Direct Measurements of Denitrification Rates in Wetland Mesocosms: A Comparison of Removal Rates of Biologically Available Nitrogen between Vegetation and Hydraulic Loading Rates Treatments

Final Project Report

July 12, 2019

South Florida Water Management District
3301 Gun Club Road
West Palm Beach, FL 33406

From:

Jeffrey Cornwell, Michael Owens and Melanie Jackson
UMCES Horn Point Laboratory

Contents

List of Tables

List of Figures

Executive Summary

A research program was carried out to determine how vegetation, hydraulic loading rates and soil treatment affect denitrification rates in the C-43 Water Quality Treatment and Testing Project (C43-WQTTP) mesocosms. The specific objectives of the work were to:

1. Determine denitrification rate differences between mesocosms
2. If differences exist, determine if hydraulic loading rate, plant community, or soil affect the degree of difference
3. Determine whether the sediments are a source or sink for nutrients in the mesocosms
4. Determine if hydraulic loading rate, plant community, or soil affect whether the sediments are a source or sink for nutrients in the mesocosms."

The benthic exchange of nitrogen (N), phosphorus (P) and oxygen (O_2) were examined in the 12 tanks of the C-43 Water Quality Treatment and Testing Project (WQTTP) mesocosm facility. Sampling took place in June and December 2018 under two different flow regimes under flow (Hydraulic Loading Rate, HLR) and no-flow (Batch 2) conditions, respectively. Measurements included ambient water quality, pore water nutrient chemistry, sediment solid phase chemistry, sediment-water dissolved nutrient exchange, and gaseous fluxes of oxygen (O_2) and di-nitrogen (N_2-N). For the sediment-water exchange component of this project, 5 cores per mesocosm were incubated, for a total of 60 cores in June and 60 cores in December. With the level of variability typical of that observed in macrophyte systems, this high degree of replication was essential.

The vegetation type (wetland plants, submerged aquatic vegetation), soil treatment (untreated native soils, soils rinsed with oxidant and acid) and two levels of hydraulic loading were represented in the mesocosms. No single treatment appeared to control denitrification. Overall, these sediments represent a net sink for nitrogen and phosphorus. Overall, the average rate of denitrification (± 1 S.D., N = 116) was 17.4 ± 23.0 mg N m^{-2} d^{-1}, with average June rates of 24.3 ± 29.7 mg N m^{-2} d^{-1} and December rates of 10.9 ± 11.4 mg N m^{-2} d^{-1}. Denitrification was in important N loss term in the WQTTP mesocosms.

Sediment is a short-term sink for organic C and N, and likely a long-term sink for phosphorus. Comparison of fluxes to organic matter pools suggest that ~2% of the sediment organic matter is remineralized on a daily basis, with ~0.35% of the sediment N pool denitrified on a daily basis. Especially for a macrophyte-based sediment system, these sediments appear to have a relatively labile pool of organic matter.

Introduction

The purpose of the contract SOW was:

> "The C-43 Water Quality Treatment and Testing Project (C43-WQTTP) is located on the Boma property, south of the C-43 canal, just upstream of the S-78 control structure (Figure 1). The C-43 WQTTP includes Phase I, a mesocosm demonstration project is being conducted to evaluate the use of wetlands vegetated with different plant communities for the removal of nitrogen from Caloosahatchee surface water. The primary objective of the mesocosm demonstration project is to assess potential surface water nitrogen removal rates using different plant communities, hydraulic loading rates, and soil. More specifically, the project assesses the removal potential for different nitrogen fractions—including the dissolved inorganic species nitrate and ammonia, which are bioavailable to microbes and plants for uptake, and dissolved organic nitrogen (DON), which has unknown bioavailability. The mesocosm demonstration project will also determine to what extent the proportion of bioavailable DON (BDON) is affected by the different treatments, including a range of hydraulic loading rates.
>
> The effects of the different mesocosm treatments on the response of the inorganic nitrogen species N_2 (di-nitrogen gas) is highly relevant to nitrogen removal from surface waters in aquatic systems. Dinitrogen gas is produced through the biogeochemical process of denitrification; the microbial transformation of biologically available dissolved nitrogen (nitrate and nitrite) to dinitrogen gas, which diffuses into the atmosphere where it is biologically unavailable to most organisms. The process of denitrification requires anoxic (no oxygen) conditions. Nitrification, the microbial transformation of ammonium (NH_4) to nitrite (NO_2) and nitrate (NO_3), is a process that requires the presence of oxygen. In aquatic sediments, anoxic and oxic zones can occur in close/immediate proximity, and nitrification can fuel denitrification in what is termed "coupled nitrification-denitrification." The presence of vegetation can increase coupled nitrification denitrification by increasing the area of oxygenated zones via oxygen produced by plant roots."

The specific objectives of the work are to:

1. Determine denitrification rate differences between mesocosms
2. If differences exist, determine if hydraulic loading rate, plant community, or soil affect the degree of difference
3. Determine whether the sediments are a source or sink for nutrients in the mesocosms
4. Determine if hydraulic loading rate, plant community, or soil affect whether the sediments are a source or sink for nutrients in the mesocosms.

This report presents the sediment flux, pore water and solid phase data sets in a relatively descriptive manner; integration with the larger data set of biogeochemical measurements in the WQTTP program will put this work in a broader context.

Methods

UMCES Personnel

The University of Maryland Center for Environmental Science (UMCES) personnel in this project are identified in Table 1.

Table 1. List of project personnel, all at UMCES Horn Point Laboratory.

	Degree	Title	Area of Expertise	Role
Cornwell, J.C.	Ph.D.	Research Professor	Sediment Biogeochemistry	Project PI, field work, report preparation
Owens, M.S.	M.S.	Advanced Senior Faculty Research Assistant	Sediment Biogeochemistry	Technical lead, field work, laboratory and data analysis, assistance with reporting
Jackson, M.	M.S.	Graduate Research Assistant	Benthic biogeochemistry	Field assistance
Owens, K.		Faculty Research Assistant	Laboratory assistance	Chemical sample preparation and analysis

Brief Mesocosm Description

The mesocosm facility is shown in Figure 1. The C-43 Water Quality Treatment and Testing Project is located on the Boma property, south of the C-43 canal, just upstream of the S-78 control structure (Figure 1). The C-43 WQTTP includes Phase I, a mesocosm demonstration project that is being conducted to evaluate the use of wetlands vegetated with different plant communities for the removal of nitrogen from Caloosahatchee surface water (Figure 1). Further details on the Phase I project are documented in the

Final Draft Report: C-43 Water Quality Treatment Area Test Facility – Mesocosm Operation and Sampling (J-Tech in association with Wetlands Solutions, Inc., 2019).

The mesocosm tanks consisted of different soil treatments, inflow rates, and vegetation types (Table 2). The SAV mesocosms were planted with Southern naiad (*Najas guadalupensis*), coontail (*Ceratophyllum demersum*) and muskgrass (*Chara spp*). Tthe wetland EMV mesocosms were planted with cattail (*Typha spp*.), bulrush (*Schoenoplectus spp*.), and spikerush (*Eleocharis spp.).* Three hydrological phases were incorporated into the experimental design, with an ~ 6 month start-up phase that was not part of the experiments, a 6 month batch phase, and a 1 y flow-through phase in which our first sample period in June 2018 was included. A six month no-flow period was established for the last 6 months of the project and UMCES sampling took place at the end of this period. Soils in this experiment were collected on-site at the Boma property and either kept unaltered or washed with hydrogen peroxide and dilute hydrochloric acid to remove labile soil nutrients. The flow regime was set to either 1.5 or 6 cm d^{-1}.

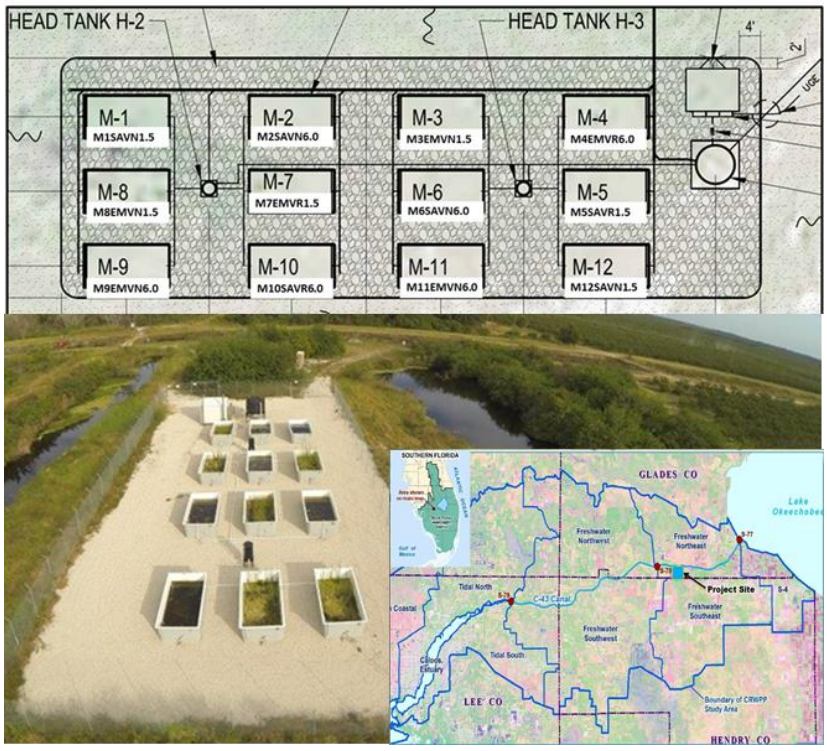

Figure 1. C-43 WQTTP mesocosm facility. Tank ID's are shown in the upper diagram and the tank M-1 is located in the lower left corner of the aerial photo.

Table 2. Description of treatments in each tank (J-Tech 2019).

Tank	Vegetation	Substrate	HLR (cm/d)	Head Tank
M-1	SAV	Native Sand	1.5	H-2
M-2	SAV	Native Sand	6.0	H-2
M-3	EMV	Native Sand	1.5	H-3
M-4	EMV	Rinsed Sand	6.0	H-3
M-5	SAV	Rinsed Sand	1.5	H-3
M-6	SAV	Native Sand	6.0	H-3
M-7	EMV	Rinsed Sand	1.5	H-2
M-8	EMV	Native Sand	1.5	H-2
M-9	EMV	Native Sand	6.0	H-2
M-10	SAV	Rinsed Sand	6.0	H-2
M-11	EMV	Native Sand	6.0	H-3
M-12	SAV	Native Sand	1.5	H-3

Ambient Water Quality

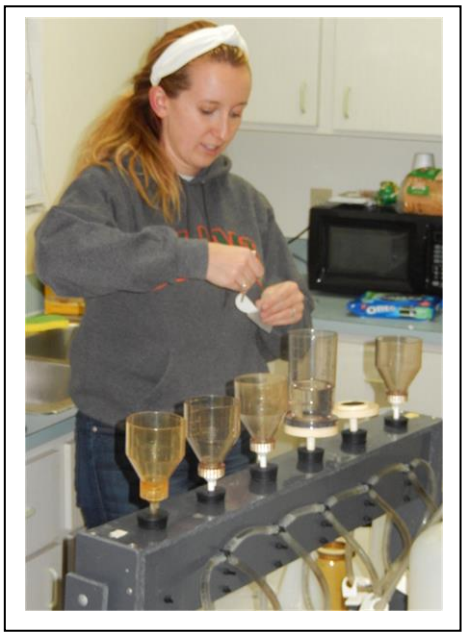

Figure 2. Filtering samples for ambient water quality.

A 2 L whole water sample was collected from each mesocosm. In June, we collected water at the tank outlet and in December water was collected by siphoning water ~ 10 cm below the water surface. The siphon used a 2 m length of tubing with vacuum used to start the siphon, with collection bottles below the tank water level. Bottles were kept out of the light. The water samples were vacuum filtered using GF/F glass fiber filters at our field laboratory for chlorophyll a, particulate P, particulate C/N analysis and suspended solids using pre-weighed filters (Figure 2) . Filtered samples were frozen for analysis of ammonium, nitrate, SRP, and TDN. Water column dissolved oxygen, temperature, salinity, and pH were measured with a YSI model 650MDS handheld logger. We measured photosynthetically active radiation (PAR) using a two channel Li Cor light meter with two underwater sensors (2π) attached to an aluminum rod system. The top sensor was held < 1 cm below the water surface and the bottom sensor was placed at the sediment surface; water depth was measured using a meter stick. Filtration of ambient water and incubation of the cores took place at UMCES' remote lab. A freezer from UMCES was used to store frozen samples.

Core Collection

A pole corer (Figure 3) was used to collect sediment cores in the mesocosm. Cores were collected in 30 cm high, 7 cm id incubation tubes (Figure 3). Approximately half of the tube was filled with sediment, leaving space for the stirring magnet suspended in the core during incubation. Undisturbed cores were collected, with minimal disturbance of the mesocosm. An o-ring fitted bottom plate was added to each core. During planning, consideration was given to filling the coring "holes" to keep the mesocosm less disturbed after sampling. Although we prepared a 3" tube to be a spacer for returning cores to the mesocosm after sampling, this approach was not implemented because the sample holes collapsed upon coring and the underlying sand did not hold its shape. At each time, 5 replicate flux cores collected in each mesocosm.

After collection, cores were placed in tall coolers in the shade. Water was added to the cooler to 1) help moderate temperatures and 2) aid in keeping pore water from draining from the sand sediments. Cores were transported to our field laboratory within 2 hours of collection.

Upon return to the incubation facility, the open sediment cores were bathed overnight in overlying water from the site's head tank. A bubble-lift system flushed the cores completely to maintain oxygen saturation (Newell et al. 2002). The overnight incubation provided the cores time to come to a thermal equilibrium; although not critical for solute fluxes, we have observed a large improvement in the performance of our denitrification measurements with overnight equilibration. Gases in the plastics can have a second order impact on our measurements and the equilibration minimizes that effect.

Figure 3. Core collection using a pole corer

Sediment-Water Exchange Methods

The measurement of sediment-water exchange in these sediments followed our approach in wetland and bottom sediments (Owens and Cornwell 2016) and has been applied to estuarine sediments (Cornwell et al. 2014; Cornwell et al. 2016), wetland sediments (Cornwell and Owens 2000; Hopfensperger et al. 2009) and aquaculture sediments (Jackson et al. 2018; Testa et al. 2015). The fluxes of N_2 and O_2 were measured using the gas ratio methods from Kana et al. (1994) in which ratios of N_2 to Ar and O_2 to Ar allowed the estimation of both denitrification and oxygen fluxes (Cornwell et al. 1999). Additional rationale for the use of this approach is found in Appendix VI. Here, we briefly describe our measurement approach; a video presentation of it is available at:

https://www.jove.com/video/54098/the-benthic-exchange-o2-n2-dissolved-nutrients-using-small-core

For both sample periods, a box truck was set up as an incubation laboratory (Figure 4). Our set-up included temperature-controlled incubators, water replacement carboys and tubing, and a CFL lighting system to be used when appropriate. A Feliz Light 6500k 250 watt full spectrum light was used. We experienced no equipment failures or any other issues using this laboratory and the gear within it. Table 3 outlines the experimental procedure.

Figure 4. A rental box truck used for an incubation laboratory (December 2018). Double wall incubators were kept at field temperatures using a heating/cooling circulator. The white PVC frame was used to hang compact fluorescent lights for illuminated incubations.

Table 3. Outline of flux sampling procedures.

Pre-Incubation – day of collection	Upon arrival at lab, cores are placed into the incubator. Site overlying water is added to the chamber to a level above the cores. T-shaped bubblers are added to pump water from cores into overlying water bath water, circulating and aerating the water. This promotes oxygen saturation and thermal equilibrium. The pre-incubation period is generally overnight, though periods as short as 2 h work well.
Setting up the experiment – day after collection	The cores are capped with o-ring sealed spinning tops; the spinners consist of Teflon-coated magnets. Care is taken to exclude bubbles. When the tops are in place, the input ports on the top are attached to tubes leading from the replacement water tank, whose bottom is placed ~1.5' higher than the core tops. A magnetic turntable is switched on to commence stirring. Between sample points, a black plastic sheet is put over the top to shield the cores from light. For illuminated incubations, a CFL light providing ~ 300 μmol photons m^{-2} s^{-1} PAR is suspended over the cores (Cornwell et al. 2008).
Gas Sample Collection	At appropriate intervals, samples are collected for gas analysis. An 8" tube is attached to the outlet of the core, the replacement water valves are opened, and a 7 mL ground glass stoppered tube was filled to overflowing, from the bottom of the tube, using gravity to push water out of the core. Sample tubes are overflowed with approximately 1 sample volumes and 10 μ L of 50% saturated $HgCl_2$ was added as a preservative. The samples are kept under water in a cooler until analysis; the temperature was ≤ ambient temperature. Samples are analyzed within 1 week of return to Maryland.
Solute Collection	A 20 mL syringe barrel was attached to the core outlet, the replacement water valves are opened, and the barrel filled to the top. The plunger is inserted and the syringe removed. All valves are closed. Samples are filtered through 0.4 μm pore size 25 mm diameter syringe filters. Samples are frozen immediately after collection and kept frozen until analysis.

The timing of sampling from the incubation cores was determined by the rate of oxygen consumption, estimated by the change in dissolved oxygen determined using a fiber-optic oxygen meter (FireStingO_2; https://www.pyroscience.com/index.html). All cores were incubated in the dark, but in instances where we had determined that light reached the bottom of the mesocosm, we did an illuminated incubation starting at the time 4 sampling point, with 3 more points added. This allowed us to have separate regressions of analyte versus time for the dark and illuminated incubations, each using 4 time points and sharing the time point when lights were turned on (Cornwell et al. 2014). We incubated a water-only core from each mesocosm to correct for water column respiration and nutrient remineralization.

Solid Phase Sediment Collection

At the end of the incubation, solid phase samples (C, N, P, chlorophyll a) were collected from the sediment surface. We let pore water drainage consolidate the floc layer to the sediment-water interface. A cut-off 10 mL syringe was used as a mini-corer and samples were collected to a depth of 1 cm. Samples were placed in 15 mL centrifuge tubes and frozen until analysis. Samples for C, N and P analyses were weighted, dried at 65°C, ground with a mortar and pestle, and saved for chemical analyses. One sample for each

analyte was collected from every incubation core. The remaining sediment in the cores was sectioned to 3 cm depth and refrigerated until grain size analysis.

Pore Water Collection

Sandy sediments are poor candidates for pore water analysis via centrifugation, as was originally planned. In November 2018 two pore water equilibrators (Hesslein 1976) were installed in each mesocosm by SFWMD personnel. These had ~8 mL of water available and these were removed during the December sampling, samples pulled up in a syringe, and filtered using a 25 mm diameter 0.4 μm pore size syringe filter (Figure 5). Samples were preserved by freezing. Two depths centered on 2 and 8.5 cm were used for analysis.

Figure 5. Collecting pore water from equilibrators, December 2018.

Chemical Analysis

The samples for chemical analysis were analyzed rapidly after arrival at the UMCES laboratory facility. Frozen samples were transported in a freezer to which dry ice was added and samples arrived solidly frozen. Dissolved gas samples with Hg preservation for N_2, O_2 and Ar last for ≥ 4 weeks and were analyzed within two weeks of collection. A listing of the chemical analysis procedures is shown in Table 4.

Table 4. Chemical analyses.

Analyte	Method	Reference
	Solutes	
Soluble reactive P (SRP)	Colorimetry	Parsons et al. (1984)
Ammonium (NH_4^+)	Colorimetry	Parsons et al. (1984)
Nitrate + nitrite (NO_x)	Vanadate reduction, colorimetry	Doane and Horwath (2003)
Dissolved organic nitrogen (DON)	Persulfate oxidation, colorimetry. Total dissolved N minus nitrate + nitrite and ammonium	Valderrama (1981)
	Gases	
Di-nitrogen, oxygen, argon (N_2, O_2, Ar)	Membrane inlet mass spectrometry	Kana et al. (1994)
Dissolved inorganic carbon (DIC)	Apollo Scitech automated IR analyzer	Cai et al. (1998)
	Solids/Particulates	
Total carbon and nitrogen	CHN analyzer	Cornwell et al. (1996)
Sediment phosphorus	Ashing, acid extraction, colorimetry	Aspila et al. (1976)
Grain size	Sieving, pipet analysis	Sweet et al. (1993)
Chlorophyll a	Fluorometry on acetone extracts	Parsons et al. (1984)

Data Analysis- Fluxes

Sediment-water exchange rates were calculated from the slope of the change of chemical constituent concentrations in the overlying water:

Equation 1

$$F = \frac{\Delta C}{\Delta t} * \frac{V}{A}$$

Where F is the flux (μmol m^{-2} h^{-1}), $\Delta C/\Delta t$ is the slope of the concentration change in overlying water (μmol L^{-1} h^{-1}), V is the volume of the overlying water (L) and A is the area of the incubated core (m^{-2}).

Data Analysis – Statistical Tests

The descriptive statistics shown in multiple tables includes measures of data means, medians, maximum and minimum values, standard deviation and standard error. When shown in the text, the mean values are always presented as ± 1 standard deviation.

Several approaches were used for statistical tests to determine if there were significant differences in the sediment-water exchange rates. The statistics were all carried out using Sigmaplot for Windows Version 11.0 (Systat Software Inc.). In the results, we first used a simple comparison of vegetation type (SAV and EMV), where EMV indicated emergent vegetation to facilitate initial data presentation. This allowed a first examination of differences. For these simple comparisons, simple T tests were invalid because the data was not normally distributed; the test that was applied was the Kruskal-Wallis One Way Analysis of Variance on Ranks (Hecke 2012). This allows for comparisons of data sets of different sizes. Significance was set at $P < 0.05$.

One way ANOVA's (Kruskal-Wallis) were also performed on all of the cores from each sample period for each unique set of conditions. For examples, 4 EMV mesocosms had native sand, with a pair from each having the same inflow rates. For the rinsed sand treatments, there the two flow regimes were not replicated. With the inclusion of SAV, there were 8 treatment types for the mesocosms and each treatment was compared using a Kruskal-Wallis one way ANOVA. Data was compared within each sample period and between sample periods.

Data Analysis – Daily Rates, Unit Conversion, Areal Extrapolation of Solids

The conversion to daily rates was carried out for O_2, N and P dark-only fluxes, with hourly rates multiplied by 24 hours:

Equation 2 – Dark only incubations

daily rate ($\mu mol\ m^{-2}\ d^{-1}$) = dark rate ($\mu mol\ m^{-2}\ h^{-1}$) * 24 h d^{-1}]

For the dark/illuminated incubations, we summed the 1) hourly rate in the dark that was multiplied by the dark hours at the time of sampling and 2) with the light rate times the hours of light:

Equation 3 – Dark/light daily rates

daily rate ($\mu mol\ m^{-2}\ d^{-1}$) = [dark rate ($\mu mol\ m^{-2}\ h^{-1}$) * night hours (h)] +
[light rate ($\mu mol\ m^{-2}\ h^{-1}$) * light hours (h)]

Light and dark hours were from the US Naval Observatory website (https://aa.usno.navy.mil/data/docs/Dur_OneYear.php) and the rates were converted afterward to mmol m^{-2} d^{-1} b dividing the daily rate in equation 2 by 1000. Although we used µmol units for dissolved concentrations and fluxes, we converted fluxes to the standard rates used by engineers (mg m^{-2} d^{-1}) using the molecular mass of O_2, N and P (32, 14 and 30.97 respectively).

The sediment-water exchange data presented here has uptake by the sediments as a negative number, with efflux from the sediments as a positive number. For presentation purposes, we use the term sediment oxygen demand, in which oxygen uptake in converted to a positive number:

Equation 4 – Sediment oxygen demand (SOCD)

Sediment oxygen demand (umol m^{-2} h^{-1}) = oxygen flux * -1.0

For the conversion of the sediment C, N and P concentrations from mg g^{-1} to g m^{-2} units, we used the bulk density (g cm^{-3}) times the area in 1 m^2 (10,000 cm^2 per m^2; our samples were from 0-1 cm). The data was then divided by 1000 to convert from mg to g.

Equation 5 – areal concentrations of C, N, P

CNP (g m^{-2}) = [bulk density (g cm^{-3}) * sample depth (cm) * 10000 cm^2 m^{-2} * CNP concentration (mg g^{-1})] * 0.001 g mg^{-1}

Field Activity Schedule/Summary

The field activity schedule is presented in Table 5. The data set are from two sampling periods, one in June and the second in December, the latter time coincided with destructive biomass sampling and cessation of the active experimental program.

Table 5. Equilibrator installation and biogeochemical sampling schedule in 2018. The flux cores were incubated the day after collection.

Date	**Flux Cores Collected**
June 20	1,2,4,5
June 21	3,7,8,11 light dark
June 22	6,9,10,12
December 10	1,2,5, 6
December 11	3,7,8,11 light dark
December 12	4,9,10,12
November 18	2 equlibrators installed by SFWMD in each tank

Results

Presentation Approach

To simplify the presentation of the data, most of the visualization of the data is carried out using comparisons of box plots that show the spread of the data and median values of the vegetation type (SAV, EMV) at each time of sampling.

Tank Water Quality

The water quality in the mesocosms was assessed at the time of core collection and all field results are presented in Appendix I. The bottom temperatures decreased from 27.3 ± 0.6 in June to 18.4 ± 0.5 °C in December. In June and December, surface water was slightly warmer than bottom waters (Figure 6). There was a broad range of dissolved oxygen concentration in both months, with average bottom concentrations of 1.6 ± 0.4 and 3.8 ± 2.0 mg L^{-1} in June and December, respectively. Most mesocosms had negligible light at the sediment surface (Appendix I), but there was sufficient light at the sediment surface in mesocosms 3, 7, 8 and 11 to warrant illuminated incubations; all 4 had EMV vegetation. The SAV mesocosms were dark at the sediment surface below the dense plant canopy.

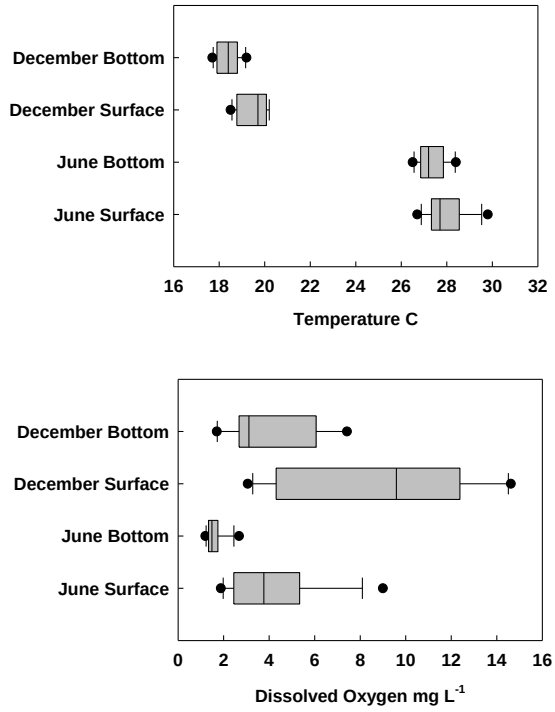

Figure 6. Temperature and dissolved oxygen concentrations of surface and bottom of mesocosm water column.

The SRP concentrations in surface waters were variable, averaging 0.6 ± 1.0 and 0.3 ± 0.2 μmol L^{-1} in June and December respectively; box plots in Figure 7 show the data range and median values. Nitrate plus nitrite concentrations were relatively low, but ammonium showed considerable variability, with some concentrations in excess of 20 μmol L^{-1}. DON concentrations were the dominant dissolve N pool, averaging 95.5±9.6 and 92.6 ± 20.5 μmol L^{-1} in June and December respectively. All ambient water nutrient data is located in Appendix II.

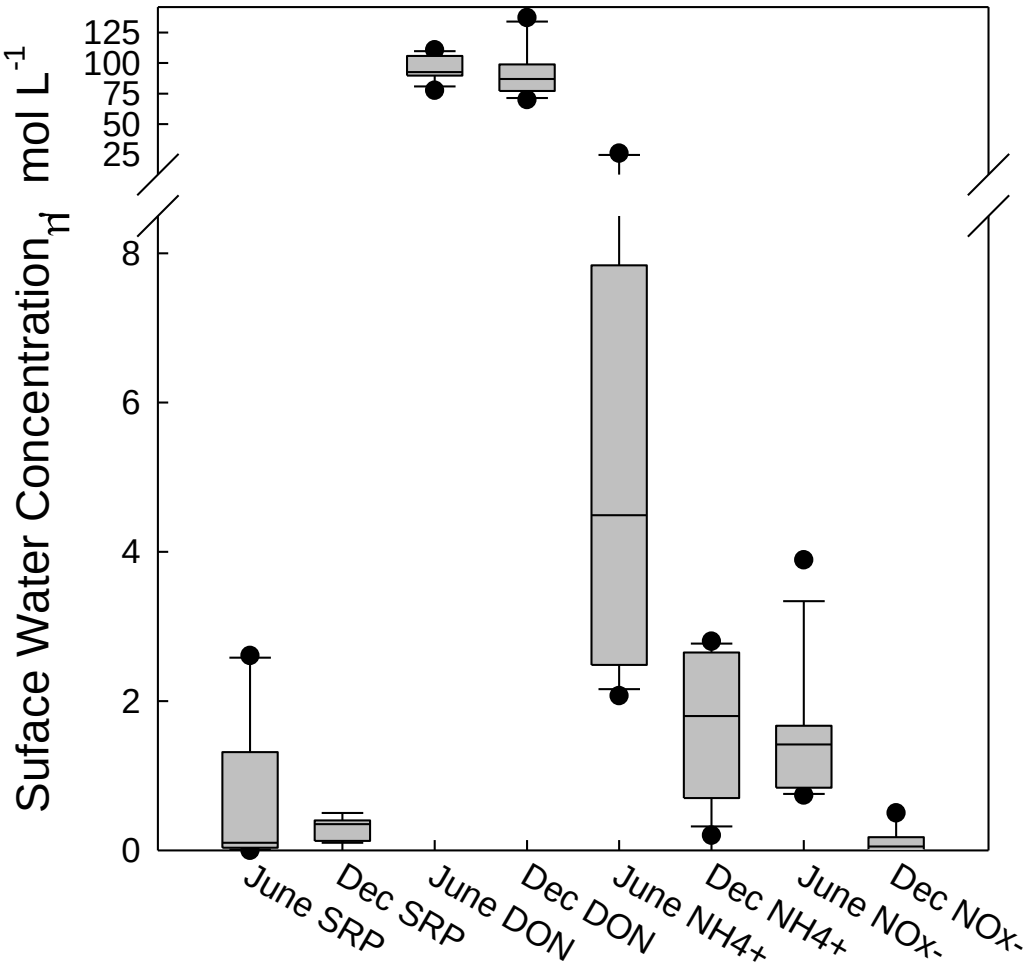

Figure 7. Surface water box plots of dissolved nutrients.

Sediment Visual Observations

The sediments had a wide variety of surface appearance. However, a several cm thick floc layer (Figure 8) was a common occurrence in almost all sediment cores. This layer was very watery and undulated when the core was moved after collection.

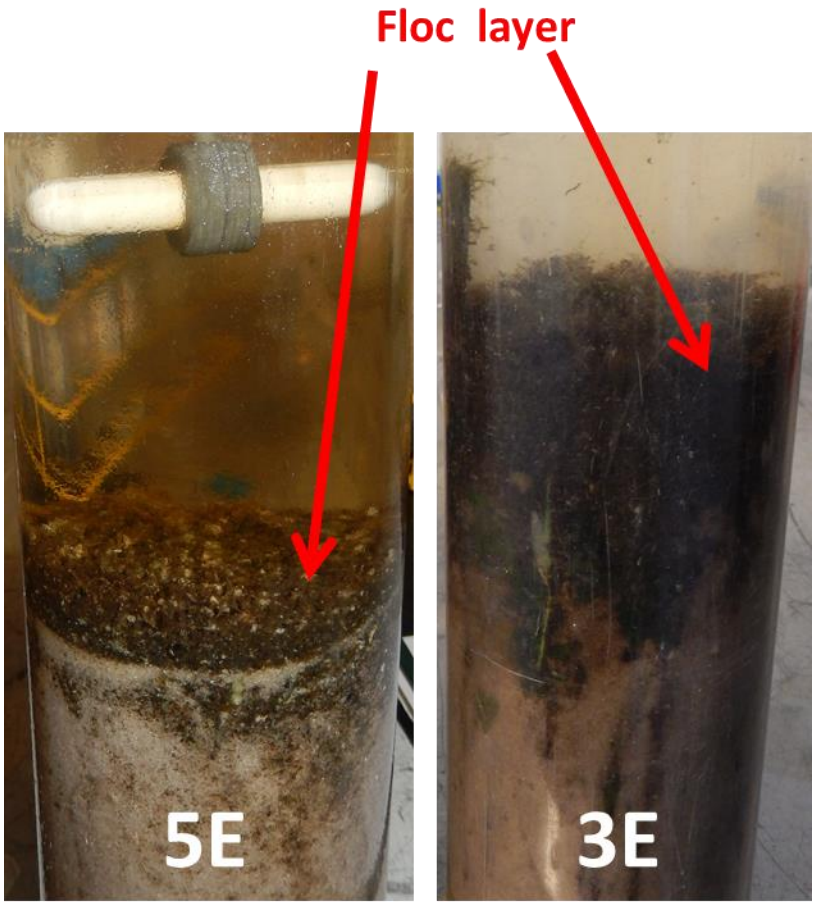

Figure 8. June 2018 photos of cores from Tank 5 (SAV) and Tank 3 (EMV).

While the thick layer of organic material and floc was found in most cores, core appearances varied within a tank (Figures 9, 10). In all cases, the underlying sand layers were obvious, with evidence that the coring activity dragged some of the surface material to greater depths. We did not observe many roots in the cores we collected.

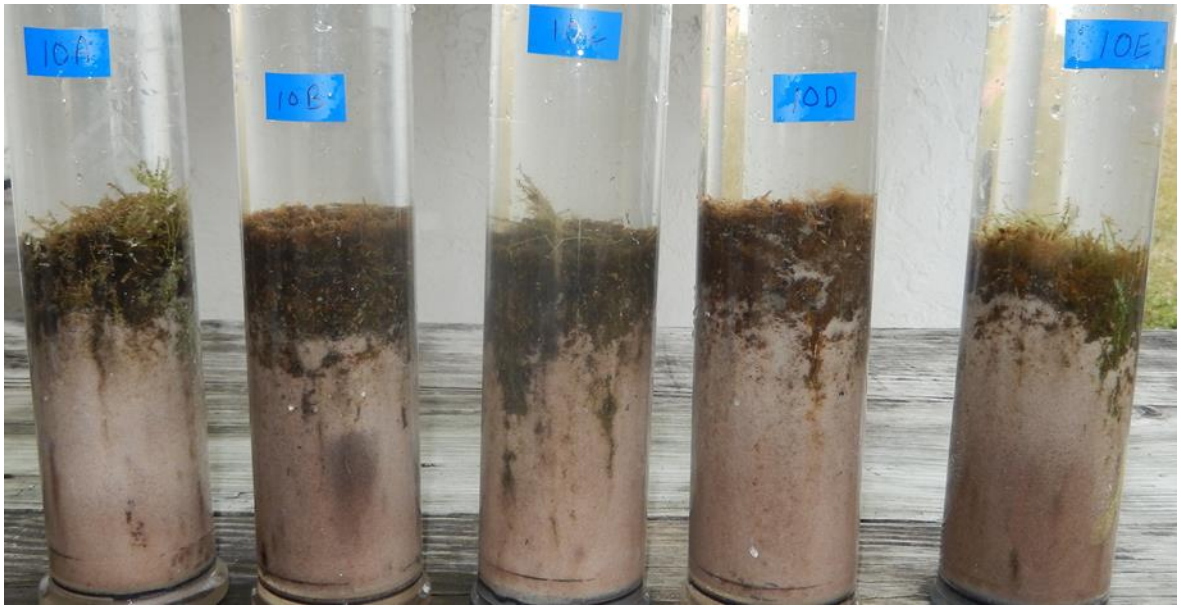

Figure 9. December 2018 photos from SAV tank 10.

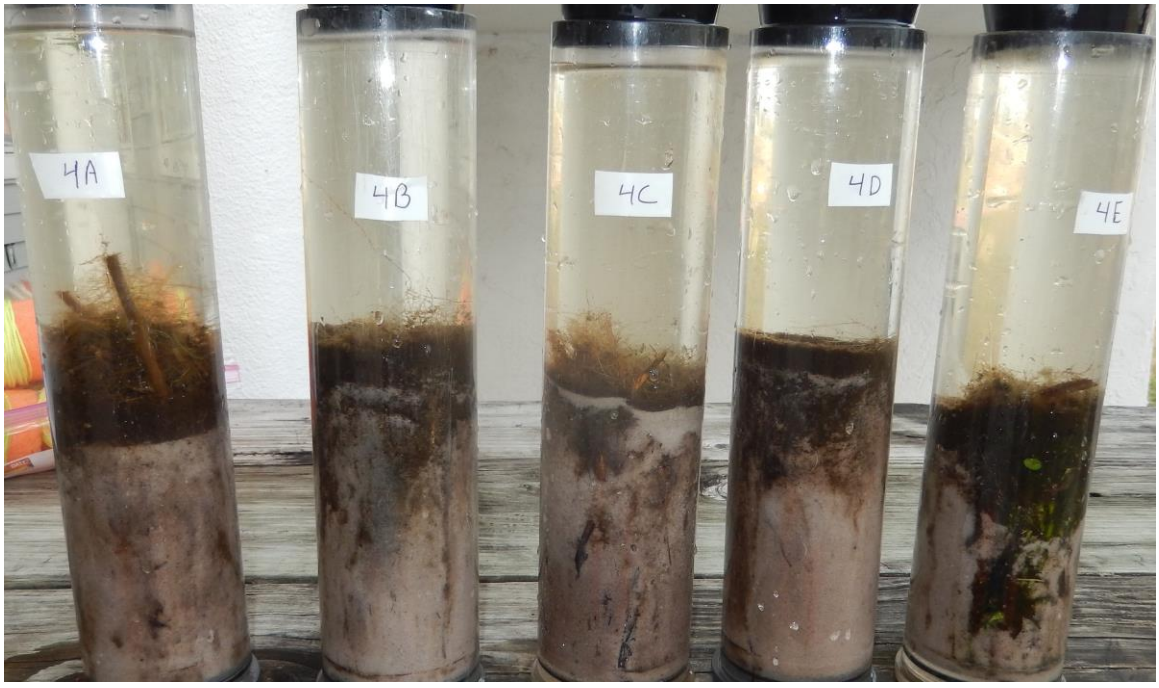

Figure 10. December 2018 photos from EMV Tank 4.

Pore Water Chemistry- December 2018

The recovery of pore water from the equilibrators was sufficient for the analyses of the nutrient elements. While the concentrations of SRP and NH_4^+ were generally much higher than observed in the tank water column, the sediment concentrations of DON were generally similar to that of the overlying water (Table 6, Figure 11). All data are available in Appendix V.

The enrichment of ammonium in the sediment pore water was high, with concentrations in the upper few cm of sediment averaging 538.1 ± 343.7 and 114.4 ± 159.7 μmol L^{-1} for SAV and EMV. Median NH_4^+ concentrations in the water column were < 5 μmol L^{-1}, indicating sediments were highly enriched in ammonium. The pore water concentrations of SRP were much lower than NH_4^+, ranging from 0.7 to 107 μmol L^{-1}. Average pore water DON concentrations were < 2 times greater than the surface water concentration.

Using a Kruskal-Wallis one way analysis of variance on ranks, the only difference of note is that in the SAV data, the 8.5 cm was higher than the data from 2 cm. The level of variability in all the pore water data suggests that small scale variability occurred in the mesocosms.

Table 6. Descriptive statistics for pore water from the two sampled depths in the two vegetation types.

		Mean	Std Dev	Std. Error	Max	Min	Median
		μmol L^{-1}					
NH_4^+	SAV 2	538.1	343.7	99.2	1269.3	3.9	460.9
	SAV 8.5	1045.7	602.8	174.0	2127.0	419.2	802.1
	EMV 2	114.4	159.7	46.1	578.0	3.4	81.4
	EMV 8.5	366.9	492.9	142.3	1514.3	0.4	140.7
SRP	SAV 2	10.0	12.0	3.5	46.5	0.7	7.5
	SAV 8.5	28.1	30.7	8.9	107.4	3.1	16.6
	EMV2	7.2	5.7	1.7	16.6	1.4	3.9
	EMV 8.5	21.3	31.5	9.1	92.7	1.9	7.1
DON	SAV 2	131.0	119.5	34.5	308.0	0.0	126.0
	SAV 8.5	115.6	105.1	30.3	277.2	0.0	91.8
	EMV 2	159.1	73.4	21.2	281.6	57.7	140.1
	EMV8.5	182.6	166.1	48.0	589.8	0.0	146.6

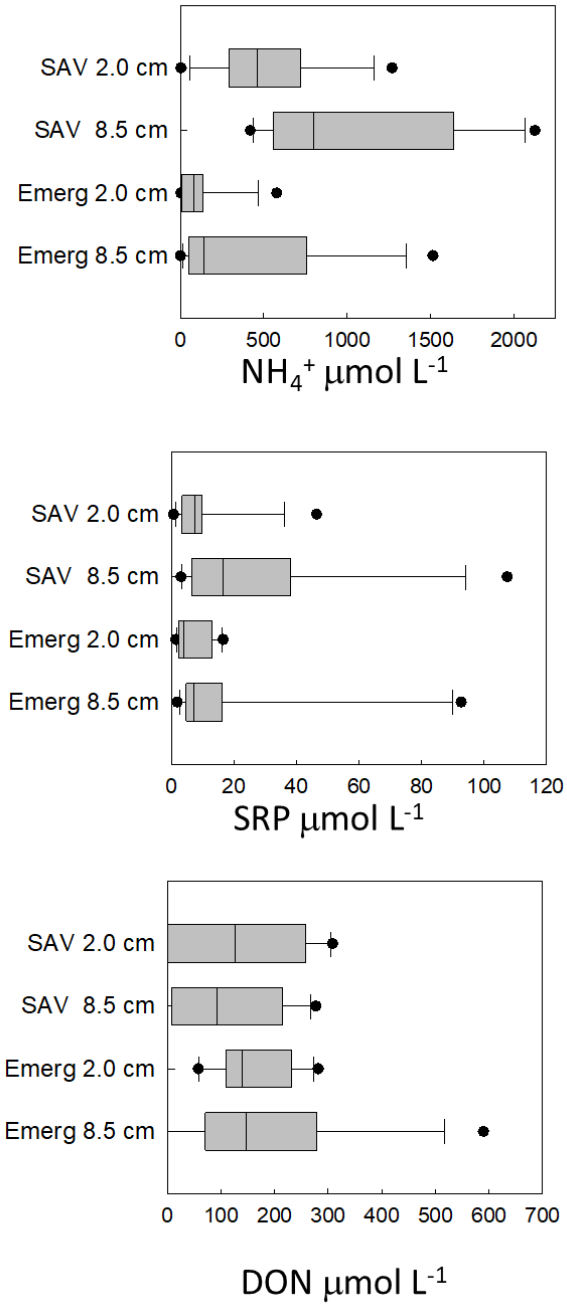

Figure 11. Box plots of pore water chemistry from December 2018. Each box represents 12 data points.

Sediment Solid Phase Chemistry and Grain Size

Biogeochemical Concentrations and Grain Size – Mass Basis

The data for solid phase chemistry and grain size consisted of 5 samples from each tank from each sampling event, for a total of 120 observations (Table 7; Appendix VI). The concentrations shown here are unusual compared to field systems in that this is a new system and the deeper sediments are largely devoid of experimental influence on the solid phase.

Sand was the predominant grain size in the top 3 cm of sediment making up 98.6 ± 0.06% and 94.5 ± 6.0% of SAV and EMV samples (Figure 12). Using a Mann-Whitney rank sum test, sand content in the SAV tanks was significantly greater than EMV tanks, and both silt and clay were significantly lower in the SAV tanks. Average proportions of grain size are depicted on Figure 12D. The percent water concentrations were significantly higher in the EMV tanks and bulk density values were significantly higher in the SAV tanks. The bulk density values are more typical of sandy environments, rather than fine-grained organic matter conditions typical of many wetlands. The nature of the fine-grained inputs are not discernable from these data; fine grained organic material may have biased these results, but visual observations suggest both EMV and SAV cores had a similar flocculent organic component.

Organic carbon concentrations were slightly less than 1% in June, significantly decreasing ($P < 0.001$) to about 0.4% in December (Figure 13). However, no equivalent changes were observed in total phosphorus. A simple interpretation would be that remineralization depleted the organic matter, decreasing N and P, but remineralized P was retained, presumably in the inorganic form. Phaeophytin a decreased from June to December ($P < 0.001$), suggesting degradation and depletion of organic matter. There were no significant changes in chlorophyll a, but the variability decreased from June to December. The molar C:N ratios were more tightly constrained in June, but SAV and EMV ratios were not significantly different at either sample time. The C:N ratios were consistent with a macrophyte origin of the organic matter.

Using a Kruskall-Wallis one way analysis of variance on ranks, there were significant decreases in organic carbon and nitrogen in December relative to June ($P < 0.001$). Total P did not change over time, phaeopigment a decreased ($P < 0.001$) from June to December for EMV vegetation, chlorophyll a did not have significant differences, and within a vegetation type, the molar C:N did not change over time.

Direct comparison to other SFWMD and J-Tech data sets is difficult; our samples were taken from the top 1 cm of sediment. Since visual examination of cores suggested that accumulation of organic matter was limited to the upper cm (in most cases), deeper sampling would result in a lower organic C, N and pigment concentration via dilution by inert sand.

Table 7. Sediment solid phase statistics for June and December samples. December data are shaded; grain size, bulk density and percent water data are for December only.

Analyte	Samples	Mean	S.D.	S.E.	Max	Min	Median
Organic C %	June SAV	0.96	0.77	0.14	3.48	0.14	0.71
	June EMV	0.94	0.89	0.16	4.37	0.15	0.61
	Dec SAV	0.36	0.27	0.05	1.10	0.10	0.20
	Dec EMV	0.46	0.54	0.10	2.80	0.10	0.30
Total N mg g^{-1}	June SAV	0.99	0.89	0.16	4.08	0.10	0.70
	June EMV	0.90	0.87	0.16	4.40	0.10	0.60
	Dec SAV	0.31	0.25	0.05	1.20	0.08	0.20
	Dec EMV	0.41	0.51	0.09	2.30	0.08	0.20
Total P mg g^{-1}	June SAV	0.09	0.06	0.01	0.29	0.03	0.08
	June EMV	0.10	0.07	0.01	0.27	0.03	0.07
	Dec SAV	0.10	0.05	0.01	0.22	0.03	0.09
	Dec EMV	0.11	0.09	0.02	0.49	0.04	0.09
Phaeophytin a mg m^{-2}	June SAV	229.9	144.8	26.4	571.0	30.2	187.9
	June EMV	329.0	388.2	70.9	2061.5	3.6	224.8
	Dec SAV	149.7	91.1	16.6	500.0	38.6	137.7
	Dec EMV	126.8	89.6	16.4	476.0	18.6	106.7
Chlorophyll a mg m^{-2}	June SAV	213.3	156.5	28.6	591.3	29.4	159.5
	June EMV	300.0	329.9	60.2	1586.3	1.7	198.2
	Dec SAV	173.2	126.8	23.2	570.2	38.9	131.1
	Dec EMV	152.6	115.0	21.0	614.4	10.8	129.1
C:N Ratio molar	June SAV	12.5	2.7	0.5	22.0	9.9	11.5
	June EMV	12.6	2.2	0.4	19.7	9.8	12.1
	Dec SAV	14.3	3.9	0.7	25.5	8.5	13.3
	Dec EMV	15.2	4.0	0.7	23.1	9.4	15.0
Sand %	Dec SAV	98.6	0.6	0.1	99.4	96.8	98.5
	Dec EMV	94.5	6.0	1.1	99.7	77.0	96.8
Silt %	Dec SAV	0.40	0.36	0.06	1.50	0.00	0.30
	Dec EMV	0.84	0.61	0.11	2.50	-0.20	0.75
Clay %	Dec SAV	1.08	0.67	0.12	2.90	0.00	0.95
	Dec EMV	4.67	5.65	1.03	21.90	0.00	2.55
Water %	Dec SAV	29.8	5.3	1.0	43.8	22.3	28.2
	Dec EMV	37.1	10.1	1.8	66.7	21.6	35.4
Bulk Density g cm^{-3}	Dec SAV	1.32	0.24	0.04	1.90	0.80	1.30
	Dec EMV	1.06	0.29	0.05	1.90	0.30	1.05

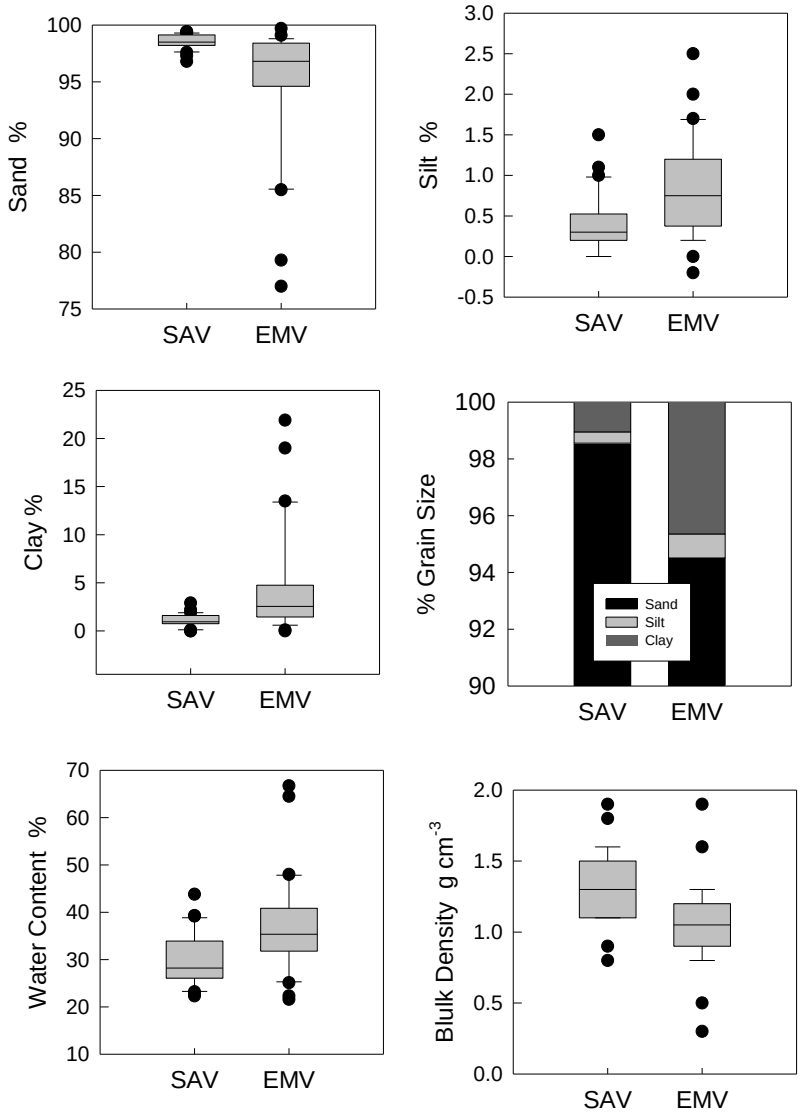

Figure 12. December 2018 solid phase physical parameters. Box plots of all data for SAV and EMV samples are presented, with each box representing 30 individual data points. The data include percentages of sand (A), silt (B), clay (C), all grain size averages as a stacked bar (D), and water content (E). Bulk density, the grams of dry material per cubic centimeter of sediment is shown in panel F.

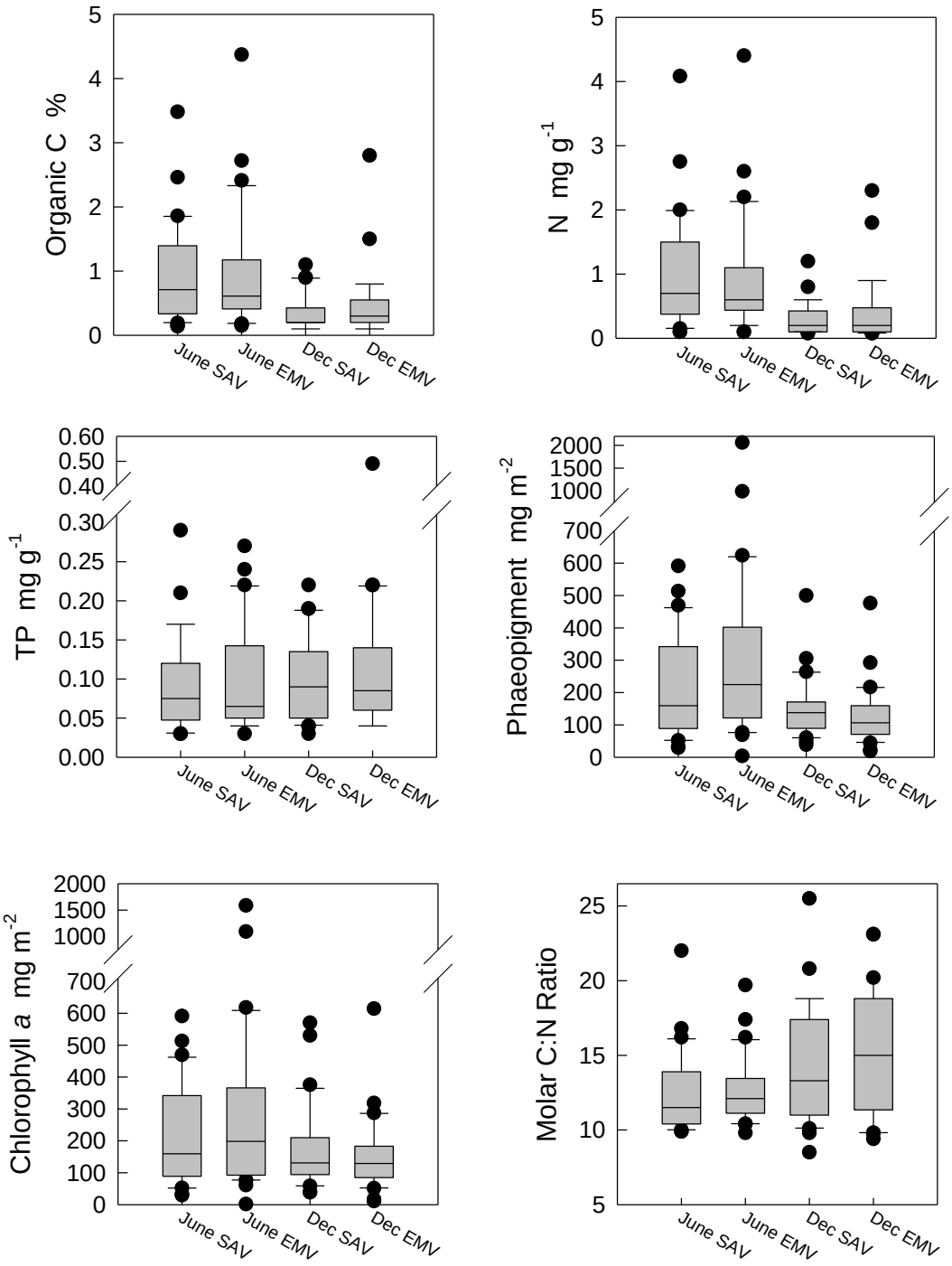

Figure 13. Solid phase chemistry, presented as box plots of the SAV and EMV tanks for both sample times. Organic C (A), total nitrogen (B), total P (C), phaeopigment a (D), chlorophyll a (E) and the molar C:N ratio are shown. These parameters were collected only in December.

Areal Concentrations

In a mass balance, the key concentration is an areal (m^2) amount of organic carbon, nitrogen and phosphorus. We can estimate the total mass of sediment in the top 1 cm of sediment by multiplying bulk density (g cm^{-3}) by the area of 10,000 cm^2 in 1 square meter to get a mass per square meter. Multiplying this areal mass by the concentration of C or N (mg g^{-1}) and converting the mass to grams, we get mass of C or N per square meter. All estimates are in Appendix VI and average data for each mesocosm are presented in Table 8. Bulk density was measured only in December and December values were applied to June calculations.

Table 8. Areal mass of C, N and P in each mesoscosm. Means are based on 5 measurements in each mesocosm, taken from the flux cores. The December data are shaded.

Mesocosm	Analyte	Mean	Std Dev	Std. Error	Max	Min	Median	Mean	Std Dev	Std. Error	Max	Min	Median
		Areal Mass g m^{-2}											
		June						December					
1	C	211	100	45	337	93	229	32	12	6	48	19	29
2	C	53	35	16	98	16	38	45	26	12	70	14	59
3	C	266	227	102	671	144	177	40	24	11	78	15	39
4	C	104	77	34	213	39	58	56	27	12	87	19	65
5	C	44	54	24	140	12	24	104	143	64	359	22	47
6	C	60	35	16	117	28	47	21	8	4	30	11	18
7	C	64	38	17	118	12	59	14	2	1	18	12	14
8	C	206	168	75	498	77	165	43	21	9	71	22	43
9	C	95	51	23	149	20	99	56	67	30	176	20	24
10	C	59	23	10	98	42	53	43	25	11	76	13	44
11	C	217	128	57	347	22	233	30	11	5	48	20	28
12	C	50	21	9	72	24	43	61	42	19	111	18	55
1	N	23.5	11.4	5.1	37.6	9.3	26.8	2.9	1.7	0.8	5.5	1.5	1.9
2	N	4.5	3.6	1.6	8.6	0.8	3.0	4.2	2.9	1.3	6.6	0.9	5.9
3	N	28.4	28.1	12.6	78.5	14.5	15.1	2.9	2.2	1.0	6.8	1.1	2.0
4	N	11.0	8.0	3.6	21.6	4.5	5.9	5.7	3.5	1.6	10.0	1.1	5.9
5	N	4.9	6.4	2.9	16.2	1.2	2.5	8.8	11.7	5.2	29.5	1.6	4.0
6	N	4.9	3.0	1.3	9.7	2.1	3.7	1.5	1.0	0.4	2.9	0.7	1.0
7	N	5.5	3.2	1.4	9.7	1.0	5.3	1.3	0.6	0.3	2.2	0.8	0.9
8	N	20.1	17.2	7.7	50.2	7.7	15.8	3.9	2.1	1.0	6.5	1.4	3.2
9	N	9.8	5.0	2.2	14.2	2.2	10.7	5.6	7.3	3.3	18.6	1.3	2.5
10	N	6.3	2.0	0.9	9.8	4.9	5.8	3.8	2.7	1.2	7.8	1.0	3.7
11	N	20.1	12.3	5.5	33.2	1.4	21.9	2.5	1.2	0.6	4.3	1.3	2.6
12	N	4.5	2.8	1.3	7.7	1.4	3.4	4.7	3.0	1.3	8.4	1.2	4.6
1	P	2.01	0.64	0.29	2.91	1.38	1.73	1.09	0.69	0.31	2.32	0.70	0.83
2	P	0.72	0.32	0.14	1.04	0.28	0.64	1.56	0.97	0.43	2.71	0.35	1.77
3	P	2.13	1.93	0.86	5.54	0.94	1.50	1.12	0.55	0.25	1.83	0.45	1.07
4	P	0.93	0.70	0.31	1.85	0.41	0.45	1.07	0.40	0.18	1.61	0.58	0.94
5	P	0.51	0.38	0.17	1.17	0.22	0.34	2.31	2.30	1.03	6.24	0.48	1.65
6	P	0.58	0.16	0.07	0.81	0.44	0.55	0.66	0.17	0.08	0.85	0.44	0.65
7	P	0.65	0.34	0.15	1.06	0.17	0.59	0.53	0.19	0.08	0.84	0.33	0.49
8	P	1.80	0.91	0.41	3.07	0.64	1.60	1.31	0.72	0.32	2.23	0.58	0.91
9	P	1.64	0.86	0.38	2.71	0.53	1.47	1.30	0.44	0.20	1.78	0.76	1.46
10	P	0.64	0.17	0.08	0.85	0.47	0.58	1.41	0.72	0.32	2.39	0.42	1.42
11	P	2.19	1.02	0.45	3.08	0.46	2.43	0.92	0.42	0.19	1.65	0.61	0.82
12	P	0.64	0.13	0.06	0.77	0.44	0.71	1.54	0.77	0.34	2.37	0.65	1.44

For C, N and P, the standard deviation of the average within a mesocosm was typically half or greater than the mean value. The high variability in each mesocosm, and between

mesocosms, is partly attributed to having variable amounts of coarse organic matter in some sites.

Statistical Analyses – Areal Solids

The data analysis for this section consists of a Kruskal-Wallis ANOVA for each unique set of experimental conditions shown in Table 9. The data arranged in this fashion are shown in Figures 14-16, with separate plots for June and December data. Within each date, there were few significant differences for C and none for N and P. For C the only difference was observed between EM1 and SAV4 in June and EM1 in June and EM1, EM2 and SAV2 in December.

Table 9. Labeling of treatment types. Not that the rinsed sand mesocosms are not replicated.

ID	Vegetation	Substrate	HLR cm d^{-1}	Tanks
EM1	EMV	Native Sand	1.5	3, 8
EM2	EMV	Native Sand	6.0	9, 11
EM3	EMV	Rinsed Sand	1.5	7
EM4	EMV	Rinsed Sand	6.0	4
SAV1	SAV	Native Sand	1.5	1, 12
SAV2	SAV	Native Sand	6.0	2, 6
SAV3	SAV	Rinsed Sand	1.5	5
SAV4	SAV	Rinsed Sand	6.0	10

A three way ANOVA (vegetation, rinsed/unrinsed, flow rate) was applied to each of the three analytes. For carbon in June, statistically significant results ($P < 0.05$) were observed between EMV and SAV treatments, with EMV > SAV. Perhaps more interesting was the observation that the rinsed sediments had lower C than the native sediments; clearly the oxidation of organic matter and mild acid extraction created significant differences. However, these observed differences were not found 6 months later and no statistical significance was observed for that sample time.

The three way ANOVA for the sediment nitrogen data showed no significant differences between EMV and SAV treatments, but for both the June and December data, sediment treatment differences were significant (rinsed < native). Initial removal of organic matter and nitrogen appear to have a more lasting effect than for carbon.

For phosphorus, a three way ANOVA showed June differences between vegetation types and between sediment treatments; no differences were observed in December. Significantly ($P < 0.05$) higher sediment P concentrations were found in EMV tanks and the rinsed sediments had lower sediment P than native sediments. No differences were observed in December.

In all cases, the sediment composition was not related to the hydrological flow regime. Overall these data suggest vegetation type and sediment treatment had on effect on sediment composition, particularly in June.

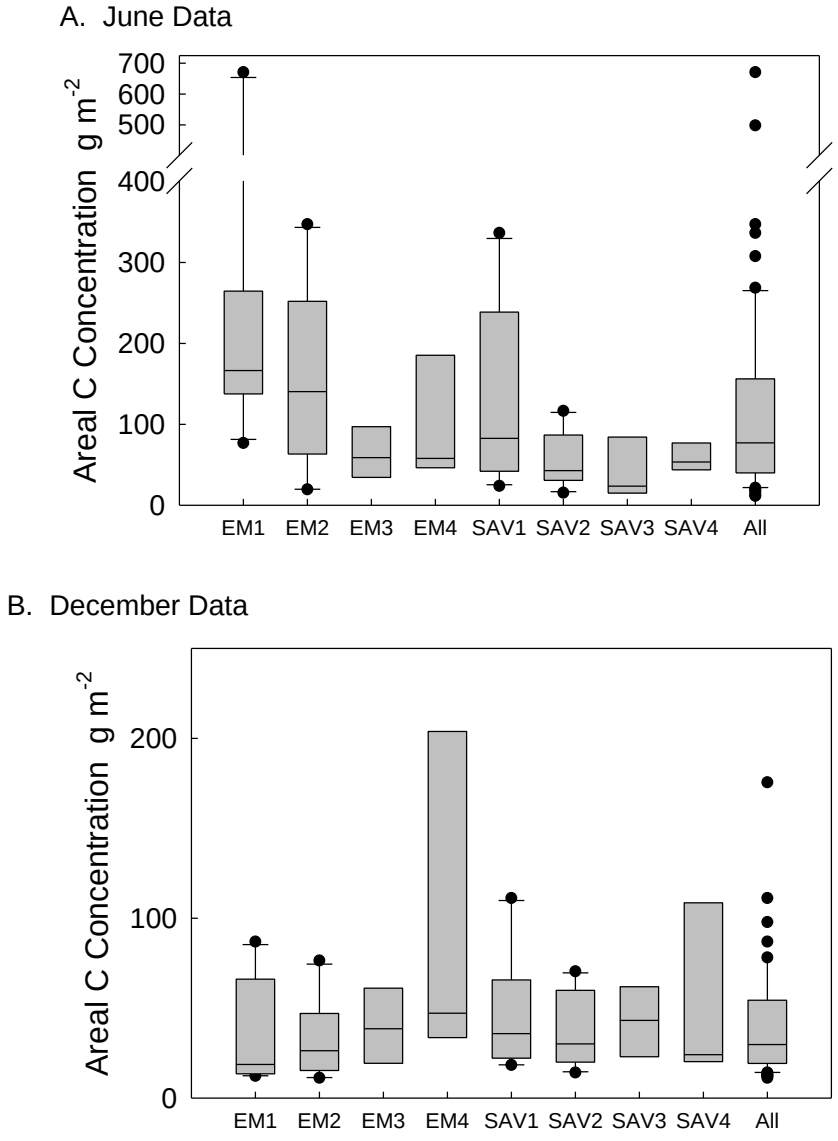

Figure 14. Areal C concentration box plots within treatments. For EM1, EM2, SAV1, and SAV2 treatments, bars are based on 10 cores; the remainder had data from 5 cores. The final box plot data is for all data combined.

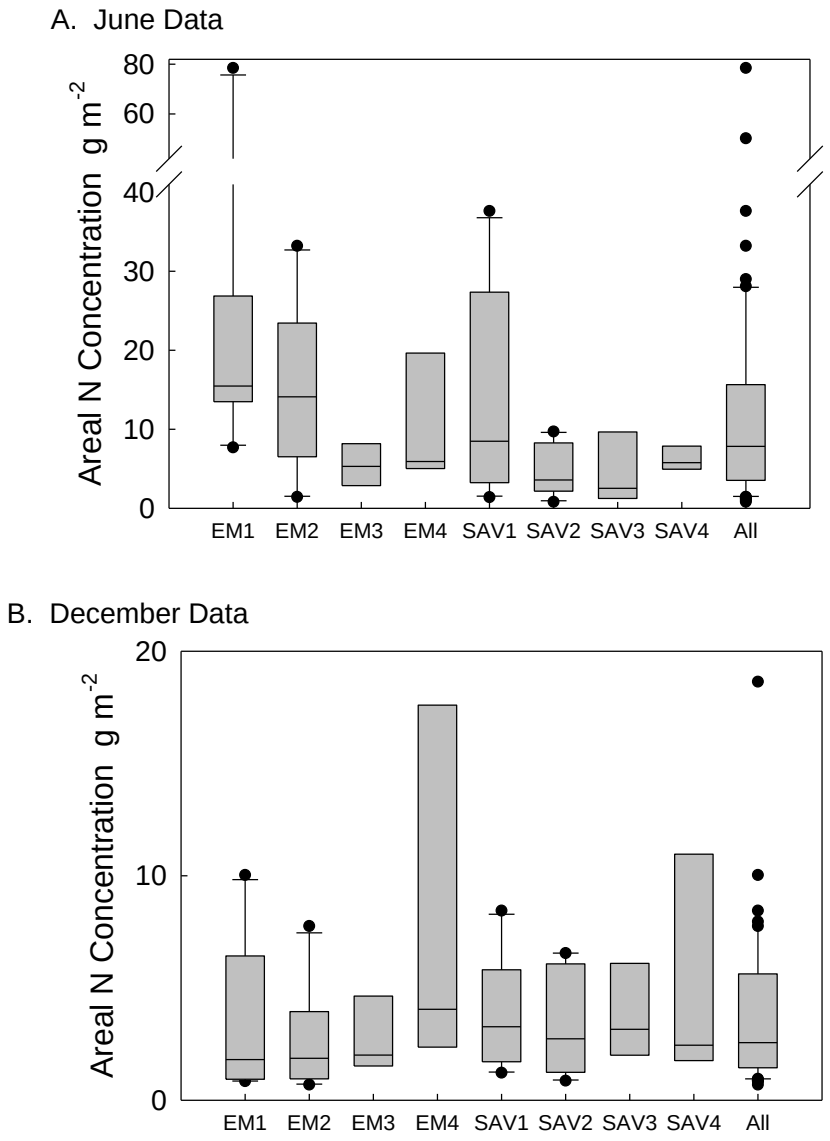

Figure 15. Areal N concentration box plots within treatments. The final box plot data is for all data combined.

A. June Data

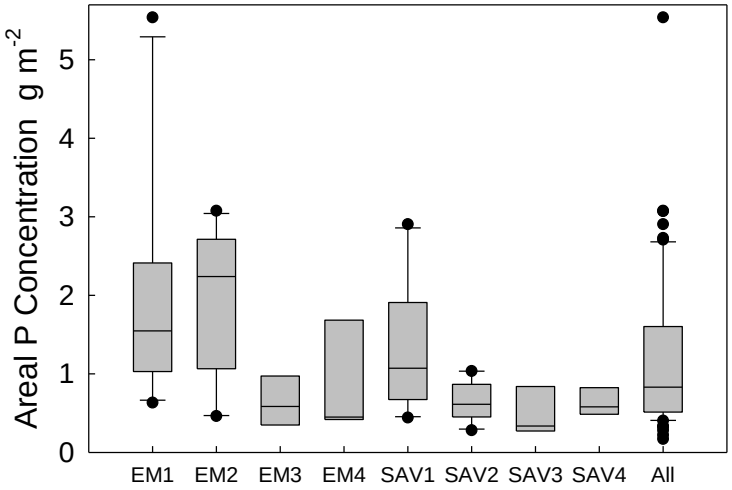

B. December Data

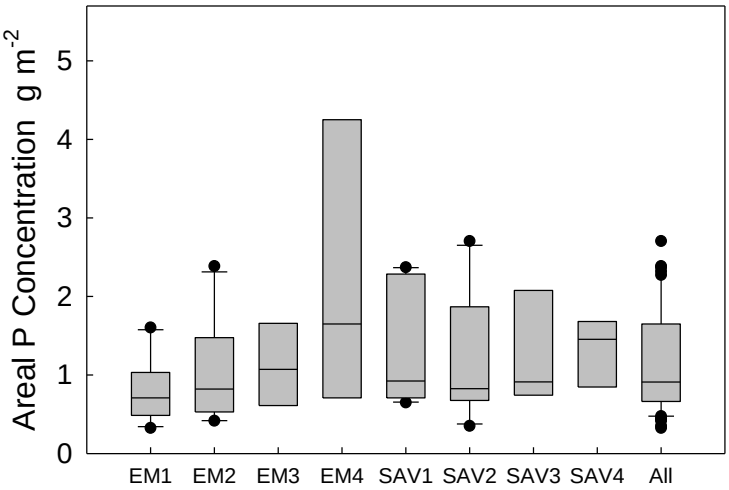

Figure 16. Areal P concentration box plots within treatments. The final box plot data is for all data combined.

Sediment-Water Exchange

In this section, the data from the June and December samples are presented as 4 separate figures. In the first figure, the flux data from all cores are presented, separating them into SAV and EMV plots, using the same scaling on a given sample date. These plots provide a snapshot view of all the data and an view of the variability in these measurements. A second page of plots shows the differences in dark and illuminated fluxes for each analyte at each time. A plot of dark versus illuminated data is used to illustrate the date spread between light-induced increases/decreases and dark data. A total of 4 mesocosms had light incubations of sediment cores; 8 did not.

After this data description, an examination of all of the nitrogen data follows, as well as an examination of whether fluxes of N_2 are relatable to fluxes of oxygen. Statistical calculations in this section are used for a comparison of vegetation type and date, and do not examine all individual treatments used in this project (See Statistical Analyses below for more detail). The data used in this section are available in Appendix IV.

Dissolved Oxygen Fluxes

Dark oxygen fluxes (Figures 17, 18; Appendix IV) ranged from -6,231 to -380 μmol m^{-2} h^{-1}. The overall variability was relatively high (Table 10), reflecting the variable inputs of organic matter.

Table 10. Dark oxygen flux statistics

	Mean	Std Dev	Std. Error	Max	Min	Median
	O_2 μmol m^{-2} h^{-1}					
June SAV	-1713	801	146	-494	-3826	-1653
June EMV	-2803	1188	217	-1470	-6231	-2468
Dec SAV	-1090	369	67	-484	-2052	-993
Dec EMV	-1070	340	62	-380	-1698	-1093

Four of the EMV tanks were incubated with illumination after the dark incubation (Figure 19A), with lower June rates of oxygen uptake in the light (Figure 19B). Production of O_2 during the incubation was not observed. In December, the same pattern was observed, but there were 5 instances where O_2 fluxes increased during illuminated incubation (Figure 20).

There was a significant decrease ($P < 0.001$) between June EMV O_2 fluxes (Figure 21) and either EMV or SAV oxygen fluxes in December. The difference between dark and illuminated oxygen fluxes is an estimate of benthic photosynthesis. In June the net photosynthesis averaged 1386 μmol m^{-2} h^{-1}, while in December is was a statistically similar 943 μmol m^{-2} h^{-1}.

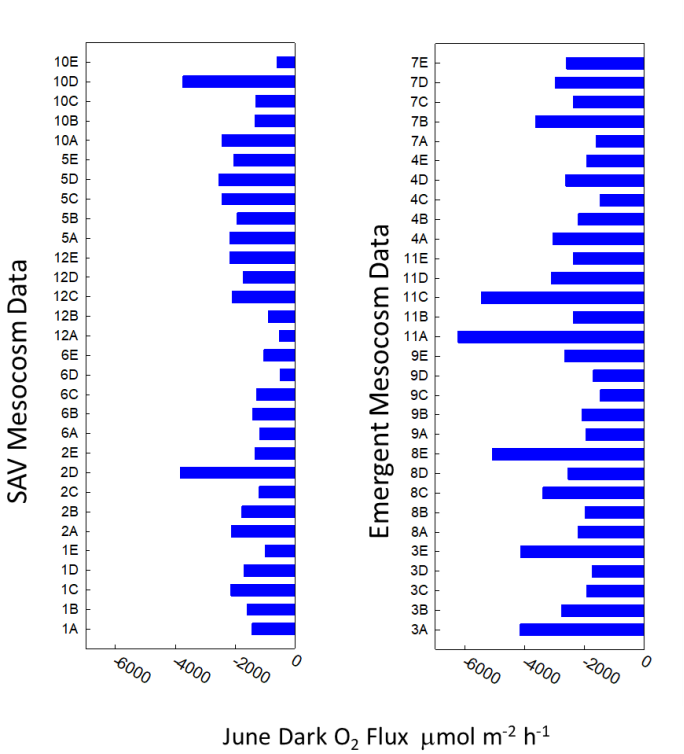

Figure 17. June 2018 oxygen fluxes. Negative rates indicate sediment uptake

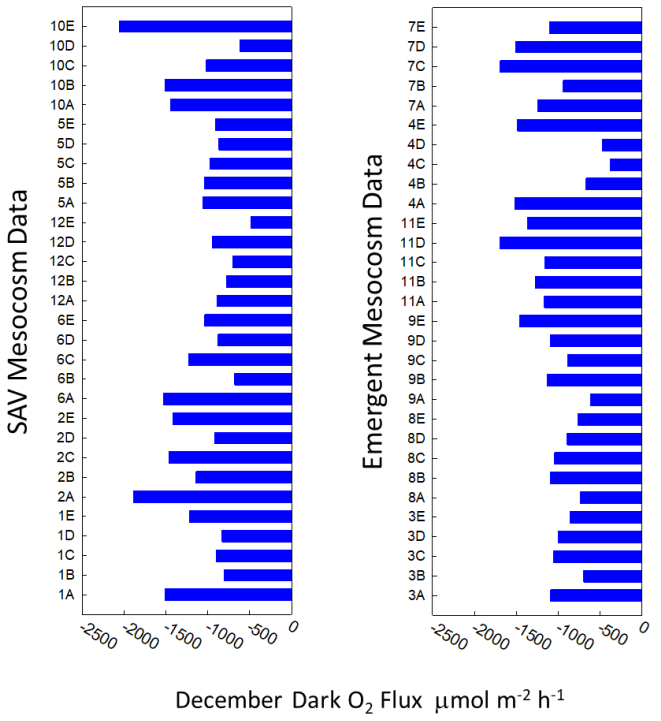

Figure 18. December 2018 oxygen fluxes.

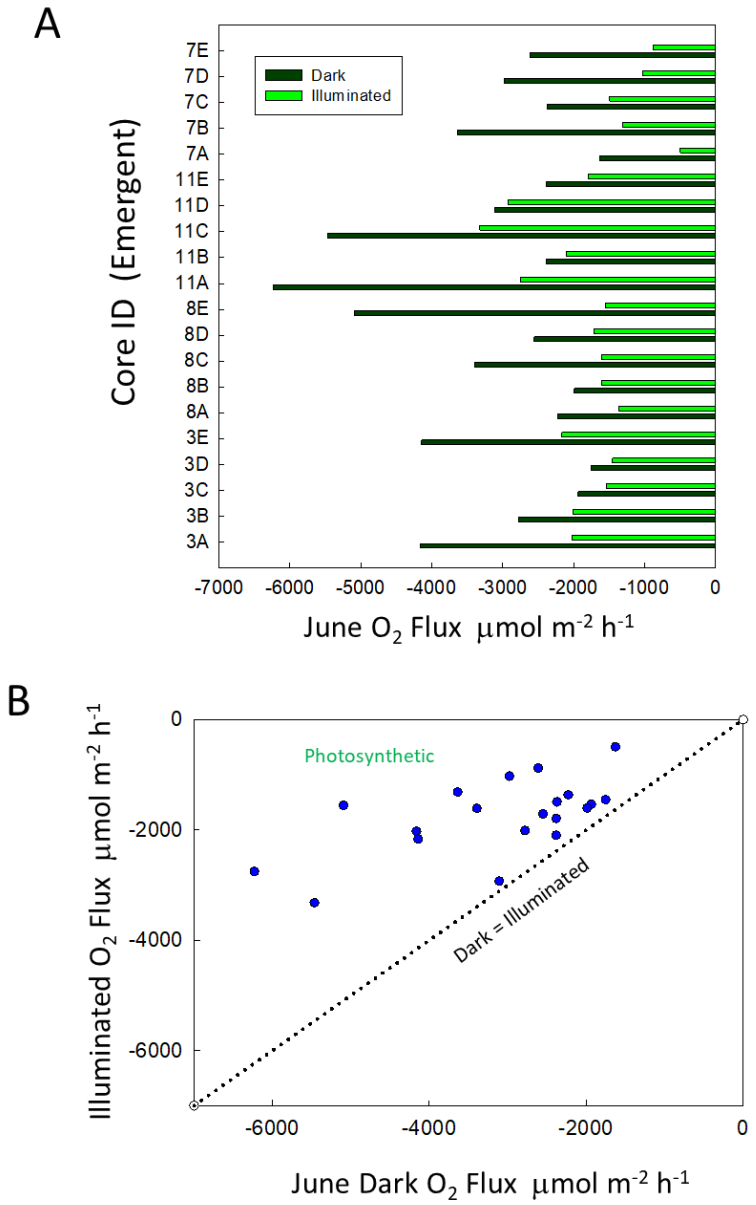

Figure 19. Plots of June dark and illuminated oxygen fluxes for all cores (A), including a plot of dark and illuminated data (B).

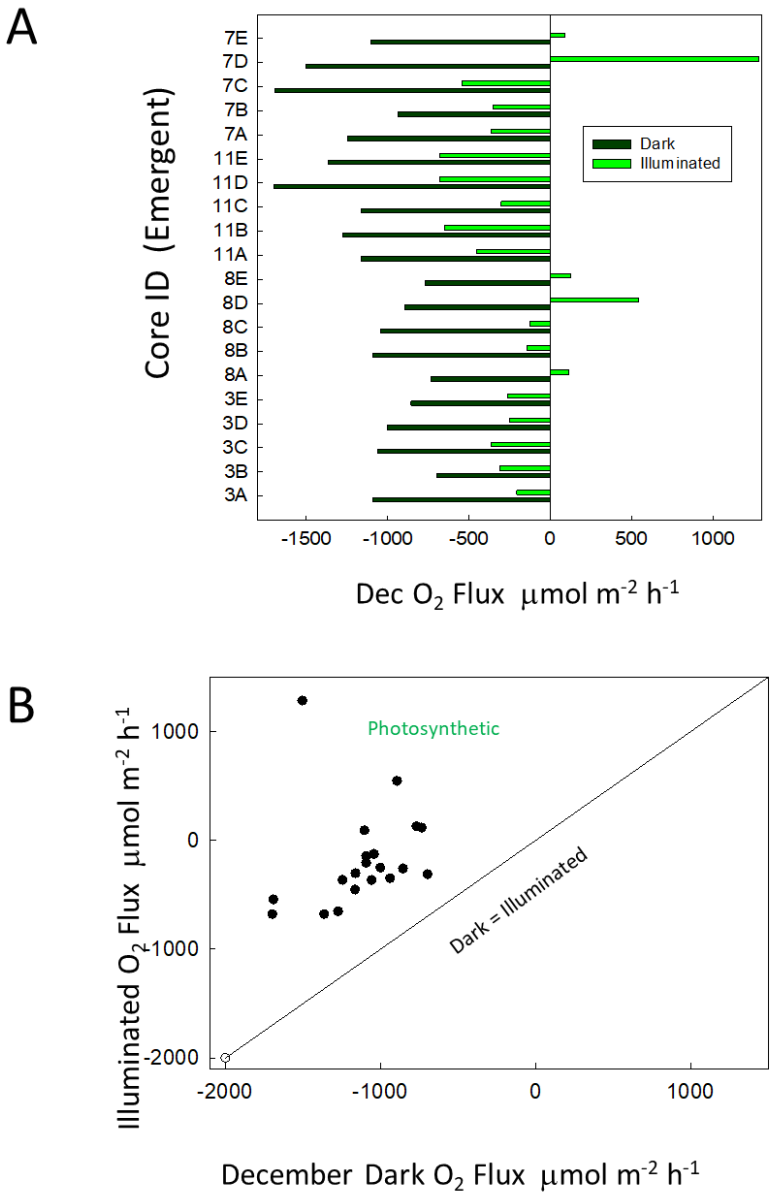

Figure 20. Plots of December dark and illuminated oxygen fluxes for all cores (A), including a plot of dark and illuminated data (B).

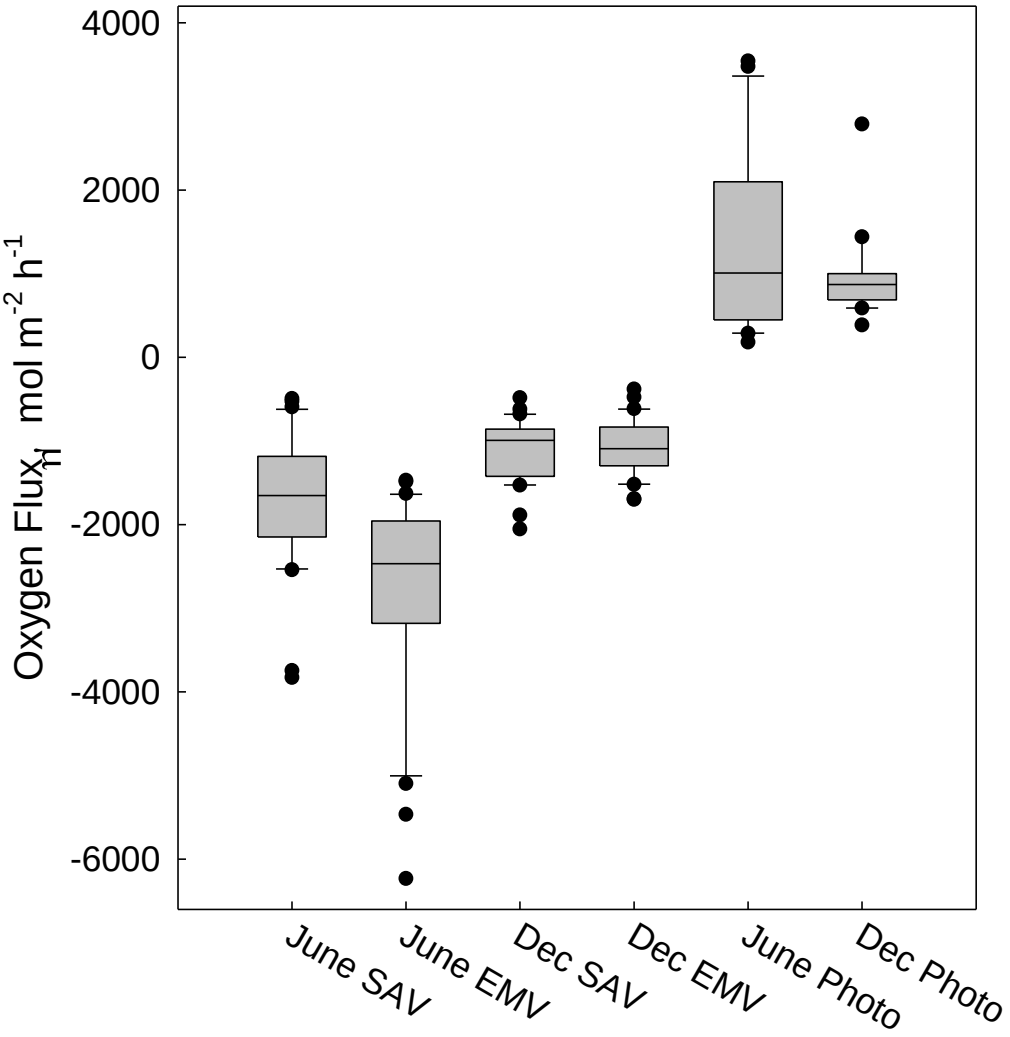

Figure 21. Box plot of all dark SAV and EMV O_2 flux data for June and December. The estimates of photosynthesis, determined by the difference between light and dark oxygen flux rates, are shown in the right two boxes. For the dark data, the June EMV O_2 data were significantly lower ($P < 0.001$; Kruskal-Wallis) than the December SAV or EMV O_2 data. For O_2, this means that the June EMV mesocosms had a higher rate of oxygen uptake.

Ammonium Fluxes

Dark NH_4^+ fluxes were generally directed out of the sediments (Figures 22, 23), with the exception of a small number that, for the most part, had small influxes. The highest efflux rates approached 500 μmol m^{-2} h^{-1}. The average June NH_4^+ flux in SAV tanks was 66.4 ± 13.6 μmol m^{-2} h^{-1} with a median rate of 52.3 μmol m^{-2} h^{-1}. In December, the SAV NH_4^+ fluxes averaged 12.9 ± 38.7 μmol m^{-2} h^{-1}, with a median rate of 33.2 μmol m^{-2} h^{-1}. June and December NH_4^+fluxes in the EMV mesocosms averaged 66.1 ± 63.1 and 34.0 ± 42.9 μmol m^{-2} h^{-1} respectively, with median rates of 68.6 and 19.0 μmol m^{-2} h^{-1}.

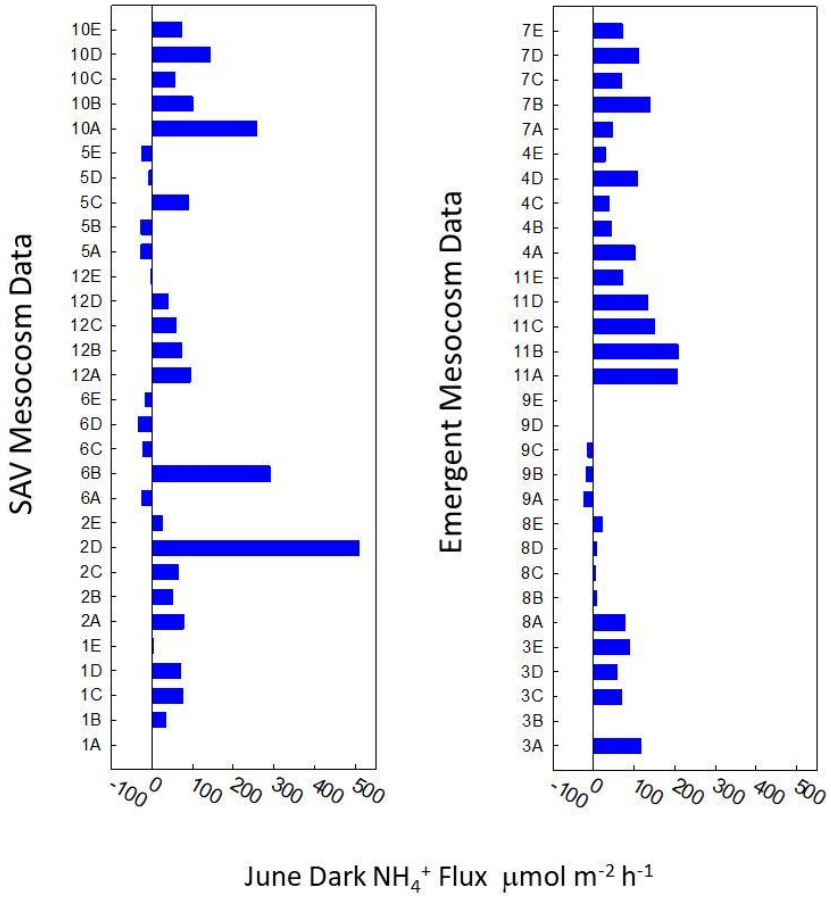

Figure 22. June 2018 NH_4^+ dark flux data.

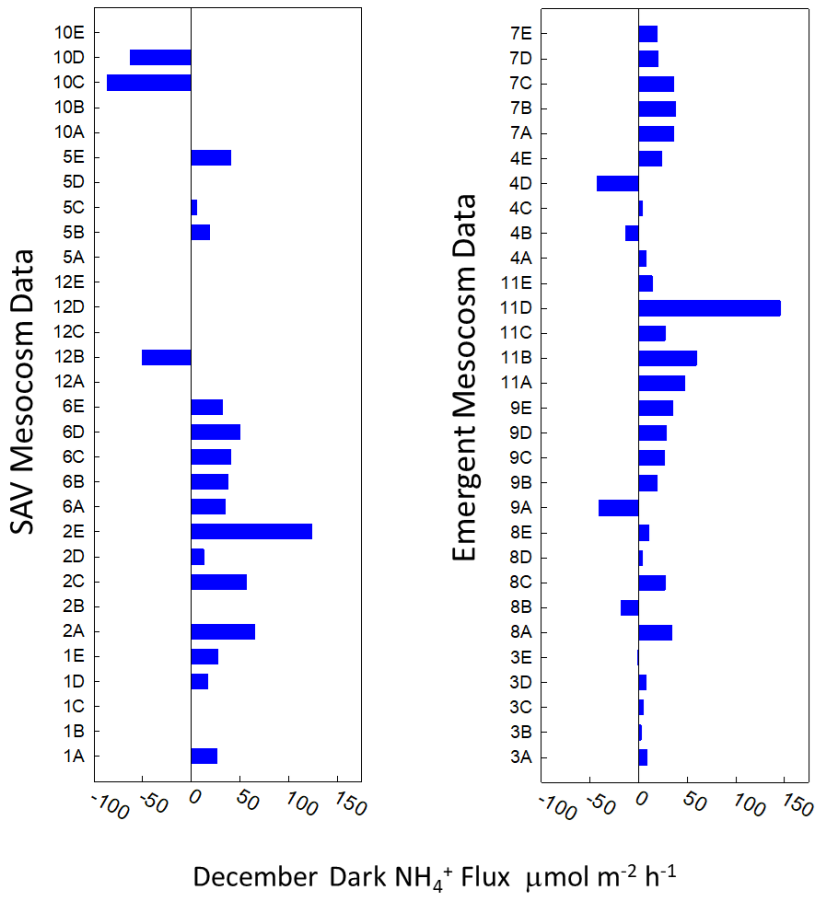

Figure 23. December 2018 NH_4^+ dark flux data.

In most, but not all cases, illumination decreased NH_4^+ fluxes (Figures 24, 25); in December two cores showed substantial increases in ammonium fluxes in the light. In June and December, 10 of 20 cores switched from NH_4^+ efflux to influx. Four cores showing an increased NH_4^+ efflux in the light. Overall, 5 cores in December showed increased efflux, or decreased influx of NH_4^+ under illuminated conditions.

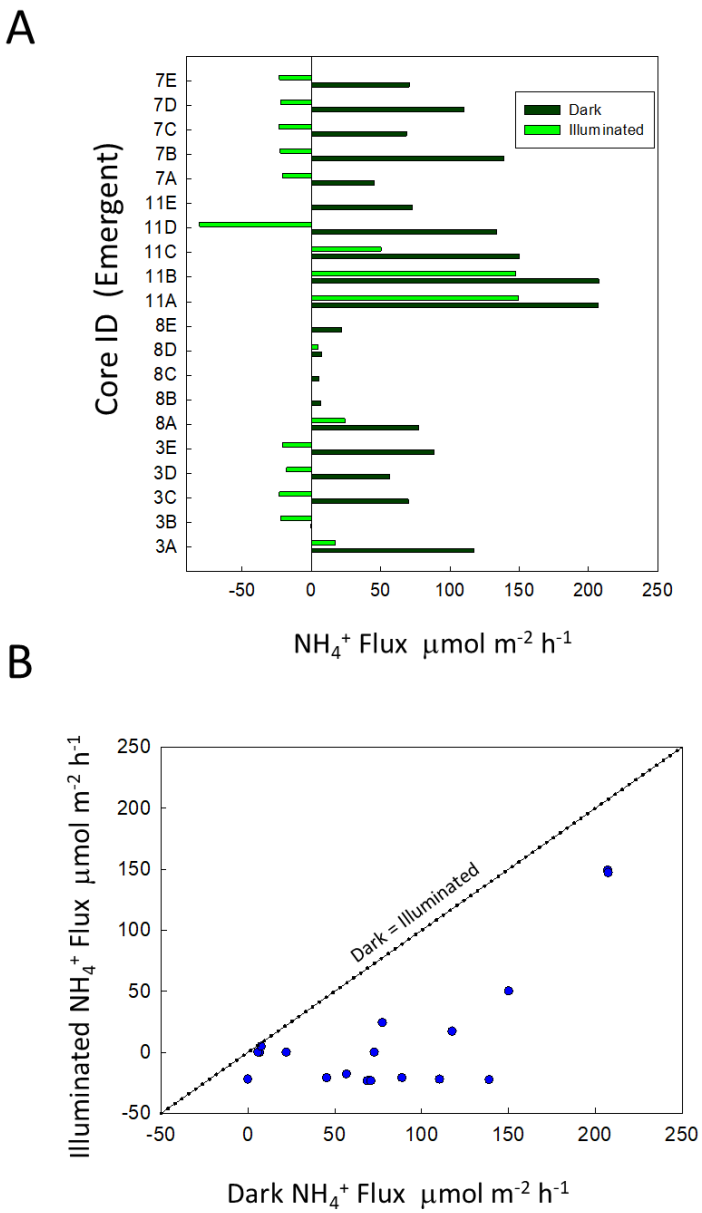

Figure 24. Plots of June dark and illuminated ammonium fluxes for all cores (A), including a plot of dark and illuminated data (B).

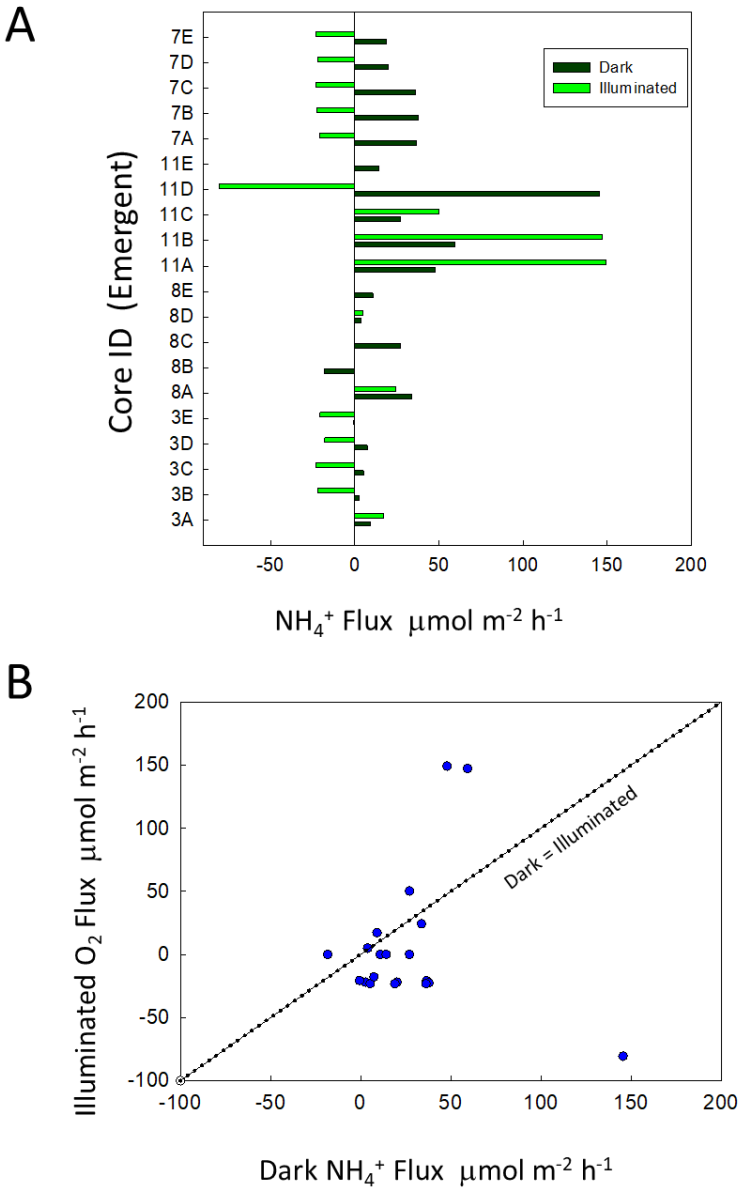

Figure 25. Plots of December dark and illuminated ammonium fluxes for all cores (A), including a plot of dark and illuminated data (B).

Fluxes of Di-Nitrogen

With five exceptions, N_2-N fluxes were directed out of the sediments (Figures 26, 27). There was a high degree of variability within most tanks, particularly in June. Rates in the SAV tanks averaged 61 ± 67 and 31 ± 21 μmol m^{-2} h^{-1} during June and December respectively, with rates in EMV tanks averaging 98±63 and 34 ± 43 μmol m^{-2} h^{-1}.

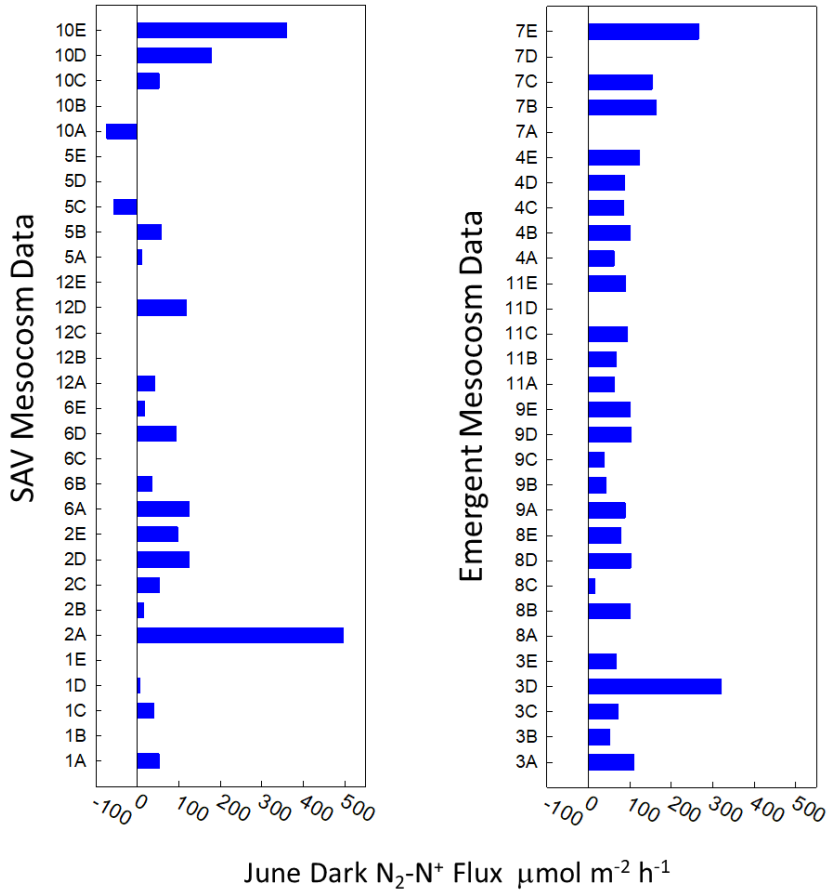

Figure 26. June 2018 N_2-N dark flux data.

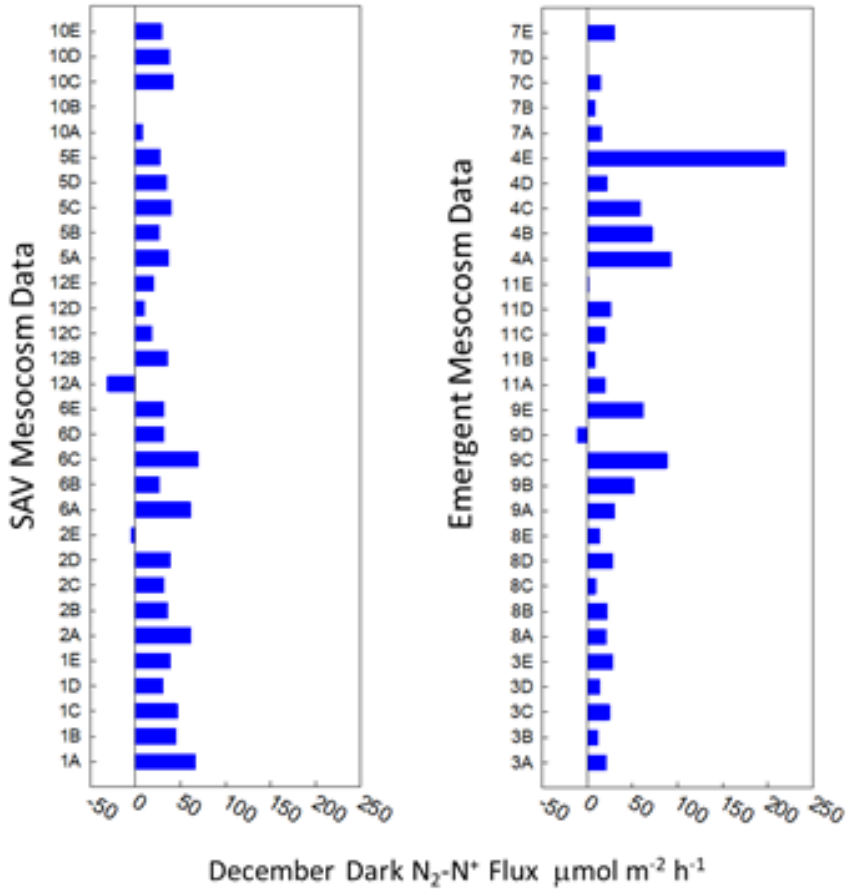

Figure 27. December 2018 N_2-N dark flux data.

With illumination, June observations indicate both increased and decreased denitrification relative to dark incubations (Figure 28). Decreased denitrification can occur with illumination because the regenerated N used for coupled nitrification is used for benthic microalgal photosynthesis, or because water column nitrate is taken up by algae. Increased denitrification in the light is usually less common in the literature. In contrast, December denitrification rates were usually suppressed by benthic photosynthesis, with most illuminated rates being very low (Figure 29).

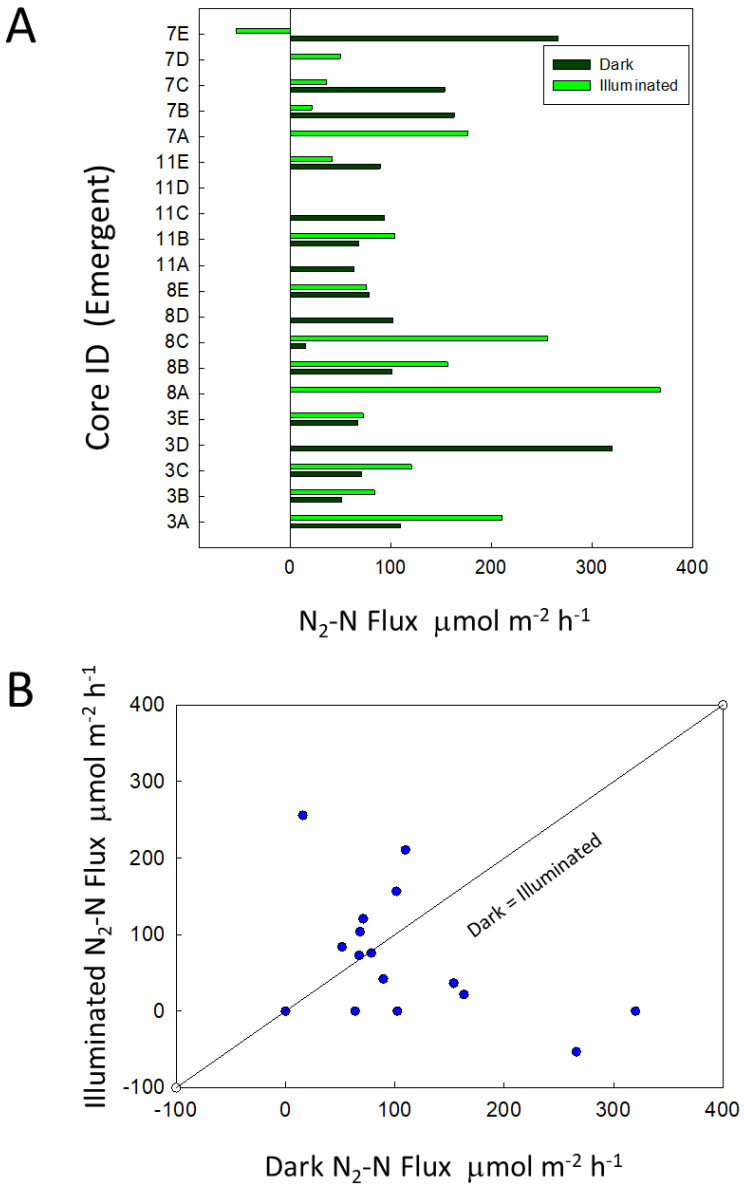

Figure 28. Plots of June dark and illuminated N_2-N fluxes for all cores (A), including a plot of dark and illuminated data (B).

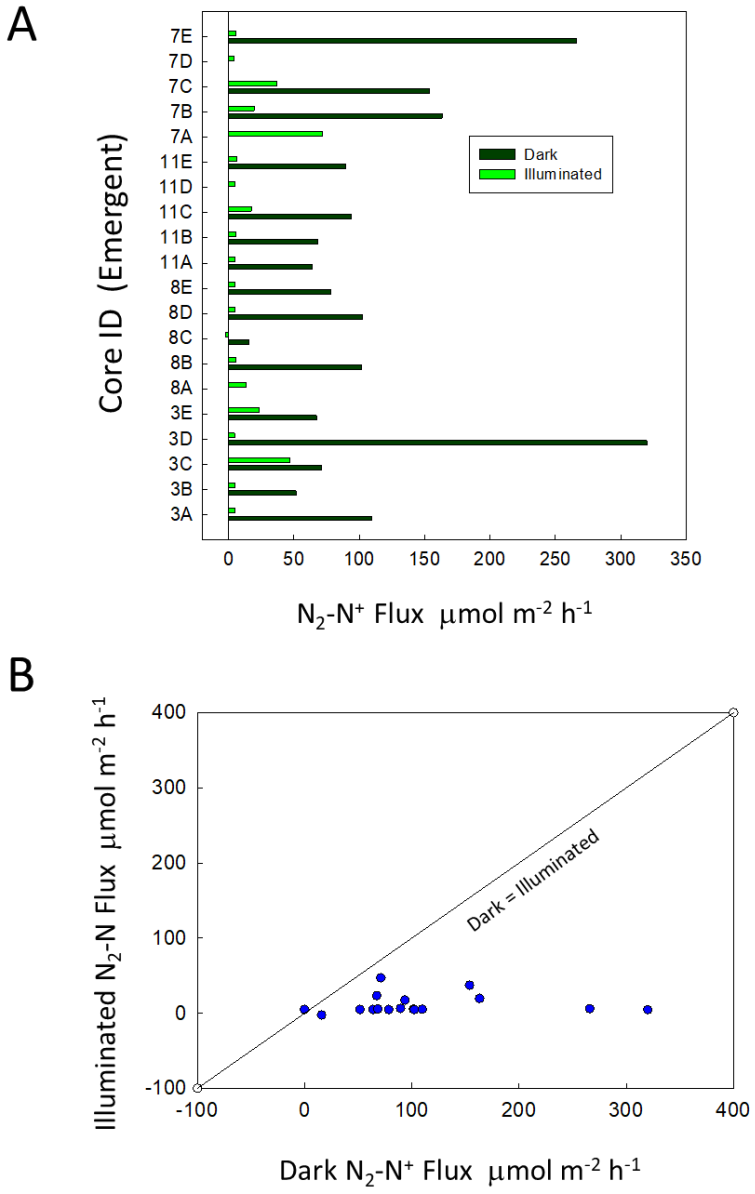

Figure 29. Plots of December dark and illuminated N_2-N fluxes for all cores (A), including a plot of dark and illuminated data (B).

Nitrate + Nitrite Fluxes

The flux of NO_x^- was often very low, with very few effluxes. In June, SAV and EMV NO_x^- flux rates averaged -41 ± 34 and -50 ± 55 μmol m^{-2} h^{-1} respectively (Figure 30). In December, SAV and EMV NO_x^- flux rates averaged -13 ± 10 and -4 ± 7 μmol m^{-2} h^{-1} respectively (Figure 31). The EMV tanks in December had 9 effluxes of NO_x^- while only 3 effluxes in all other treatments and times. This suggests that in some cores, nitrification is taking place at a rate in which denitrification cannot consume all of the nitrate.

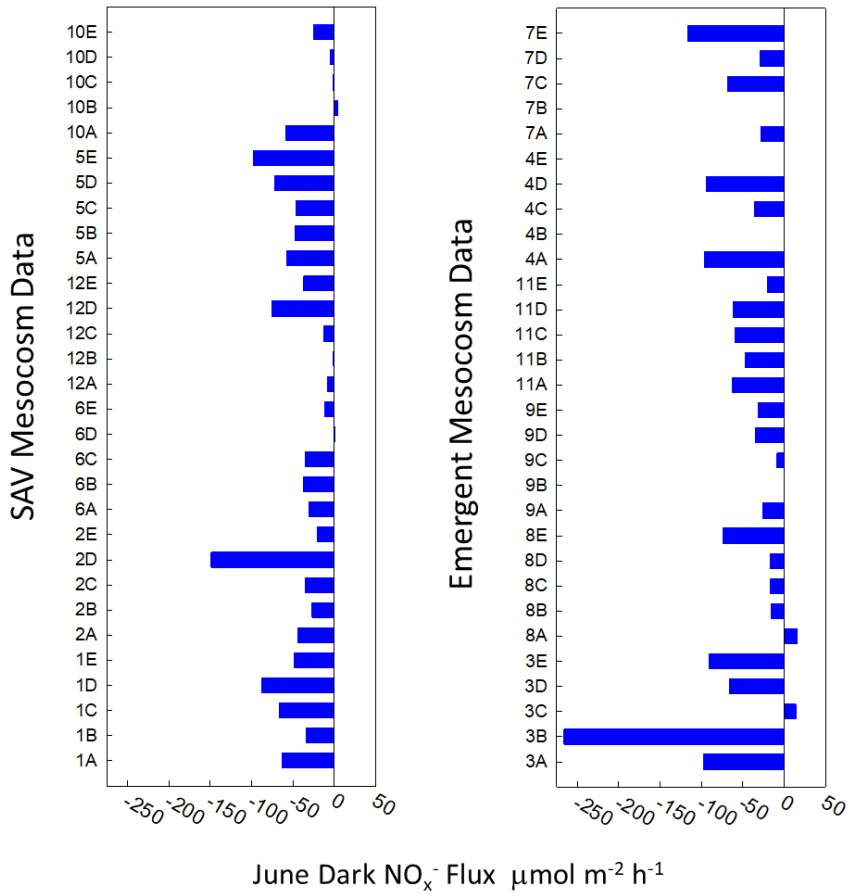

Figure 30. June 2018 NO_x^- dark flux data

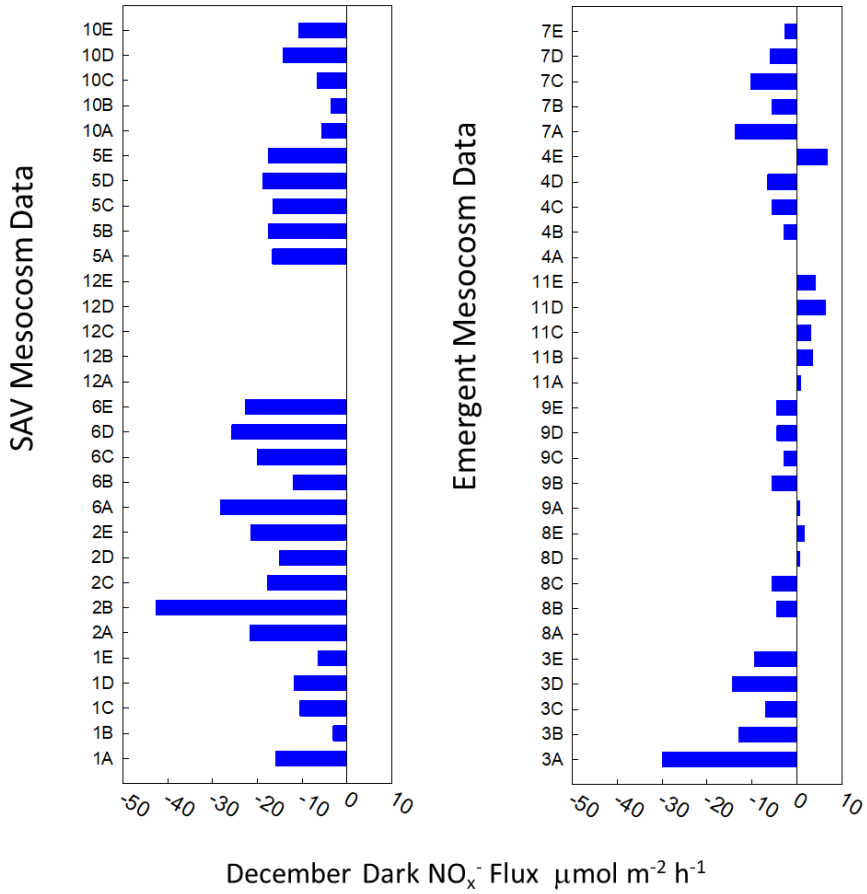

Figure 31. December 2018 NO_x^- dark flux data

Unlike O_2, N_2-N and NH_4^+ fluxes, the changes in NO_x^- fluxes with illumination were not unidirectional; with 59% of fluxes having increases with illumination in June (Figure 32). In December, 37% of cores had increased fluxes, 37% had decreased fluxes, and the remainder did not change (Figure 33).

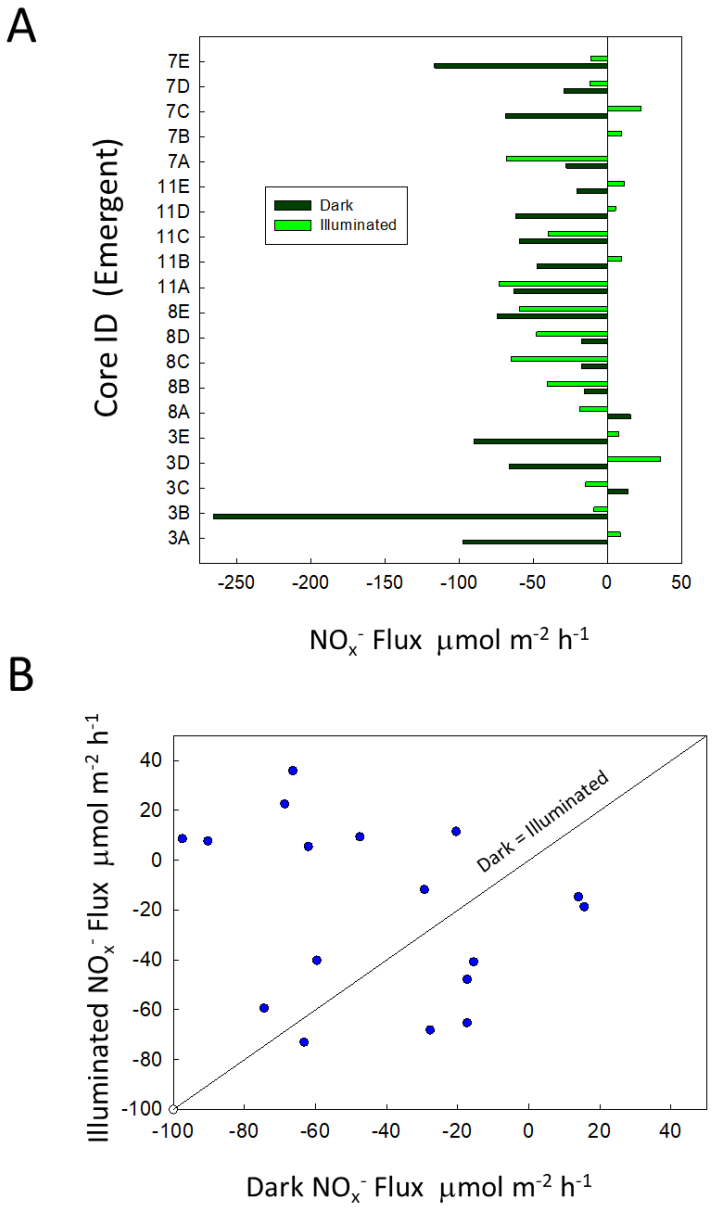

Figure 32. Plots of June dark and illuminated NO_x^- fluxes for all cores (A), including a plot of dark and illuminated data (B).

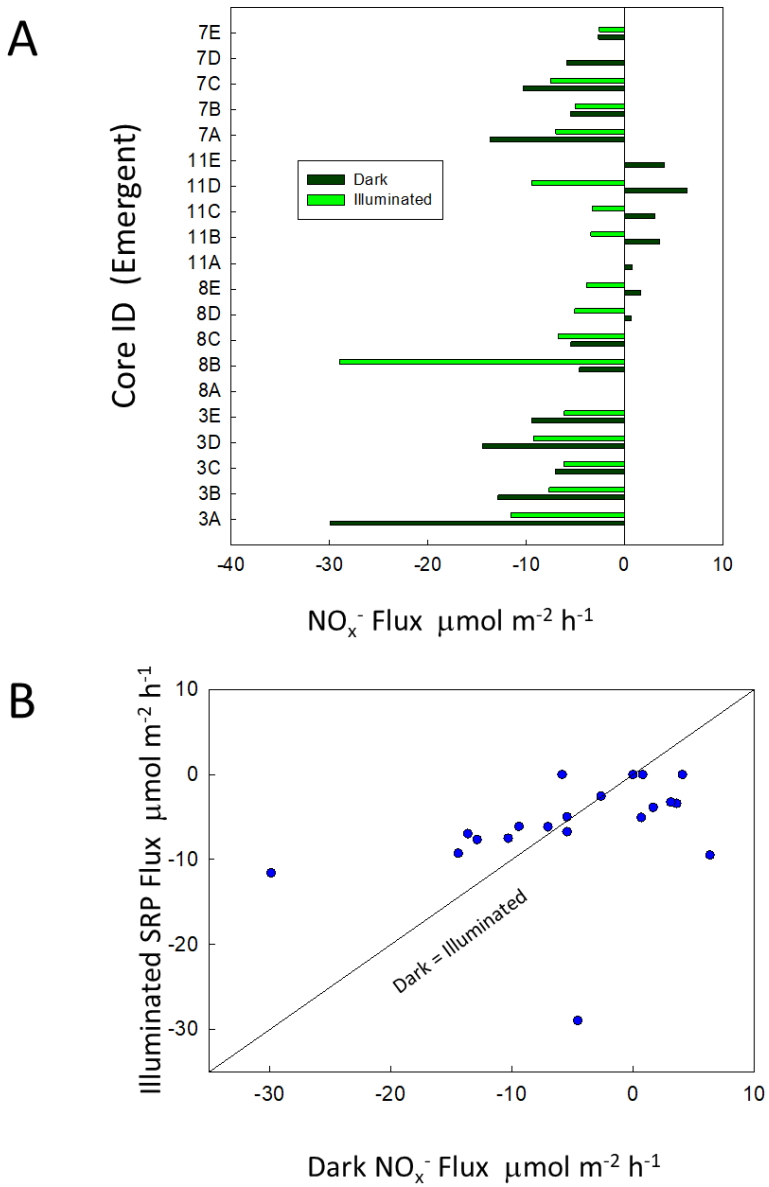

Figure 33. Plots of December dark and illuminated NO_x^- fluxes for all cores (A), including a plot of dark and illuminated data (B).

Dissolved Organic Nitrogen Fluxes

The fluxes of DON were highly variable and directed both into and out of sediments (Figures 34, 35). In many studies (Cowan and Boynton 1996), simple interpretations of DON fluxes are difficult. In this work, we observed 15 of 60 June dark incubations had non-interpretable flux time courses, decreasing to 6 of 60 in December. Under illumination, 2 of 20 and 6 of 20 time course in June and December respectively were not interpretable (Figures 36, 37). In June, illumination resulted in mostly lower effluxes of DON, while results were mixed in December.

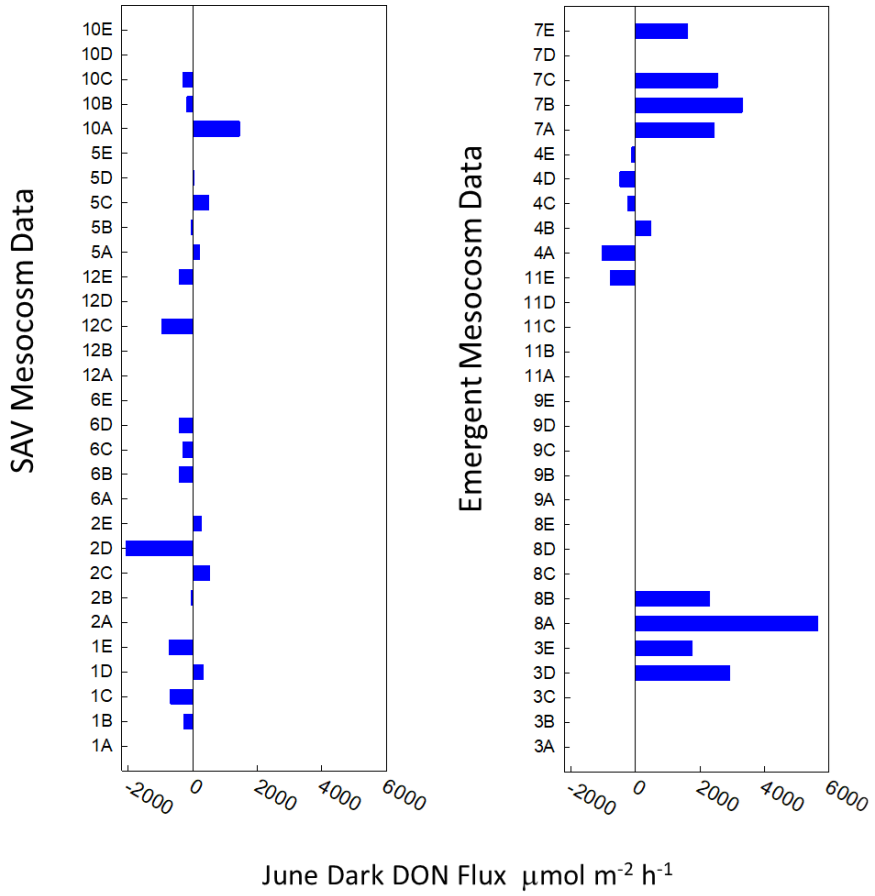

Figure 34. June 2018 DON dark flux data

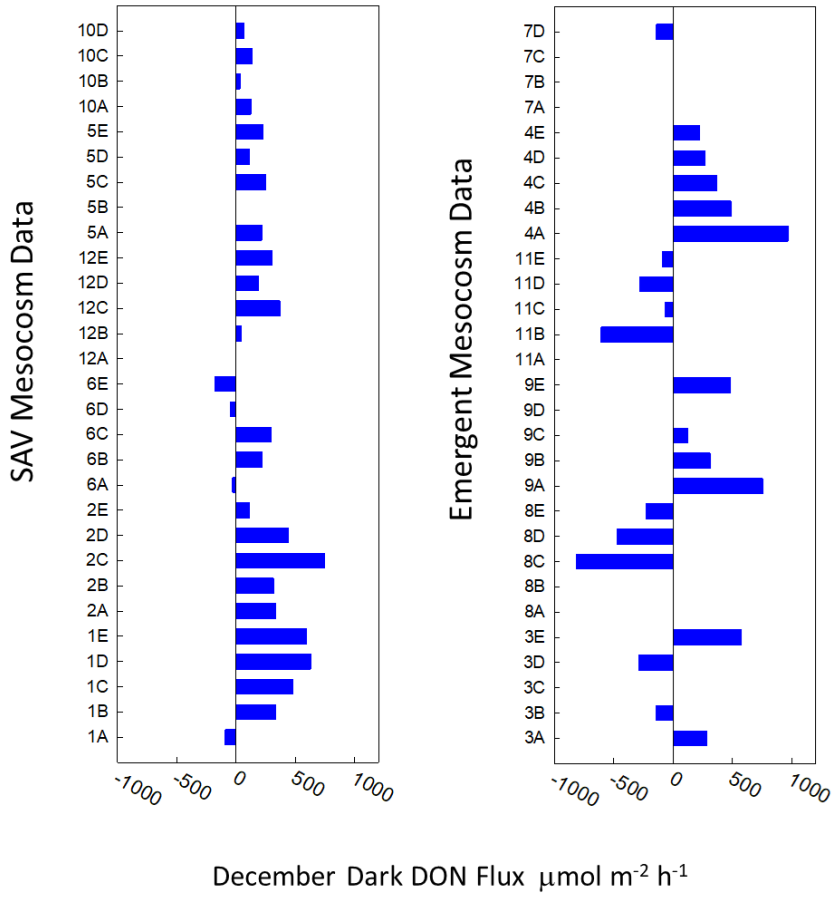

Figure 35. December 2018 DON dark flux data

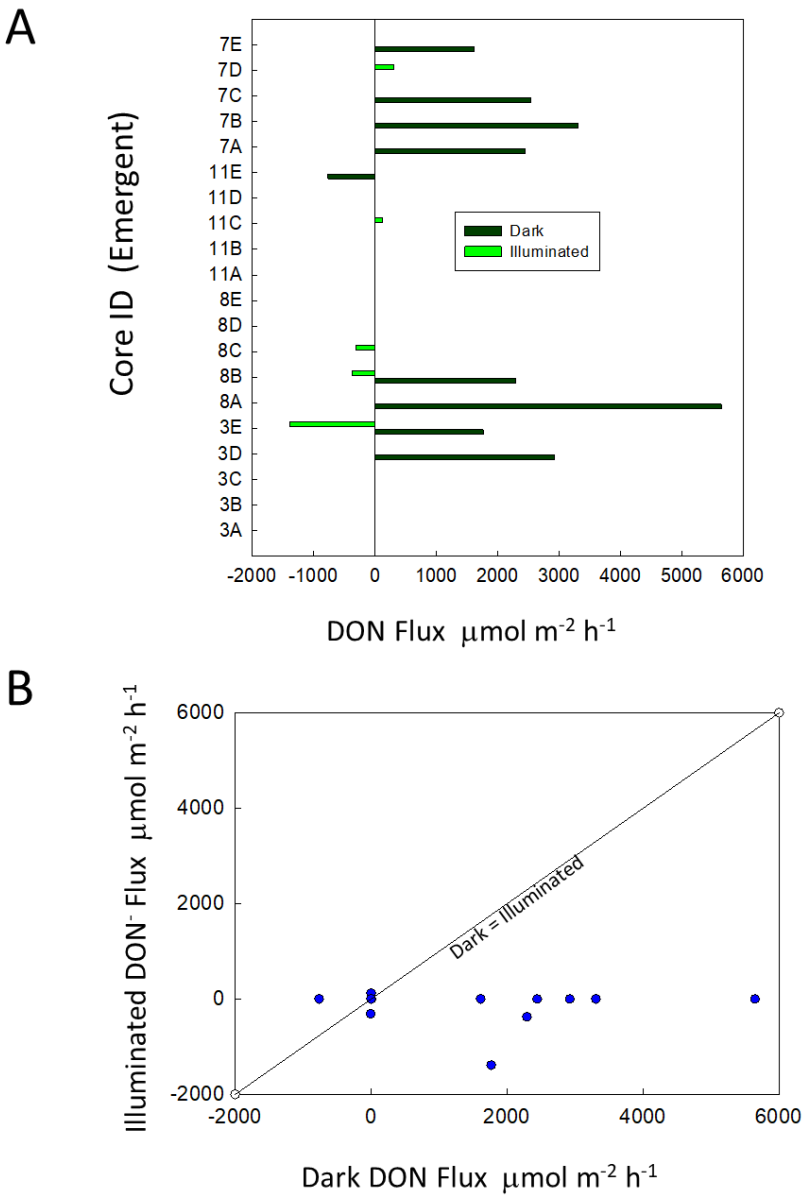

Figure 36. Plots of June dark and illuminated DON fluxes for all cores (A), including a plot of dark and illuminated data (B).

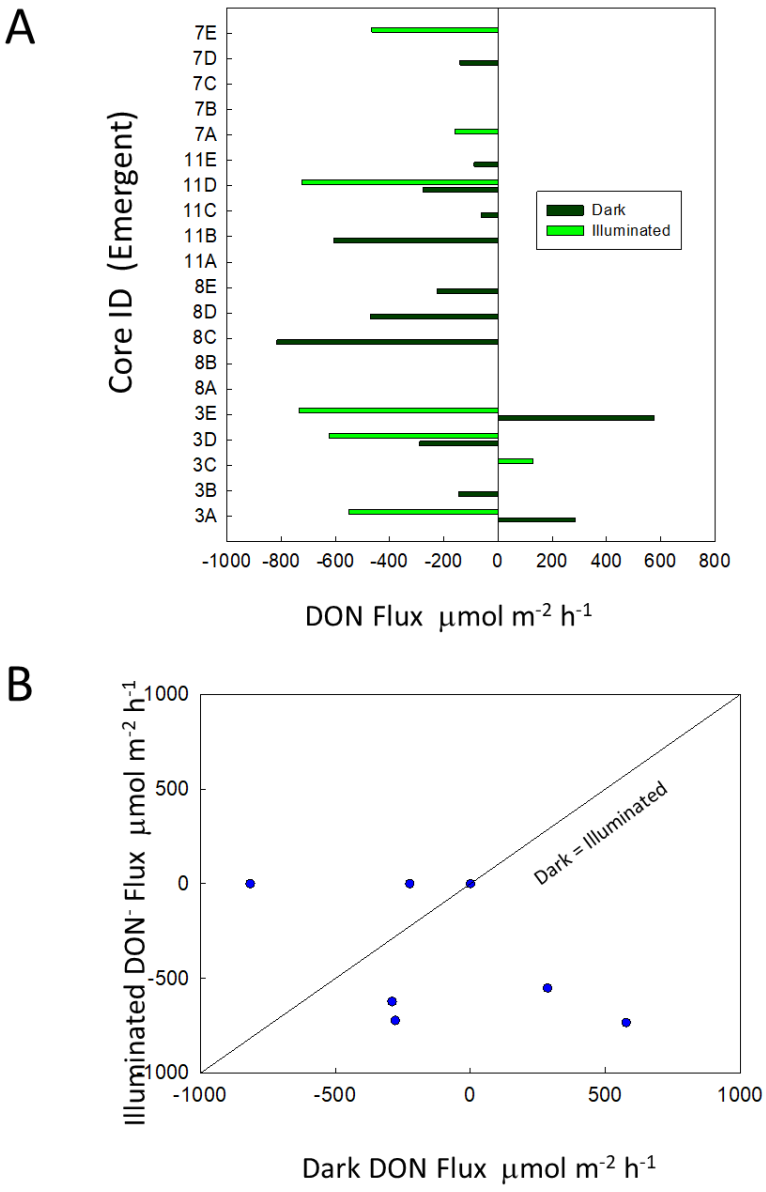

Figure 37. Plots of December dark and illuminated DON fluxes for all cores (A), including a plot of dark and illuminated data (B).

Soluble Reactive Phosphorus Fluxes

With few exceptions, sediments in these mesocosms were not a source of soluble reactive P to the water column (Figures 38, 39). Average flux rates were -22 ± 19, -31 ± 30, -1.9 ± 2.4, and -0.6 ± 2.0 µmol m^{-2} $h^{-1}$for June SAV, June EMV, December SAV and December EMV. The effect of light on SRP fluxes in June was mixed, with some increases and a lot of decreases relative to dark fluxes (Figure 40), while in December most fluxes had only minor changes with illumination (Figure 41).

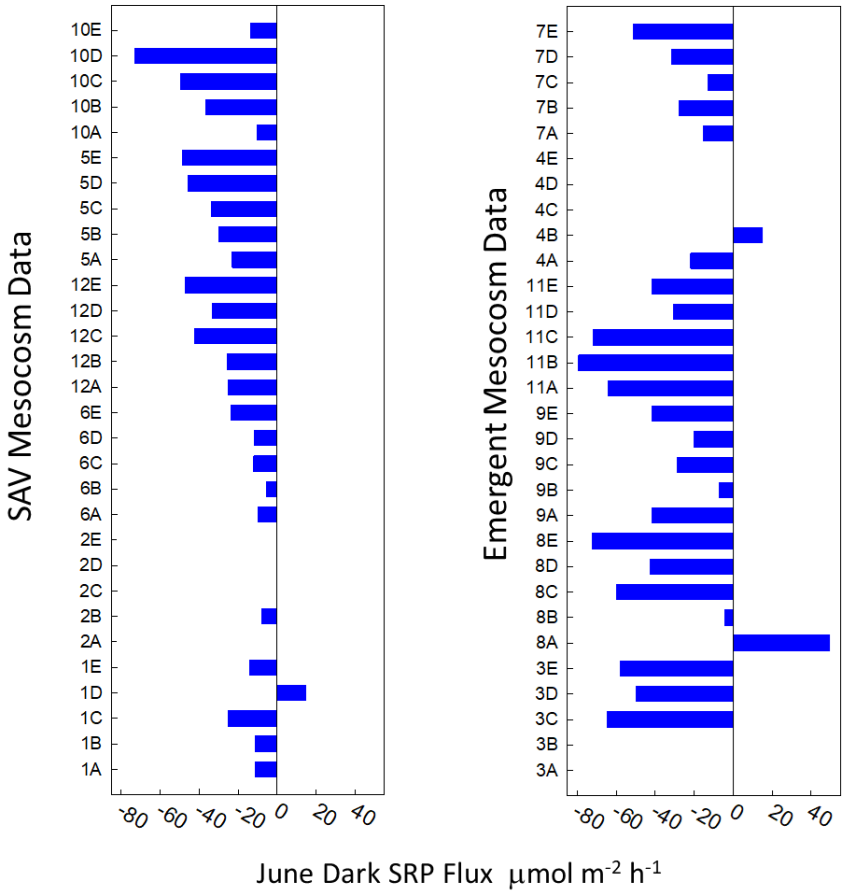

Figure 38. June 2018 SRP dark flux data.

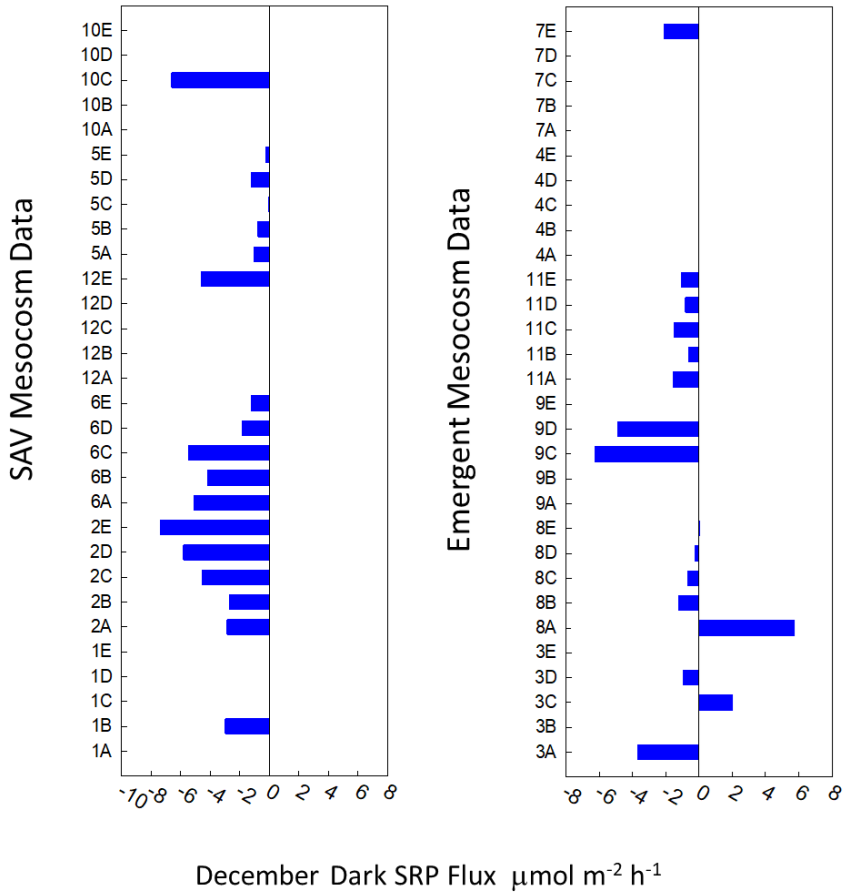

Figure 39. December 2018 SRP dark flux data.

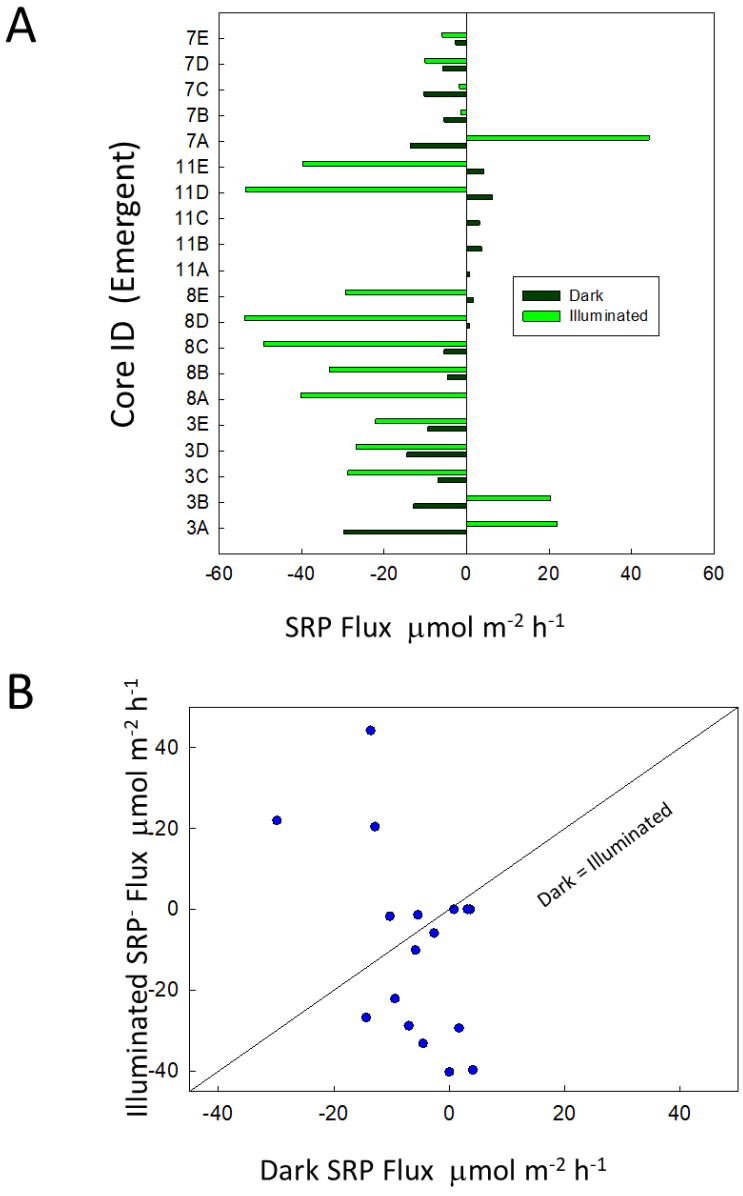

Figure 40. Plots of June dark and illuminated SRP fluxes for all cores (A), including a plot of dark and illuminated data (B).

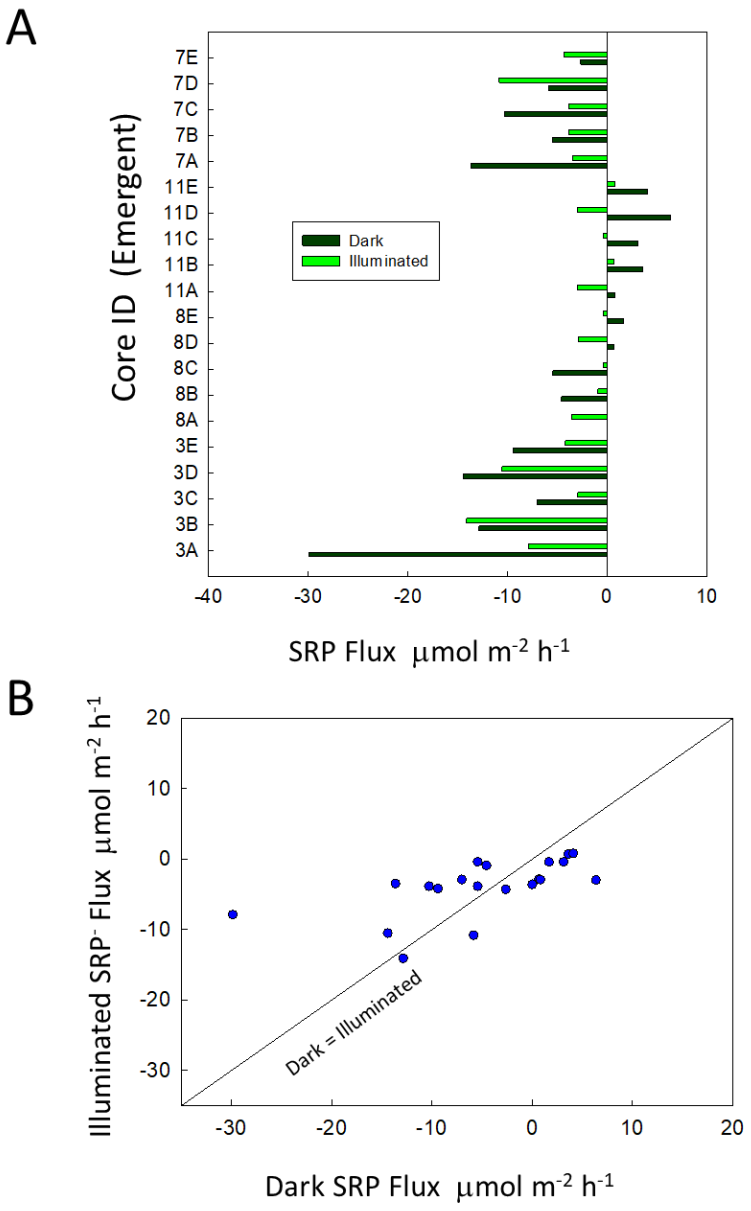

Figure 41. Plots of December dark and illuminated SRP fluxes for all cores (A), including a plot of dark and illuminated data (B).

Statistical Analyses - Fluxes

In the previous section, statistical analyses have been used largely at the descriptive level to help characterize the data. The data has been examined largely by considering EMV versus SAV comparisons without examination of treatment effects. Here we examine the various treatments with a goal of informing SFWMD which treatments are most effective at removing nitrogen from the mesocosms. The experiments break down to 8 different treatments that are shown in Table 9. We use the daily units of sediment-water exchange (mg m^{-2} d^{-1}) to make the extrapolation to mass numbers easier and to combine the light and dark data into single numbers. This analysis is restricted to N_2-N, O_2 and NH_4^+, the most important fluxes within these mesocosms.

For one way ANOVA's, we used the categories from Table 9 and compared all treatments and times (Figure 42). The sediment-water exchange rates within each grouping were not normally distributed, all failing the normality test (Shapiro-Wilk; $P < 0.050$). Thus the comparison was made on ranks. All pairwise comparisons were made and there was insufficient statistical power in this data set to identify any significant differences. High variability reduced the power of tests of inference to detect statistically significant differences; with high within-group variability, larger among-group differences were needed for statistical significance.

A one way ANOVA on O_2 showed most pairwise comparisons were generally not testable, with the only significant results showing that EM1 in December was significantly lower than June rates in EM2, EM3, EM4 and SAV3. With N_2, high variability within a treatment hindered comparison. For NH_4^+, the only significance was the SAV4 in June was higher than SAV3 and SAV4 in December.

As with the oxygen, one way ANOVA on N_2-N daily fluxes showed no pairwise differences, although as with oxygen, almost all comparisons were not testable. For NH_4^+ a significant pairwise difference was observed between June and December data for the category EM1 (native sand, HLR = 1.5), with June NH_4^+ effluxes higher than December. For nitrate (data not shown), the only pairwise difference was between the categories June SAV3 and August EM2; this difference has little relevance to this study.

Overall, the key response variable for this project was the flux of N_2-N. There were no simple statistical relationships between vegetation types, flow regime, or sediment treatments.

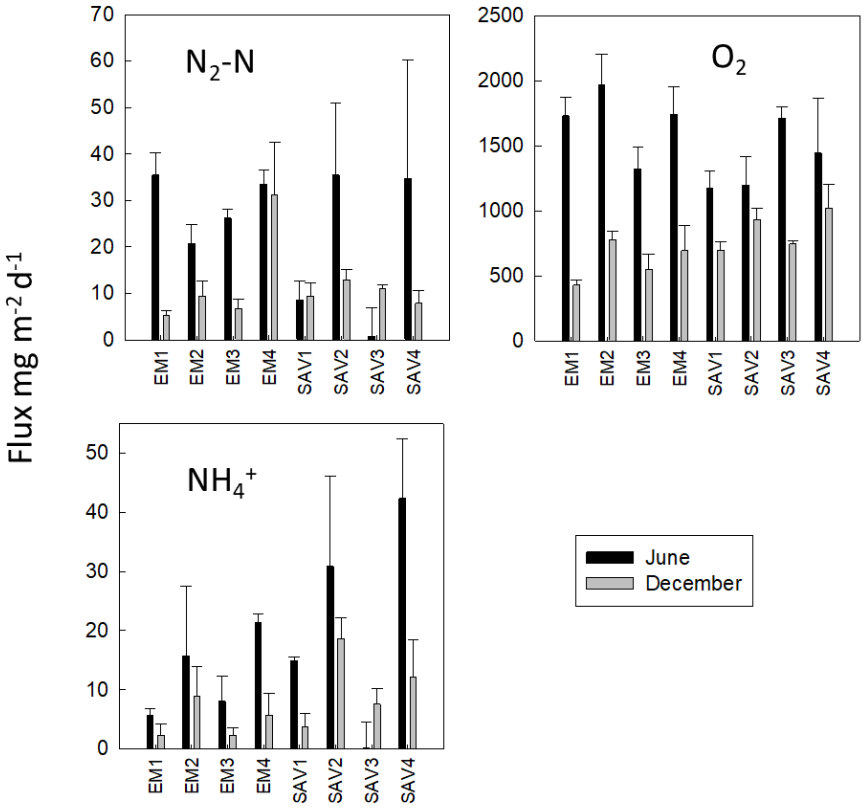

Figure 42. Mean (± S.E.) sediment-water exchange rates for each of the treatment types in Table 9. There are 10 data points represented in EM1, EM2, SAV1 and SAV2, with 5 data points in the remainder.

Discussion

Nitrogen Summary

In Table 11 and Figure 43, summary statistics and box plots of all the N data are presented. The potential remineralization rate of particulate N, estimated from C:N stoichiometry and the oxygen flux, is presented in Table 11 as "N Remin". The oxygen flux is assumed to be equivalent to a dissolved inorganic carbon flux, and N remineralization is 1/13 of the oxygen flux:

Equation 7

N Remin (μmol m^{-2} h^{-1}) = - O_2 flux (μmol m^{-2} h^{-1}) / 13 (13 is the sediment C:N ratio)

The remineralization rates are generally higher than the sum of the N fluxes, suggesting a net sink of dissolved N in the sediments.

Table 11. Collated dark N fluxes. Nitrogen remineralization (N Remin) is estimated from oxygen fluxes, using an average sediment C:N ratio of 13.0 derived from these mesocosms. This assumes that material of this composition is remineralized, that oxygen is an excellent proxy for carbon remineralization, and that both methanogenesis and sulfate reduction are minimal.

Date	Type	Analyte	Mean	Std Dev	Std Error	Max	Min	Median
2018			μmol m^{-2} h^{-1}					
June	SAV	N_2-N	61.3	115.0	21.0	496.9	-73.6	25.6
June	SAV	NH_4^+	66.4	113.6	20.7	510.0	-33.4	52.3
June	SAV	NO_x^-	-41.0	33.8	6.2	3.9	-148.9	-36.3
June	SAV	N Remin	131.8	61.6				
June	EMV	N_2-N	98.3	67.0	12.9	320.1	0.0	89.2
June	EMV	NH_4^+	66.1	63.1	11.7	207.3	-22.8	68.6
June	EMV	NO_x^-	-49.6	55.0	10.2	15.6	-265.9	-34.4
June	EMV	N Remin	216.7	91.4				
December	SAV	N_2-N	31.5	21.0	3.8	69.4	-31.0	33.2
December	SAV	NH_4^+	12.9	38.7	7.1	123.6	-86.8	2.8
December	SAV	NO_x^-	-13.4	10.0	1.8	0.0	-42.6	-14.6
December	SAV	N Remin	83.9	28.4				
December	EMV	N_2-N	34.0	42.9	7.8	219.0	-10.7	21.3
December	EMV	NH_4^+	19.1	33.1	6.0	145.6	-42.6	19.0
December	EMV	NO_x^-	-4.2	7.4	1.3	6.8	-29.9	-4.4
December	EMV	N Remin	82.3	26.2				

For the nitrogen balance, Figure 43 provides a good summary of all observations:

- Overall, fluxes of N_2-N and NH_4^+ are the major effluxes of N in these experimental ecosystems and had relatively similar rates. The flux of ammonium represents the only recycling of sediment N that could result in the production of algae.
- Denitrification is a major part of the sediment N cycle.
- Nitrate uptake is a general feature of these mesocosms.
- Although variability masks differences from a statistical viewpoint, there are seasonal decreases from June to December in rates of metabolism and N recycling.

Denitrification was not a simple function of sediment oxygen uptake, or sediment metabolism. There were no significant relationships between sediment oxygen demand and denitrification (Figure 44). The term sediment oxygen demand uses oxygen consumption by sediments as a positive value, enhancing visualization.

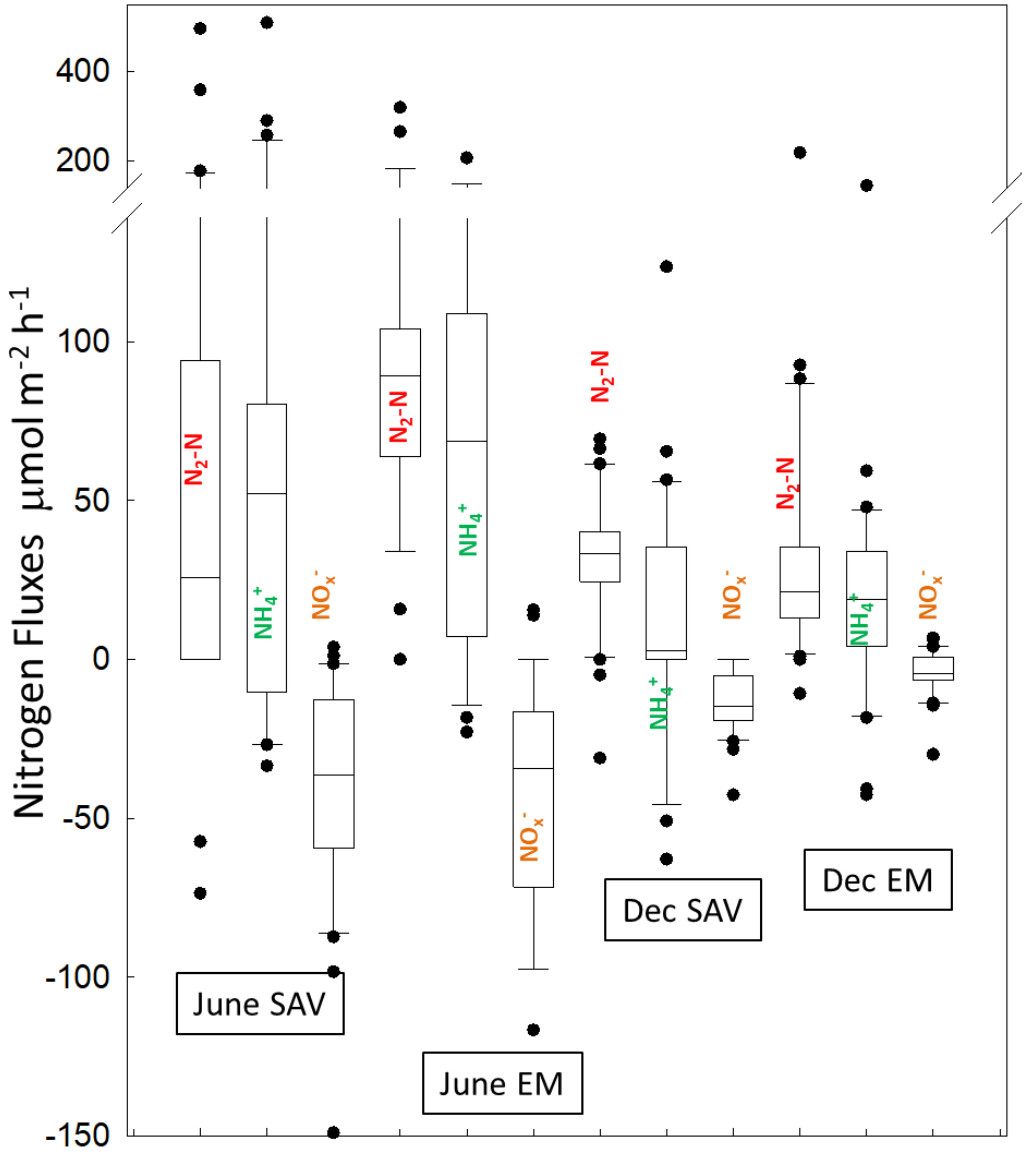

Figure 43. Box plots of all dark N fluxes. Note that some of the most negative rates (outliers) were not included to allow better visualization of the data. Using a Kruskall-Wallis one way analysis on ranks, significance was generally found only between the NO_x^- fluxes and the N_2-N and NH_4^+ fluxes. The denitrification data was not significantly different by treatment or time. The ammonium data were not significantly different by treatment or time.

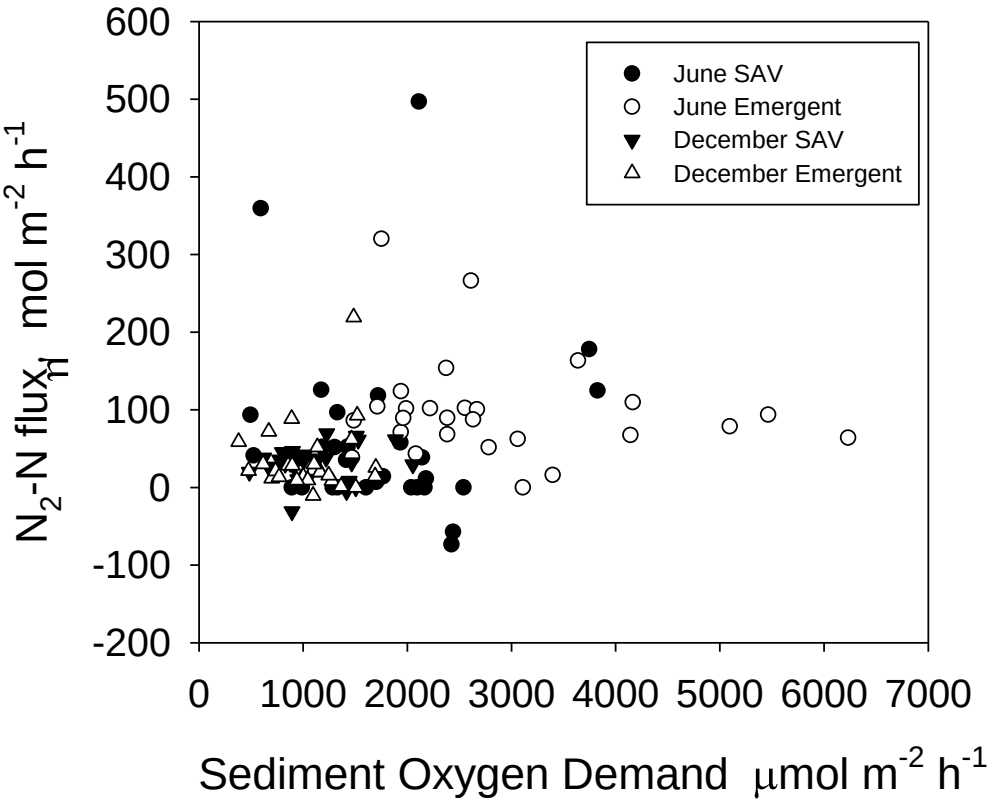

Figure 44. Plot of N_2-N flux versus oxygen demand for June and December SAV and EMV data. No significant relationship was observed. Note that sediment oxygen demand is the opposite sign of sediment flux, making oxygen uptake a positive term.

Does Light at the Sediment Surface Matter?

Measurements of sediment-water exchange generally are carried out using dark incubations similar to those used in our dark-only incubations. Even in shallow water habitats, the effects of illumination are often not assessed (Gardner and Mccarthy 2009; Hopfensperger et al. 2009; Merrill and Cornwell 2000; Piehler and Smyth 2011). The competition between autotrophs and microbes for ammonium can result in changes in nutrient fluxes and denitrification (Risgaard-Petersen 2003)

The effects of benthic microalgae and other photosynthetic communities at the sediment water interface can have a large impact on estimation of the net ecosystem effect of sediments (Cornwell et al. 2014; Cornwell et al. 2008; Sundback et al. 2000). The oxygen flux data show the instantaneous effect of benthic algal production on net fluxes. If we examine the effect on a daily basis the effects are more fairly compared. Daily rates are estimated by multiplying the daylight hours by illuminated flux rates, plus the night time duration multiplied by the dark rate. In Figure 45, plots A and B illustrate the effect of including illuminated incubations versus non-inclusion. Plot C shows a plot of the more-correct dark-light approach with a dark only oxygen flux. For all project observations, the daily net sediment oxygen flux for dark-light incubations is 70 ± 15 % of light incubations. This is a substantial correction.

The daily ammonium effluxes decreased when light incubations are included (Figure 46). When proper accounting of illuminated conditions was included, daily June and December dark-light rate estimates were 46 and 72 % of dark only incubations.

Using the same approach as for oxygen, the daily fluxes of N_2-N (Table 12; Figure 47) showed a consistent decrease when comparing the dark-light incubations to dark only incubations. June and December light-dark fluxes of N_2-N were 80 and 94% of dark only incubations.

The daily NO_x^- influx estimates increased substantially in June when dark-light incubations are compared to dark only incubations, decreasing to 55% of the dark rate (Figure 48). During December, no differences were evident.

The key point of this examination of approaches is that illumination matters and the net balance of nitrogen and oxygen within these experimental systems requires this more thorough approach. When sediments are not illuminated in the tanks, these dark-light incubations are not necessary.

Table 12. Daily rates of nitrogen fluxes, comparing dark only to dark + light incubations.

		Mean	Std Dev	Std. Error	Max	Min	Median
		mmol m^{-2} d^{-1}					
N_2-N	June Dark	2.56	1.96	0.48	7.68	0.00	2.15
	June Dark + Light	2.07	1.07	0.27	4.02	0.00	1.97
	December Dark	0.40	0.21	0.05	0.72	0.00	0.42
	December Dark + Light	0.38	0.24	0.05	0.96	0.05	0.35
NH_4^+	June Dark	1.99	1.50	0.34	4.98	0.00	1.72
	June Dark + Light	0.92	1.24	0.28	4.17	-0.31	0.39
	December Dark	0.63	0.81	0.18	3.49	-0.44	0.47
	December Dark + Light	0.46	0.85	0.19	3.39	-0.73	0.29
NO_x^-	June Dark	-1.60	1.52	0.38	0.33	-6.38	-1.50
	June Dark + Light	-0.89	0.74	0.19	-0.05	-2.83	-0.81
	December Dark	-0.12	0.21	0.05	0.15	-0.72	-0.12
	December Dark + Light	-0.13	0.15	0.03	0.06	-0.53	-0.10

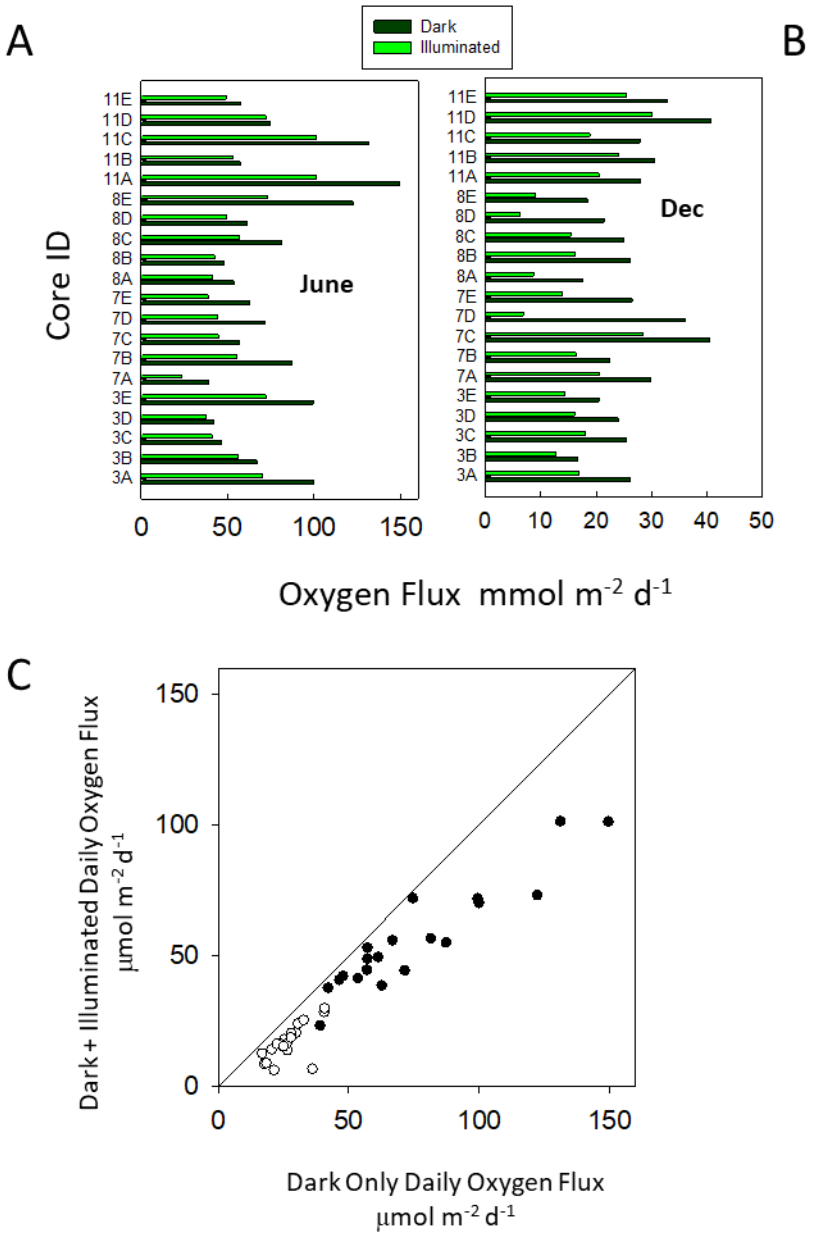

Figure 45. Daily oxygen demand showing differences when illuminated incubations are included. Dark rates and dark + illuminated rates are presented as bar plots in panel A (June) and panel B (December). In panel C, dark+ illuminated rates are plotted versus rates using only dark data. The dark symbols are from June, the open symbols are from December.

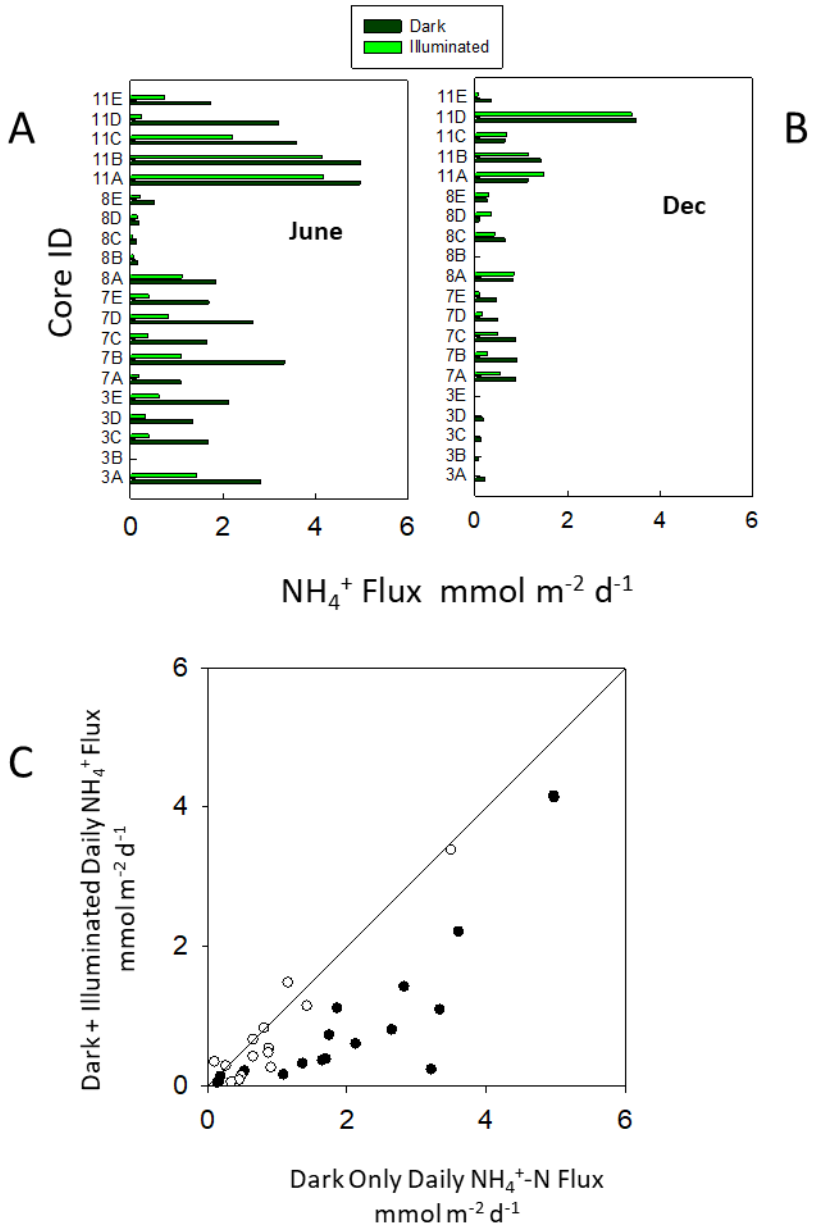

Figure 46. Daily ammonium fluxes showing differences when illuminated incubations are included. Dark rates and dark + illuminated rates are presented as bar plots in panel A (June) and panel B (December). In panel C, dark+ illuminated rates are plotted versus rates using only dark data. The dark symbols are from June, the open symbols are from December.

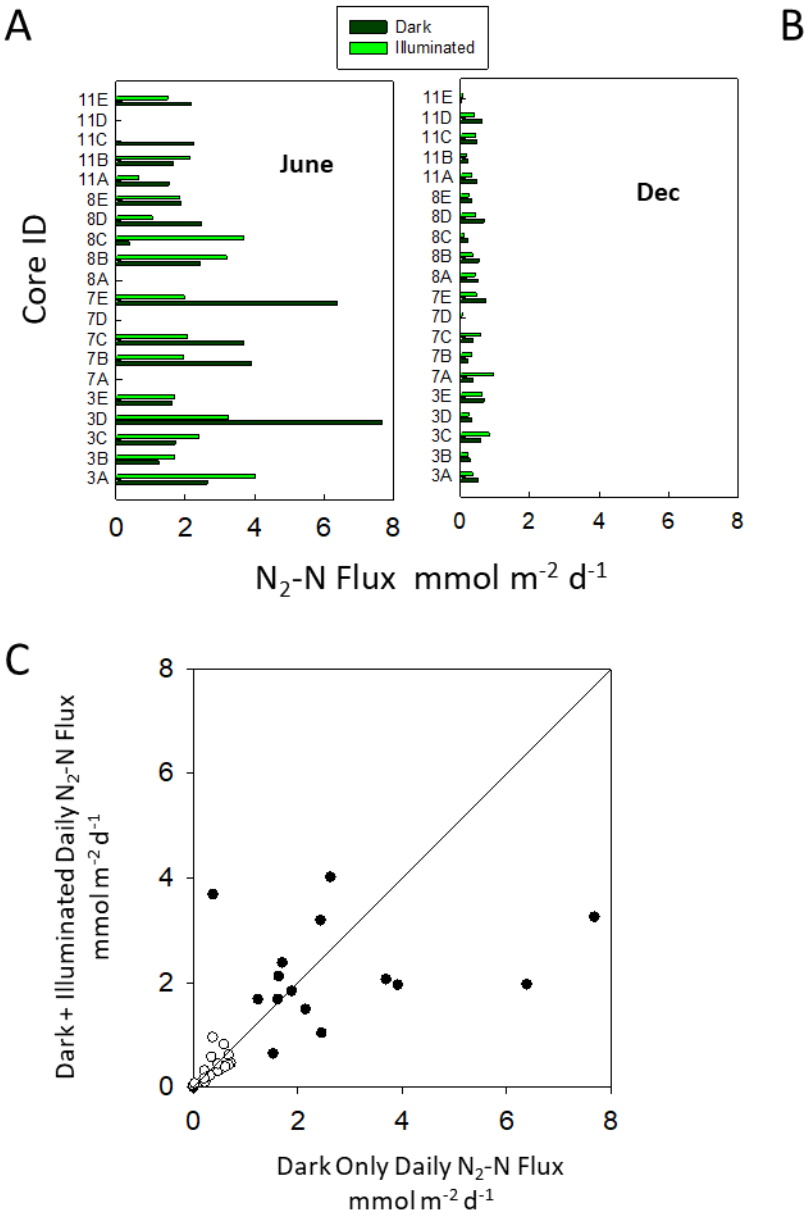

Figure 47. Daily N_2-N fluxes showing differences when illuminated incubations are included. Dark rates and dark + illuminated rates are presented as bar plots in panel A (June) and panel B (December). In panel C, dark+ illuminated rates are plotted versus rates using only dark data. The dark symbols are from June, the open symbols are from December.

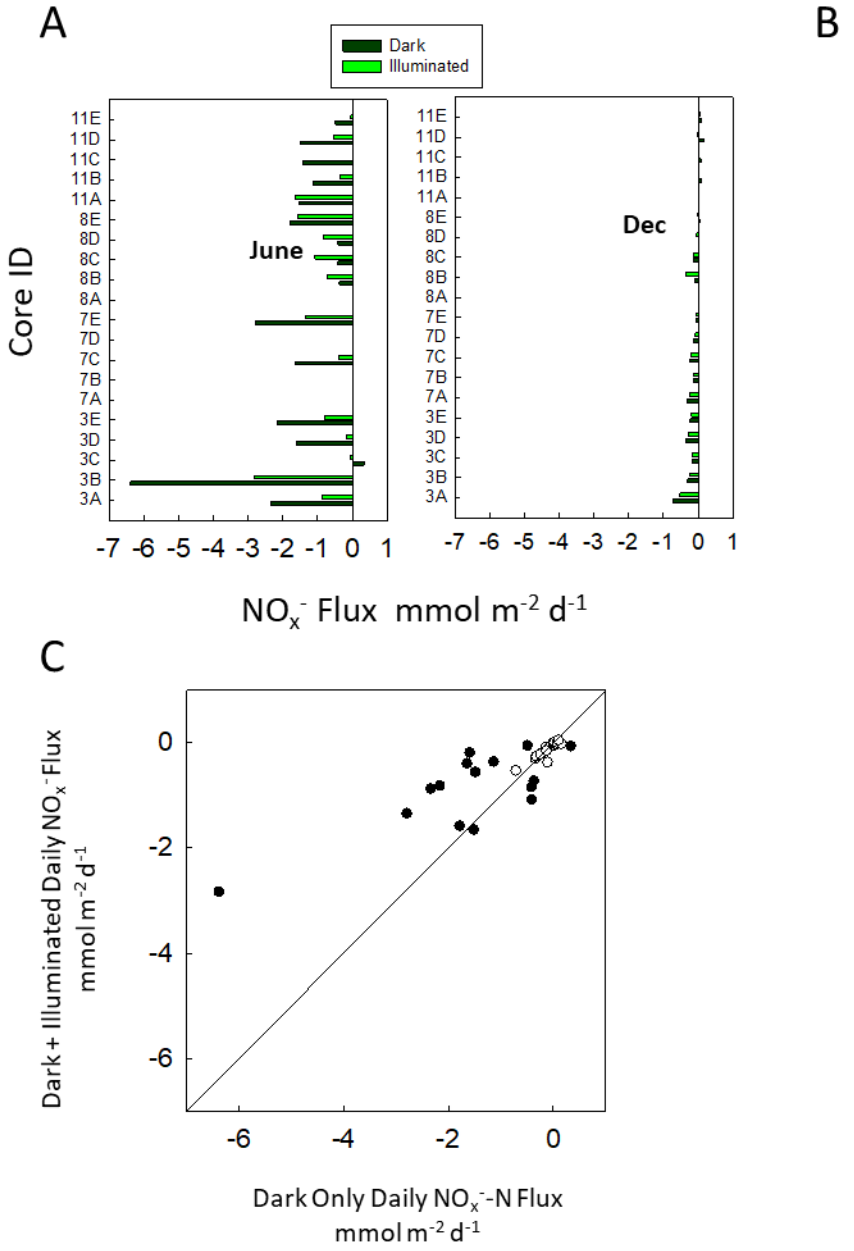

Figure 48. Daily NO_x^- fluxes showing differences when illuminated incubations are included. Dark rates and dark + illuminated rates are presented as bar plots in panel A (June) and panel B (December). In panel C, dark+ illuminated rates are plotted versus rates using only dark data. The dark symbols are from June, the open symbols are from December.

Relating Fluxes to Sediment C and N Pools

The turnover of organic matter in the sediments can be determined in a number of ways. Rates of decomposition can be best estimated from comparing fluxes of dissolved inorganic carbon (DIC) to the pool of organic carbon in the sediments (Burdige 1991). In this study, we did not measure DIC fluxes but can use the fluxes of oxygen as a proxy, recognizing that 1) upward fluxes of methane that were not reoxidized would result in oxygen underestimating overall rates of C decomposition; 2) any storage of reduced S or Fe would result in an underestimation of decomposition; and 3) nitrification would result in an over-estimation of DIC production (Banta et al. 1994). However, these effects are likely to be small and result in minimal change in the data interpretation.

The estimation of turnover rate, expressed as inverse time, can be carried out:

Equation 6

Turnover time (d^{-1}) = analyte flux rate (g m^{-2} d^{-1}) / pool size (g m^{-2})

The flux rates are converted from mg m^{-2} d^{-1} to g m^{-2} d^{-1} by dividing by 1000. Because our 0-1 cm sampling for analysis of C, N and P encompassed virtually all of the fine organic matter in the sediments, we can use the areal mass of C and N determined previously (g cm^{-3}; Appendix VI). Thus, the turnover rate for each core can be estimated, with O_2 as a proxy for DIC fluxes and N_2-N providing an estimate of the sediment N turnover into N_2.

As with most rate parameters in this study, the variability for carbon turnover estimates are high within a given treatment group (Figure 49), median rates for each treatment ranging from 0.01 to 0.08 d^{-1} and mean rates ranged from 0.01 to 0.07 d^{-1}. Comparison of groups revealed few significant differences between treatments or times. The decreased rate of oxygen uptake in December, relative to June, was compensated for by a decreased organic carbon pool in the sediments.

In the different treatments, the mean turnover rate of sediment organic N to N_2 ranged from 0.002 to 0.013 d^{-1},with median rates ranging from 0.001 to 0.008 d^{-1} (Figure 50). Thus, conversion of organic N in the sediments to N_2 consumes ~ 0.1 to 0.8% of the sediment organic N pool on a daily basis. There were no significant treatment differences, and high rates in carbon turnover did not appear to be related to the rates of N turnover. Aggregation of all of the data for June and December (Figure 51) showed little temporal change.

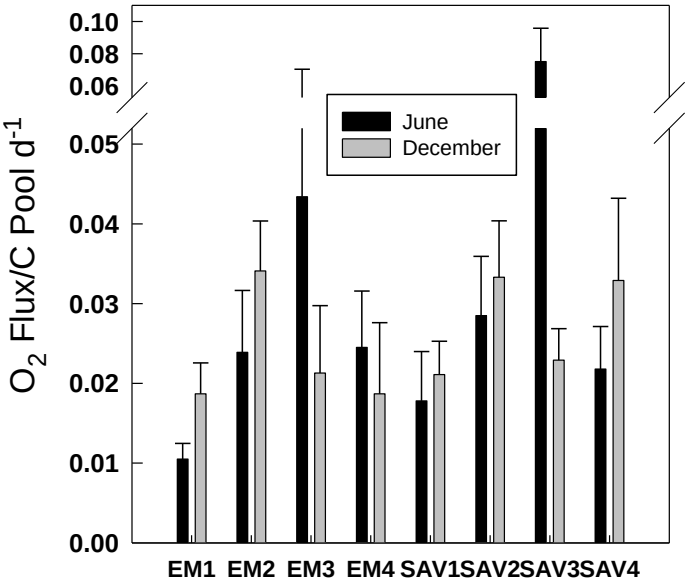

Figure 49. Mean (± S.E.) organic matter decomposition rates for each of the treatment types in Table 9. Rates are expressed on an inverse day, with a rate of 0.01 suggesting that 1% of the organic C is remineralized in a day. Only EM1 and SAV3, both in June, are significantly different (ANOVA on Ranks).

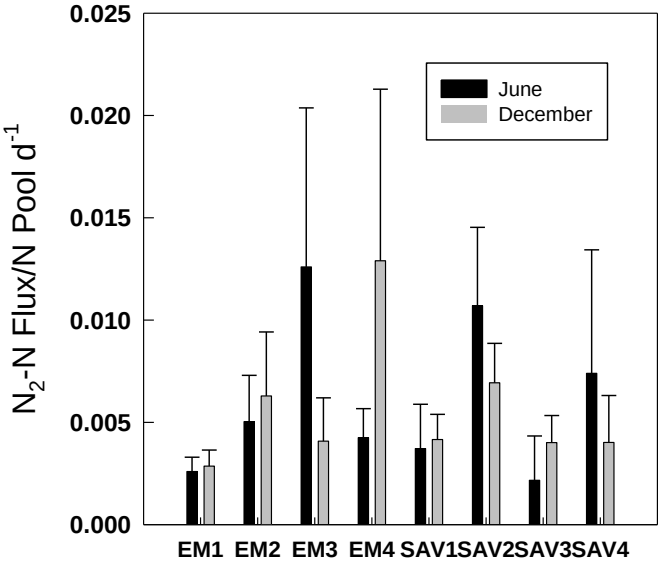

Figure 50. Mean (± S.E.) nitrogen turnover rates (into N_2) for each of the treatment types in Table 9. There were no significant differences. A rate of 0.005 indicates that 0.5% of the sediment pool is converted to N_2 on a daily basis.

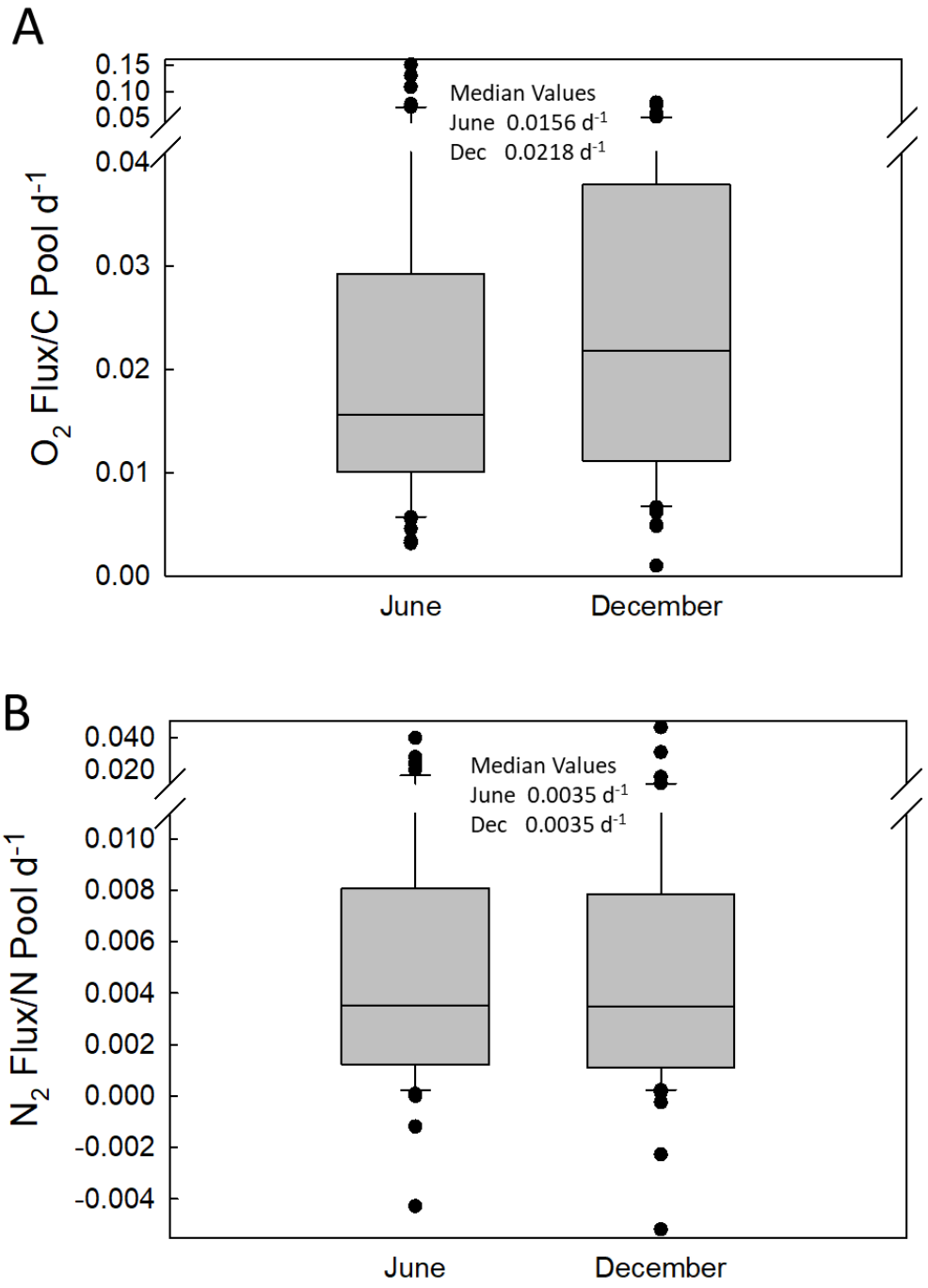

Figure 51. Carbon decomposition (A) and nitrogen decomposition (B) to N_2 rates relative to C and N pools, using data from all core incubations.

The decomposition rate data allow a comparison to rates in other ecosystems. The inverse day units compensate for different concentrations of organic matter and allow a more universal comparison. These data are also useful in a modeling context, providing data for estimating sediment diagenetic rates and simplifying the computations in spatially-explicit water quality models (Ditoro 2001; Laurent et al. 2016; Testa et al. 2013; Westrich and Berner 1984). The rates are an indication of organic matter reactivity.

Comparison of carbon decomposition turnover rates from different systems enables placing organic matter in surficial mesocosm sediment in a broader perspective. While rates for conversion of sediment organic matter to N_2 are not generally available, there is more data available for carbon turnover (Table 13). The rate of C turnover in these mesocosms (~ 0.02 d^{-1}) was several orders of magnitude higher that rates from "old" organic matter in wetland peats and tidal marshes, ~ 10 times higher than the turnover rates expected from aged, algal-derived organic matter, and about half of the rate of algal organic matter that is < 1 month old. These data suggest that the sediment organic matter was relatively reactive, that the reactivity did not appear to change over time, and that it was likely to fuel sediment respiration for many months. The increase in median turnover rate in December relative to June suggests that some aspect of organic matter quality, rather than just temperature, results in microbial decomposition rate change.

Table 13. Rates of C and N turnover. Median rates from this study are contrasted to carbon turnover estimates from other studies.

Pool/Flux	Season Time	Median Turnover Rate d^{-1}	Data Source
Wetland Mesocosm C/O_2	June	0.0156	This Study
	Dec	0.0218	
Wetland Mesocosm N/N_2	June	0.0035	This Study
	Dec	0.0035	
Algal G1 Rate C/CO_2		0.035	(Ditoro 2001)
Algal G_2 Rate C/CO_2		0.0018	(Ditoro 2001)
Chesapeake Wetland C/O_2 (deep horizons)		0.00006	(Cornwell et al. 2018)
Northern peat sediments (eroding)		0.0001	(St. Louis et al. 2003)

It might be expected that the rate of carbon turnover would have an effect on the efficiency of organic N conversion to N_2, mainly because we would expect carbon decomposition to be highly related to the remineralization from organic N to inorganic N. The initial product of decomposition is NH_4^+, and a variety of sediment processes are needed to both oxidize the NH_4^+ to NO_3^-, and reduce NO_3^- to N_2. A comparison of the two rates (Figure 52) showed that the proportional production of N_2 form organic N was significantly correlated to the turnover of organic carbon, though low R^2 values suggest these slopes provide little prediction of denitrification rates.

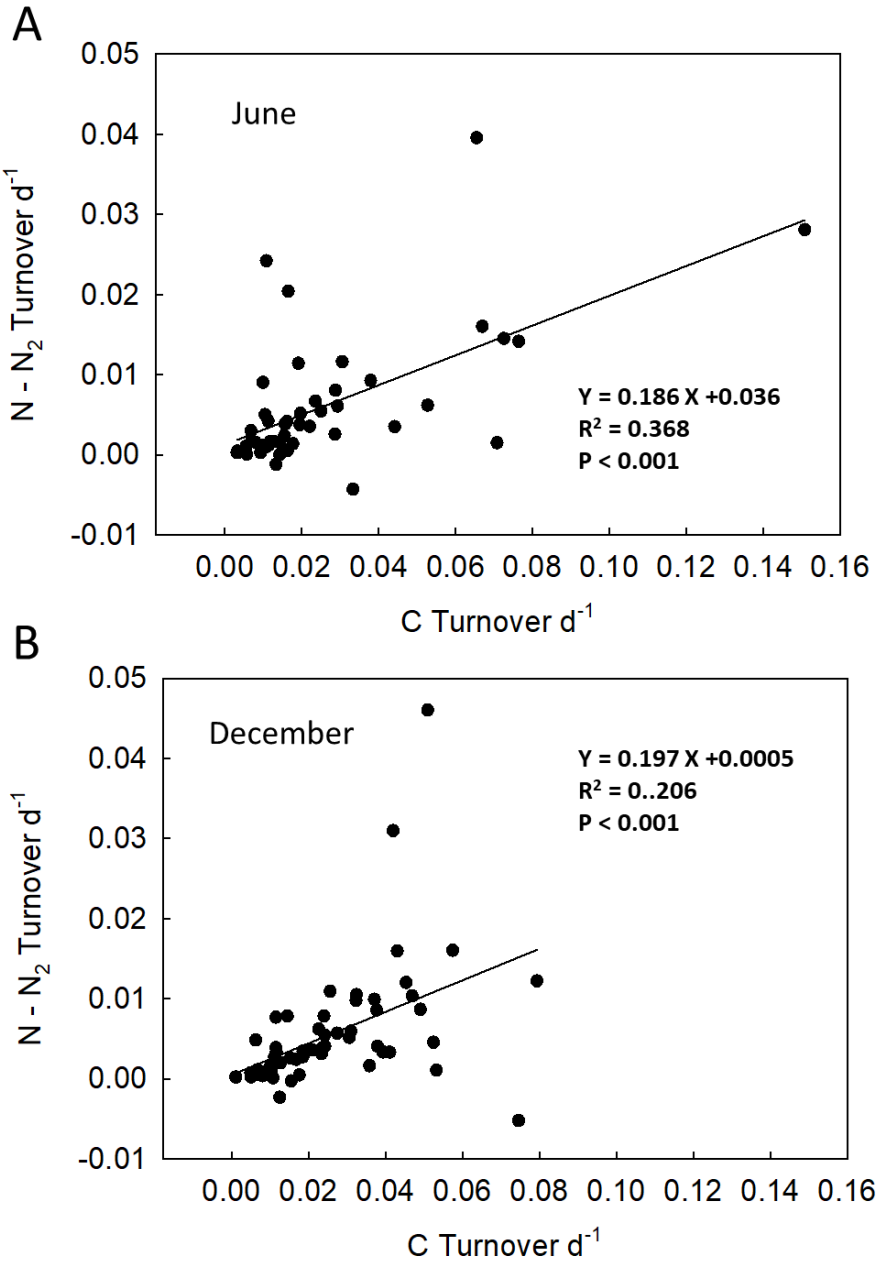

Figure 52. Plots of the rate of N_2 turnover of sediment N versus the rate of organic C turnover for June (A) and December (B). Each data point represents an individual core. Regressions are significant.

The key points to be derived from this data analysis are:

- The organic matter on the sediment surface in the mesocosm was quite reactive.
- Over the course of 6 months, including shutting off water exchange, the reactivity of organic carbon relative to oxygen uptake and of organic nitrogen relative to N_2 production did not change. This suggests a continual resupply of similar organic matter.
- For organic matter diagenesis, ~ 2% of the surficial sediment organic matter was remineralized in 1 day. For organic nitrogen diagenesis, ~ 0.35 % of the surficial pool was converted into N_2 on a daily basis.
- The turnover of organic N to N_2 (d^{-1}) was significantly correlated with the turnover of organic C, with a reactivity ratio of 0.2.

Final Observations

The first part of this section is organized around the questions posed by SFWMD for the C43-WQTTP mesocosm study. The latter part will delve into controlling mechanisms and the meaning of these mesocosm results to full scale implementation.

Objective 1. Determine denitrification rate differences between mesocosms

This objective has several components: the accurate assessment of denitrification rates (e.g. N_2-N fluxes) in each core and a comparison of rates between mesocosms and between treatments. With regard to the measurement of denitrification, these sediments were generally "well-behaved" in the sense that readily interpretable changes in the N_2:Ar ratios in core incubations yielded state of the art denitrification measurements. The O_2, NH_4^+ and NO_x^- flux rates are consistent with the overall rates of metabolism in the sediment and indicate there is a biogeochemical coherence in the data set.

Shallow water and wetland ecosystems, as well as the mesocosms, have a considerable amount of spatial variability. In the mesocosms, variability in biogeochemical pools and rates was relatively high, especially compared to non-vegetated shallow water systems. Our sampling took place between the plants and variable amounts of coarse and fine organic matter likely was a part of the heterogeneity of rates. The use of 5 cores per mesocosm per sample time is unprecedented and likely represents a minimum number to best assess the average rates in each mesocosm. Differences in denitrification rates between individual mesocosms were not observed.

Objective 2. If differences exist, determine if hydraulic loading rate, plant community, or soil affect the degree of difference

For denitrification, the within-tank variability resulted in no significant general conclusions relative to treatment. Within a single sample date, there were no significant

differences in denitrification rates for any of the individual treatments (one way ANOVA).

Objective 3. Determine whether the sediments are a source or sink for nutrients in the mesocosms

The source/sink question involves two components. Carbon and nutrient burial occurs after deposition, though a determination of a long-term burial mass is not possible in these short-term experiments. For nitrogen, NH_4^+ effluxes represent a return to the water column of fixed N. The dominant inorganic N flux is N_2-N efflux and is a dominant N loss term in these small ecosystems, barring large DON export, if observed in the mass balance (J-Tech 2019).

Objective 4. Determine if hydraulic loading rate, plant community, or soil affect whether the sediments are a source or sink for nutrients in the mesocosms.

The general conclusion of nutrient sinks/source is not generally affected by hydraulic loading rate, plant community, or soil treatment. The observations that denitrification is an important N sink and that sediment P retention was high are relatively independent of the initial mesocosm conditions.

Environmental Controls

The key controls on the ability of aquatic sediments to retain or release nutrients include:

- Rate of supply of labile and refractory organic matter. The labile organic matter is largely derived from the macrophytes, or perhaps algal epiphytes, and because of the nature of the experiment, the sediments start with virtually no sediment "memory" that would be typical of sediments in a wetland or shallow water system that has accumulated organic matter for decades. Median C and N pools were 77 and 7.8 g m^{-2} respectively in June, decreasing to 30 and 2.6 g m^{-2} in December. A measure of organic matter reactivity based on oxygen uptake and C pools suggest that ~2% of the organic matter is metabolized per day. The decrease in organic pools suggested that the supply after cessation of hydraulic exchange did not keep up with metabolism. The turnover of sediment organic N to N_2-N was ~ 0.35% per day.
- Bottom water oxygen. Low bottom water oxygen can have a negative impact on denitrification via the inhibition of nitrification (Cornwell et al. 1999). This limits denitrification rates.
- Illumination. Light has the beneficial effect of increasing incorporation of N and P in benthic microalgal communities, but can result in decreased rates of denitrification (Risgaard-Petersen 2003).
- Vertical mixing and organic matter export. The mesocosm environment is relatively quiescent and along with the plant community, the walls inhibit wind-mixing of the water. The depletion of oxygen may be increased in a mesocosm relative to open ecosystems, perhaps resulting in lower efficiencies for denitrification relative to other N cycling pathways. The flocculent layer in the

bottom of the mesocosm is a dominant feature of the mesocosm that may not be replicated in open water systems.

Concluding Remark

Although there is considerable variability in biogeochemical rate measurements, the water quality value of these macrophyte mesocosms is clear. Denitrification is an important N sink in these systems.

Acknowledgements

This work was funded by SFWMD under Contract No. 4600003691 with UMCES. Cassondra Thomas and Thomas Behlmer (SFWMD) installed the pore water equilibrators. Kabrena Owens assisted with almost all laboratory analyses. We thank Meg Maddox and Erica Kiss of UMCES HPL analytical services for pigment and CHN analyses.

References

Aspila, K. I., H. Agemian, and A. S. Y. Chau. 1976. A semi-automated method for the determination of inorganic, organic and total phosphate in sediments. Analyst 101: 187-197.

Banta, G. T., A. E. Giblin, J. Tucker, and J. E. Hobbie. 1994. Comparison of two indirect methods for estimating denitrification rates for Buzzards Bay, Massachusetts, p. 203-209. In K. R. Dyer and R. J. Orth [eds.], Changes in fluxes in estuaries: implications from science to management. Olsen & Olsen.

Burdige, D. J. 1991. The kinetics of organic matter mineralization in anoxic marine sediments. Journal of Marine Research 49: 727-761.

Cai, W.-J., Y. Wang, and R. E. Hodson. 1998. Acid-base properties of dissolved organic matter in the estuarine waters of Georgia, USA. Geochimica et Cosmochimica Acta 62: 473-483.

Cornwell, J. C., P. M. Glibert, and M. S. Owens. 2014. Nutrient fluxes from sediments in the San Francisco Bay Delta. Estuaries and Coasts 37: 1120-1133.

Cornwell, J. C., W. M. Kemp, and T. M. Kana. 1999. Denitrification in coastal ecosystems: environmental controls and aspects of spatial and temporal scale. Aq. Ecol. 33: 41-54.

Cornwell, J. C., M. Owens, T. M. Kana, E. M. Bailey, J. Barnes, and W. R. Boynton. 2008. An assessment of processes controlling benthic nutrientf in the Caloosahatchee River and Estuary and the St. Lucie River and Estuary. UMCES Technical Series Contribution TS-552-08.

Cornwell, J. C., and M. S. Owens. 2000. Nitrogen Cycling in Florida Bay Mangrove Environments: Sediment-Water Exchange and Denitrification. University of Maryland CES.

Cornwell, J. C., M. S. Owens, W. R. Boynton, and L. A. Harris. 2016. Sediment-Water Nitrogen Exchange along the Potomac River Estuarine Salinity Gradient. Journal of Coastal Research 32: 776-787.

Cornwell, J. C., A. Sanford, M. Owens, and Z. Vulgaropulos. 2018. An Investigation of the Composition and Reactivity of Material Eroded from Chesapeake Bay Marshes. Final Report to United States Army Corps of Engineers (ERDC-EL), UMCES Contribution TS-715-18.

Cornwell, J. C., J. C. Stevenson, D. J. Conley, and M. S. Owens. 1996. A sediment chronology of Chesapeake Bay eutrophication. Estuaries 19: 488-499.

Cowan, J. L. W., and W. R. Boynton. 1996. Sediment-water oxygen and nutrient exchanges along the longitudinal axis of Chesapeake Bay: Seasonal patterns, controlling factors and ecological significance. Estuaries 19: 562-580.

Ditoro, D. M. 2001. Sediment flux modeling. Wiley-Interscience.

Doane, T. A., and W. R. Horwath. 2003. Spectrophotometric determination of nitrate with a single reagent. Analytical Letters 36: 2713-2722.

Gardner, W. S., and M. J. McCarthy. 2009. Nitrogen dynamics at the sediment-water interface in shallow, sub-tropical Florida Bay: why denitrification efficiency may decrease with increased eutrophication. Biogeochemistry 95: 185-198.

Hecke, T. V. 2012. Power study of anova versus Kruskal-Wallis test. Journal of Statistics and Management Systems 15: 241-247.

Hesslein, R. H. 1976. An in situ sampler for close interval pore water studies. Limnology and Oceanography 21: 912-914.

Hopfensperger, K. N., S. S. Kaushal, S. E. G. Findlay, and J. C. Cornwell. 2009. Influence of Plant Communities on Denitrification in a Tidal Freshwater Marsh of the Potomac River, United States. Journal of Environmental Quality 38: 618-626.

Inglett, K. S., T. M. Kana, and S. M. An. 2013. Denitrification measurement using membrane inlet mass spectrometry, p. 503-518. In R. D. DeLaune, K. R. R. Reddy, C.J. and J. P. Megonigal [eds.], Methods in Biogeochemistry of Wetlands. Soil Science Society of America Book Series. Soil Science Society of America.

J-Tech. 2019. In association with Wetland Solutions, Inc. Final Project Report - Final Draft: C-43 Water Quality Treatment Area Test Facility - Mesocosm Operation and Sampling. Deliverable 8.2 prepared for the South Florida Water Management District, West Palm Beach, FL. April 2019.

Jackson, M., M. S. Owens, J. C. Cornwell, and M. L. Kellogg. 2018. Comparison of methods for determining biogeochemical fluxes from a restored oyster reef. Plos One 13: e0209799.

Jacobs, A. E., and J. A. Harrison. 2014. Effects of floating vegetation on denitrification, nitrogen retention, and greenhouse gas production in wetland microcosms. Biogeochemistry 119: 51-66.

Kana, T. M., C. Darkangelo, M. D. Hunt, J. B. Oldham, G. E. Bennett, and J. C. Cornwell. 1994. Membrane inlet mass spectrometer for rapid high-precision determination of N2, O2, and Ar in environmental water samples. Analytical Chemistry 66: 4166-4170.

Knowles, R. 1990. Acetylene inhibition technique: development, advantages, and potential problems, p. 151-166. In N. P. Revsbech and J. Sorensen [eds.], Denitrification in Soil and Sediment. Plenum Press.

Koop-Jakobsen, K. 2008. Gaseous loss of nitrogen in tidal marsh sediments: factors controlling denitrification and anammox. Boston University.
Laurent, A., K. Fennel, R. Wilson, J. Lehrter, and R. Devereux. 2016. Parameterization of biogeochemical sediment–water fluxes using in situ measurements and a diagenetic model. Biogeosciences 13: 77-94.
Merrill, J. Z. 1998. Denitrification in the Maryland National Estuarine Research Reserves. Final report to NOAA, Award #NA770R0251. UMCES Horn Point Laboratory.
---. 1999. Tidal freshwater marshes as nutrient sinks: particulate nutrient burial and denitrification. Ph.D. University of Maryland.
Merrill, J. Z., and J. C. Cornwell. 2000. The role of oligohaline marshes in estuarine nutrient cycling, p. 425-441. In M. P. Weinstein and D. A. Kreeger [eds.], Concepts and Controversies in Tidal Marsh Ecology.
Middelburg, J. J., K. Soetart, and P. M. J. Herman. 1996. Evaluation of the nitrogen isotope-pairing method for measuring benthic denitrification: A simulation analysis. Limnology and Oceanography 41: 1839-1844.
Newell, R. I. E., M. S. Owens, and J. C. Cornwell. 2002. Influence of simulated bivalve biodeposition and microphytobenthos on sediment nitrogen dynamics. Limnology and Oceanography 47: 1367-1369.
Nielsen, L. P. 1992. Denitrification in sediment determined from nitrogen isotope pairing. Fems Microbiol Ecol 86: 357-362.
Owens, M. S., and J. C. Cornwell. 2010. Nutrient flux study: results from the Murderkill River – Marsh Ecosystem. Final Report to Kent County (DE) Levy Court. Chesapeake Biogeochemical Associates.
---. 2016. The Benthic Exchange of O_2, N_2 and Dissolved Nutrients Using Small Core Incubations. Journal of Visualized Experiments 114: e54098.
Parsons, T. R., Y. Maita, and C. M. Lalli. 1984. A Manual of Chemical and Biological Methods for Seawater Analysis. Pergamon Press.
Piehler, M. F., and A. R. Smyth. 2011. Habitat-specific distinctions in estuarine denitrification affect both ecosystem function and services. Ecosphere 2: 1-16.
Poe, A. C., M. F. Pichler, S. P. Thompson, and H. W. Paerl. 2003. Denitrification in a constructed wetland receiving agricultural runoff. Wetlands 23: 817-826.
Racchetti, E. and others 2011. Influence of hydrological connectivity of riverine wetlands on nitrogen removal via denitrification. Biogeochemistry 103: 335-354.
Risgaard-Petersen, N. 2003. Coupled nitrification-denitrification in autotrophic and heterotrophic estuarine sediments: On the influence of benthic microalgae. Limnology and Oceanography 48: 93-105.
Scott, J. T., M. J. Mccarthy, W. S. Gardner, and R. D. Doyle. 2008. Denitrification, dissimilatory nitrate reduction to ammonium, and nitrogen fixation along a nitrate concentration gradient in a created freshwater wetland. Biogeochemistry 87: 99-111.
Shiau, Y. J., V. Dham, G. L. Tian, and C. Y. Chiu. 2016. Factors Influencing Removal of Sewage Nitrogen Through Denitrification in Mangrove Soils. Wetlands 36: 621-630.
Sorensen, J. 1978. Capacity for denitrification and reduction of nitrate to ammonia in a coastal marine sediment. Applied and Environmental Microbiology 35: 301-305.

St. Louis, V. L., A. D. Partridge, C. A. Kelly, and J. W. M. Rudd. 2003. Mineralization rates of peat from eroding peat islands in reservoirs. Biogeochemistry 64: 97-110.
Sundback, K., A. Miles, and E. Goransson. 2000. Nitrogen fluxes, denitrification and the role of microphytobenthos in microtidal shallow-water sediments: an annual study. Marine Ecology-Progress Series 200: 59-76.
Sweet, S. T., J. M. Wong, J. M. Brooks, and T. L. Wade. 1993. Sediment grain size analysis, p. II.23-II.26. In G. G. Lauenstein and A. Y. Cantillo [eds.], Sampling and Analytical Methods of the National Status and Trends Program. NOAA.
Testa, J. M. and others 2015. Modeling the impact of floating oyster (Crassostrea virginica) aquaculture on sediment-water nutrient and oxygen fluxes. Aquaculture Environment Interactions 7: 205-222.
Testa, J. M., D. C. Brady, D. M. Di Toro, W. R. Boynton, J. C. Cornwell, and W. M. Kemp. 2013. Sediment flux modeling: Simulating nitrogen, phosphorus, and silica cycles. Estuarine Coastal and Shelf Science 131: 245-263.
Thompson, S. P., M. F. Piehler, and H. W. Paerl. 2000. Denitrification in an estuarine headwater creek within an agricultural watershed. Journal of Environmental Quality 29: 1914-1923.
Valderrama, J. C. 1981. The simultaneous analysis of total nitrogen and total phosphorus in natural waters. Marine Chemistry 10: 109-122.
Van Raalte, C. D., and D. G. Patriquin. 1979. Use of the acetylene blockage technique for assaying denitrification in a salt marsh. Marine Biology 52: 315-320.
Westrich, J. T., and R. A. Berner. 1984. The role of sedimentary organic matter in bacterial sulfate reduction: the G model tested. Limnology and Oceanography 29: 236-249.

Appendix I: Field Sampling Data

Table 14. Field Measurements June 2018

Tank #	Sensor Depth	Temperature ºC	DO mg L^{-1}	DO % Saturation	Conductivity µS/cm	Salinity	pH	Light (PAR) µmol m^{-2} s^{-1}	Water Depth m
	Surface	28.4	5.54	70.5	431.9	0.19	7.67	875.0	
1	Bottom	27.2	1.40	17.8	468.0	0.21	7.22	0.24	0.63
	Surface	27.6	4.75	56.9	497.9	0.23	7.22	1171	
2	Bottom	26.8	1.34	16.8	573.0	0.27	7.05	0.09	0.625
	Surface	27.3	2.28	29.0	494.7	0.23	6.98	236.8	
3	Bottom	27.3	1.57	20.0	498.9	0.23	6.94	10.12	0.342
	Surface	26.7	1.88	23.3	504.0	0.23	6.86	128.9	
4	Bottom	26.5	1.34	16.8	508.0	0.24	6.80	0.00	0.330
	Surface	28.9	4.02	53.1	479.9	0.21	7.08	915.3	
5	Bottom	28.4	1.2	15.5	546.0	0.24	6.99	0.97	0.608
	Surface	28.6	4.45	57.6	502.0	0.22	7.11	865.5	
6	Bottom	27.4	1.30	16.6	523.0	0.24	7.01	0.17	0.565
	Surface	28.3	2.94	38.4	576.0	0.26	6.99	936.0	
7	Bottom	28.0	1.62	21.0	572.0	0.26	6.96	224.7	0.302
	Surface	27.4	3.06	38.7	471.7	0.22	6.98	368	
8	Bottom	27.1	1.79	22.7	470.6	0.22	6.96	21.6	0.280
	Surface	27.8	9.00	116.6	524.0	0.24	7.00	165.7	
9	Bottom	27.0	2.68	34.4	539.0	0.25	6.94	0.50	0.325
	Surface	27.6	3.51	45.4	511.0	0.23	6.99	896.1	
10	Bottom	26.7	1.34	16.8	515.0	0.24	6.99	0.03	0.645
	Surface	27.3	2.22	28.5	524.0	0.24	6.96	75.5	
11	Bottom	27.2	1.62	21.1	524.0	0.24	6.95	8.5	0.324
	Surface	29.8	5.98	78.6	427.4	0.18	7.36	911.1	
12	Bottom	28.3	1.91	26.5	426.0	0.19	7.44	0.03	0.620

Table 15. Field Measurements December 2018

Tank #	Sensor Depth	Temperature ºC	DO mg L^{-1}	DO % Saturation	Conductivity µS/cm	Salinity	pH	Light (PAR) µmol m^{-2} s^{-1}	Water Depth m
	Surface	20.2	14.25	158.5	384.4	0.20	8.25	251.0	
1	Bottom	17.7	1.7	16.4	369.4	0.21	7.94	0.0	0.57
	Surface	20.0	14.62	159.3	426.6	0.23	8.61	269	
2	Bottom	18.6	6.06	70.1	413.5	0.23	8.54	0.0	0.57
	Surface	19.6	4.60	52.1	424.6	0.23	8.43	45.0	
3	Bottom	19.2	3.12	33.7	421.4	0.23	8.23	2.5	0.27
	Surface	18.7	4.21	46.5	953	0.54	7.91	37.0	
4	Bottom	n.d.	n.d.	n.d.	n.d.	n.d.	n.d.	0.00	0.10
	Surface	19.8	10.18	113.0	636	0.34	8.08	187.0	
5	Bottom	17.9	3.11	37.4	630	0.34	8.04	0.05	0.57
	Surface	20.1	12.47	136.5	443.9	0.24	8.50	109	
6	Bottom	17.9	3.11	44.8	456.8	0.26	8.32	0.05	0.52
	Surface	19	7.09	79.0	825	0.46	8.16	52.0	
7	Bottom	19	6.93	78.6	825	0.46	8.05	28	0.27
	Surface	19.4	3.06	111.5	398.7	0.22	8.18	15	
8	Bottom	18.2	1.79	30.1	413.3	0.23	8.06	0.10	0.25
	Surface	18.7	9.00	41.4	608	0.34	7.86	5.0	
9	Bottom	18.4	2.68	38.1	614	0.34	7.75	0.50	0.24
	Surface	20.0	12.12	135.9	805	0.44	7.93	144	
10	Bottom	18.5	3.35	35.8	842	0.48	7.91	0	0.60
	Surface	18.5	3.79	40.0	489.5	0.27	7.93	33	
11	Bottom	18.4	3.05	33.0	490.5	0.27	7.86	5.0	0.25
	Surface	20.2	11.22	125.5	429	0.23	8.08	180	
12	Bottom	18.8	7.42	81.3	432.5	0.24	8.13	0.02	0.60

Appendix II. Ambient Water Sampling Chemistry

Table 16. Ambient Water Quality June 2018

Tank #	SRP	NH_4^+	NO_x^-	DON	DOP	TSS	Carbon	Nitrogen	Molar Ratio
	μmol L^{-1}	μmol L^{-1}	μmol L^{-1}	μmol L^{-1}	μmol L^{-1}	mg L^{-1}	mg L^{-1}	mg L^{-1}	C/N
1	0.05	21.48	2.05	77.72	1.93	13.95	1.60	0.20	9.19
2	0.03	26.08	1.68	90.76	1.84	9.62	1.80	0.24	8.69
3	0.00	7.11	1.47	88.23	1.86	8.49	1.80	0.14	15.57
4	0.28	8.08	3.89	93.25	1.82	7.83	1.48	0.17	9.89
5	0.03	2.87	1.37	90.26	2.19	4.97	0.81	0.06	15.13
6	1.66	5.46	0.84	107.09	2.18	10.18	8.78	0.60	17.21
7	0.05	2.56	1.26	91.84	1.93	8.44	1.99	0.13	17.85
8	0.05	3.52	0.74	89.53	2.04	11.58	3.06	0.28	12.92
9	2.51	2.07	1.47	110.78	2.49	8.49	4.23	0.48	10.35
10	0.20	6.01	1.63	97.58	2.59	10.78	4.66	0.43	12.55
11	2.61	2.46	0.79	101.97	2.51	11.90	4.06	0.34	13.92
12	0.15	2.37	0.84	107.15	2.18	15.33	6.24	0.69	10.62

Table 17. Ambient Water Quality December 2018. BDL = below detection limit.

Tank #									Particulate	Particulate	
	SRP	NH_4^+	NO_x^-	TN	DON	TSS	Fya	Chl a	Carbon	Nitrogen	Molar
	μmol L^{-1}	μmol L^{-1}	μmol L^{-1}	μmol L^{-1}	μmol L^{-1}	mg L-1	ug L-1	ug L-1	mg L-1	mg L-1	C/N
1	0.3	2.8	0.5	86.2	82.4	12.5	1.6	3.0	1.3	0.1	9.2
2	0.4	0.6	0.1	93.4	92.6	8.6	2.9	5.1	1.0	0.1	8.7
3	0.1	2.7	0.0	88.0	88.0	3.1	2.9	12.8	0.5	0.0	15.1
4	0.1	2.7	BDL	127.4	82.9	17.0	3.9	73.5	0.6	0.1	10.3
5	0.4	1.8	0.1	90.7	86.1	4.4	2.1	5.4	0.7	0.1	15.6
6	0.2	1.0	BDL	72.5	126.5	4.1	0.8	1.8	1.2	0.2	9.9
7	0.4	2.5	BDL	77.4	70.0	8.2	2.6	13.5	0.7	0.1	17.2
8	0.1	2.0	0.0	96.5	75.3	4.1	1.4	6.2	0.5	0.0	17.8
9	0.2	1.3	BDL	85.5	100.0	7.0	6.8	14.8	1.5	0.2	12.5
10	0.4	1.8	0.4	101.3	74.6	6.1	4.0	7.0	1.6	0.1	13.9
11	0.5	0.6	0.1	76.4	95.8	4.3	1.8	2.0	0.9	0.1	12.9
12	0.5	0.2	0.2	137.4	137.2	42.9	4.8	63.0	10.8	1.4	10.6

Appendix III. Core Photos

June 2018

1

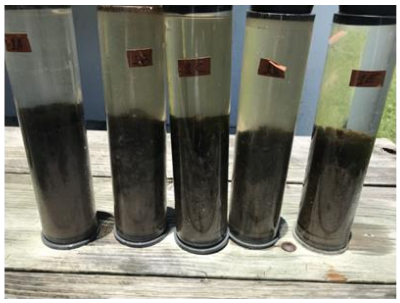

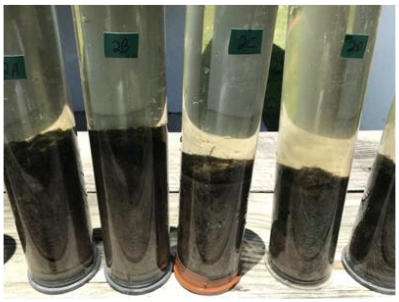

2

3

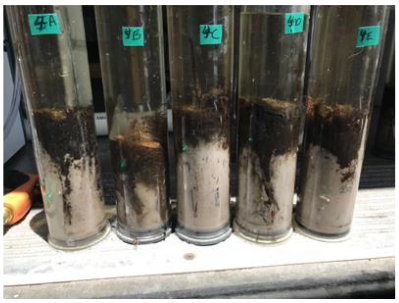

4

5

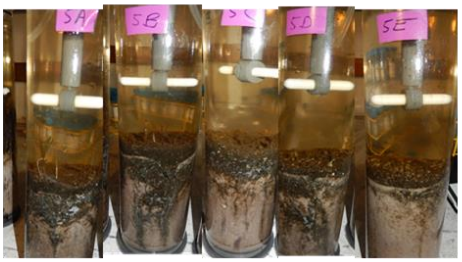

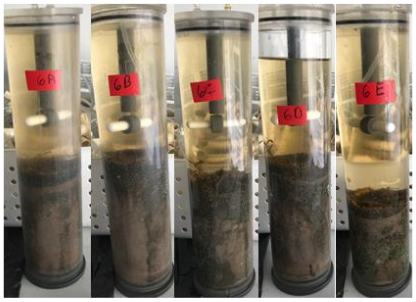

6

7

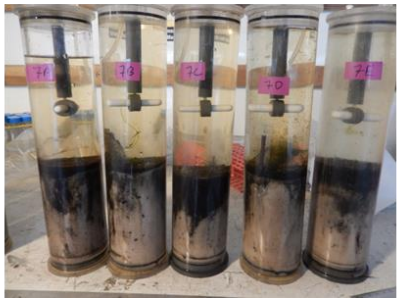

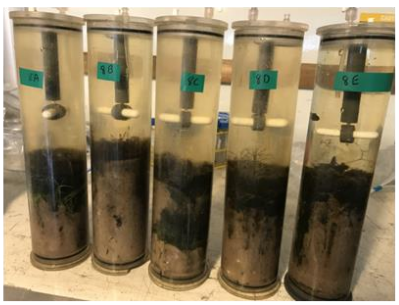

8

June 2018

9

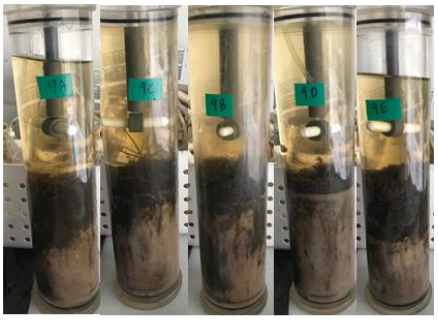

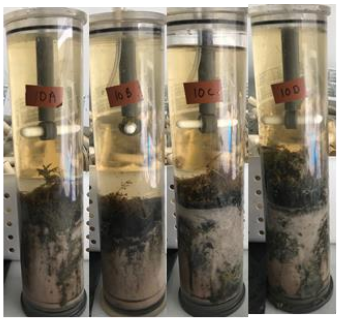

10

11

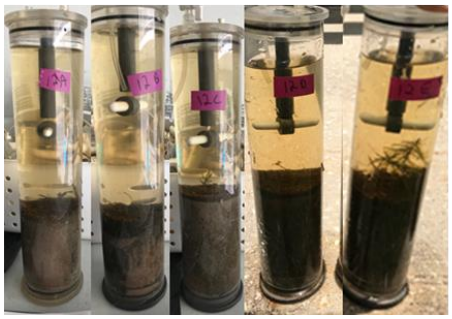

12

December 2018

1

2

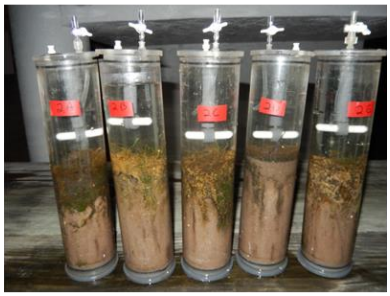

3

4

5

6

7

8

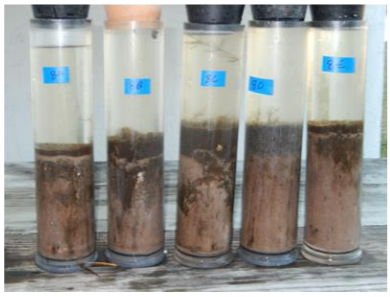

December 2018

9

10

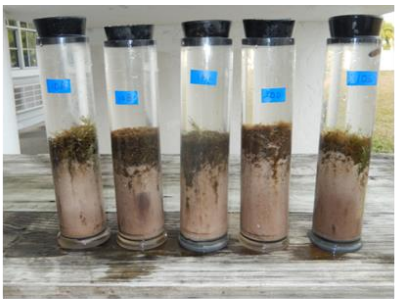

11

12

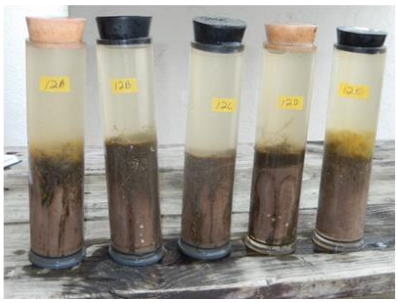

Appendix IV. Sediment-water Exchange Rates

Table 18. June 2018 sediment-water exchange, mass units on a daily basis. n.d. indicates non-interpretable fluxes. Dark and light data were used to calculate daily rates when illuminated incubations were carried out, taking into account day and night time duration.

Tank	Core	Type	O_2	N_2-N	NH_4^+	NO_x^-	SRP	DON
			mg m^{-2} d^{-1}					
1	A	SAV	-1095.8	17.6	-0.3	-21.2	-8.5	4.0
	B	SAV	-1231.1	0.0	11.6	-11.4	-8.4	-95.4
	C	SAV	-1644.1	12.9	25.5	-22.3	-18.7	-231.5
	D	SAV	-1307.3	2.3	23.1	-29.3	10.8	109.7
	E	SAV	-758.4	0.0	1.2	-16.2	-10.6	-246.6
2	A	SAV	-1620.9	167.0	26.0	-14.7	0.0	1.9
	B	SAV	-1356.8	4.7	16.4	-9.0	-5.9	-18.1
	C	SAV	-912.4	17.6	21.5	-12.0	0.0	176.7
	D	SAV	-2938.7	41.9	171.4	-50.0	0.0	-693.6
	E	SAV	-1019.7	32.4	8.4	-6.9	0.0	90.9
3	A	EMV	-2250.2	56.3	20.1	-12.2	n.d.	n.d.
	B	EMV	-1793.2	23.6	-4.3	-39.6	n.d.	n.d.
	C	EMV	-1308.2	33.4	5.5	-0.9	-32.7	n.d.
	D	EMV	-1210.7	45.6	4.6	-2.5	-27.2	416.1
	E	EMV	-2304.3	23.6	8.6	-11.4	-27.7	-17.4
4	A	EMV	-2350.7	20.9	34.1	-32.5	-16.2	-344.5
	B	EMV	-1703.5	34.2	14.6	0.0	11.1	162.2
	C	EMV	-1141.7	28.9	12.4	-12.2	0.0	-81.5
	D	EMV	-2021.5	29.4	36.1	-31.5	0.0	-161.1
	E	EMV	-1489.1	41.6	9.8	0.0	0.0	-39.0
5	A	SAV	-1673.8	3.8	-9.0	-19.5	-17.2	67.1
	B	SAV	-1485.5	19.4	-9.0	-15.9	-22.3	-14.3
	C	SAV	-1873.4	-19.2	29.9	-15.5	-25.2	167.1
	D	SAV	-1950.4	0.0	-2.7	-24.0	-34.0	13.8
	E	SAV	-1565.4	0.0	-8.7	-33.0	-36.3	n.d.
6	A	SAV	-901.3	42.2	-8.4	-10.2	-7.3	n.d.
	B	SAV	-1084.9	11.8	97.6	-12.6	-4.1	-141.0
	C	SAV	-985.3	0.0	-7.7	-12.0	-8.9	-106.2
	D	SAV	-379.4	31.4	-11.2	0.4	-8.8	-141.8
	E	SAV	-794.6	5.4	-5.6	-3.9	-17.6	n.d.

Table 18 (continued) 1. June 2018 sediment-water exchange, mass units on a daily basis. Dark/light differences are accounted for where appropriate. n.d. indicates non-interpretable fluxes.

Tank	Core	Type	O_2	N_2-N	NH_4^+	NO_x^-	SRP	DON
			mg m^{-2} d^{-1}					
7	A	EMV	-747.8	n.d.	2.4	-17.1	14.2	347.8
	B	EMV	-1764.4	27.4	15.4	n.d.	-9.3	470.8
	C	EMV	-1431.1	29.0	5.3	-5.4	-4.8	n.d.
	D	EMV	-1422.8	n.d.	11.4	-6.5	-14.2	n.d.
	E	EMV	-1238.3	27.6	5.6	-18.8	-18.7	229.5
8	A	EMV	-1328.4	n.d.	15.7	-1.4	-1.6	803.9
	B	EMV	-1354.8	44.7	1.0	-10.1	-15.5	253.5
	C	EMV	-1815.2	51.7	0.8	-15.1	-39.8	n.d.
	D	EMV	-1585.1	14.6	2.0	-11.7	-36.5	n.d.
	E	EMV	-2344.6	25.9	3.1	-22.1	-35.4	n.d.
9	A	EMV	-1506.2	30.0	-7.7	-8.7	-30.9	n.d.
	B	EMV	-1598.3	14.5	-6.1	0.0	-5.2	0.0
	C	EMV	-1128.8	12.9	-4.8	-2.9	-21.3	n.d.
	D	EMV	-1315.9	35.0	-0.7	-11.6	-14.8	n.d.
	E	EMV	-2049.9	33.7	n.d.	-10.7	-30.9	n.d.
10	A	SAV	-1861.2	-24.7	86.7	-19.6	-7.8	486.7
	B	SAV	-1021.1	0.0	33.5	1.3	-27.3	-63.7
	C	SAV	-1000.3	17.4	18.7	-0.5	-37.0	-102.9
	D	SAV	-2876.8	59.8	47.8	-1.7	-54.2	0.0
	E	SAV	-455.0	120.8	24.8	-8.6	-10.1	0.0
11	A	EMV	-3243.5	9.1	58.4	-23.1	-20.2	0.0
	B	EMV	-1701.3	29.7	58.0	-4.9	-25.0	n.d.
	C	EMV	-3245.2	n.d.	31.1	-16.3	-22.6	23.8
	D	EMV	-2305.8	0.0	3.4	-7.8	-32.7	0.0
	E	EMV	-1567.4	20.9	10.3	-0.7	-30.2	-108.8
12	A	SAV	-403.4	13.8	31.5	-2.7	-18.6	0.0
	B	SAV	-683.6	0.0	24.3	-0.5	-19.1	0.0
	C	SAV	-1609.5	0.0	20.0	-4.3	-31.4	-323.8
	D	SAV	-1320.8	39.7	12.9	-25.4	-24.6	0.0
	E	SAV	-1663.0	0.0	-1.2	-12.4	-35.2	-137.5

Table 19. December 2018 sediment-water exchange, mass units on a daily basis. Dark/light differences are accounted for where appropriate. n.d. indicates non-interpretable fluxes.

Tank	Core	Type	O_2	N_2-N	NH_4^+	NO_x^-	SRP	DON
			mg m^{-2} d^{-1}					
1.0	A	SAV	-1159.9	22.3	8.8	-5.4	0.0	-30.7
	B	SAV	-614.8	15.2	0.0	-1.0	-2.2	111.0
	C	SAV	-689.4	15.6	0.0	-3.5	0.0	159.8
	D	SAV	-635.8	10.2	5.6	-4.0	0.0	210.5
	E	SAV	-937.9	12.8	9.2	-2.2	0.0	198.7
2.0	A	SAV	-1448.8	20.7	22.0	-7.3	-2.1	112.6
	B	SAV	-873.6	11.9	0.0	-14.3	-2.0	105.4
	C	SAV	-1125.7	10.7	19.0	-5.9	-3.4	250.9
	D	SAV	-702.9	13.0	4.3	-5.1	-4.3	147.5
	E	SAV	-1087.5	-1.6	41.5	-7.2	-5.5	37.0
3.0	A	EMV	-541.5	4.7	-1.6	-7.3	-4.1	-27.0
	B	EMV	-406.0	2.9	-1.3	-3.6	-4.6	n.d.
	C	EMV	-580.0	11.5	-0.5	-2.2	-0.1	n.d.
	D	EMV	-517.2	3.2	-0.4	-4.1	-3.8	-146.4
	E	EMV	-456.9	8.8	-2.3	-2.7	-1.4	1.2
4.0	A	EMV	-1166.2	31.1	2.6	0.0	0.0	325.5
	B	EMV	-513.6	24.1	-4.4	-1.0	0.0	164.4
	C	EMV	-291.9	19.7	1.3	-1.9	0.0	123.9
	D	EMV	-365.0	7.2	-14.3	-2.2	0.0	91.3
	E	EMV	-1139.5	73.6	7.9	2.3	0.0	74.2
5.0	A	SAV	-813.0	12.4	0.0	-5.6	-0.8	73.0
	B	SAV	-799.7	8.8	6.4	-5.9	-0.6	n.d.
	C	SAV	-744.8	13.3	1.9	-5.5	0.0	83.5
	D	SAV	-666.3	11.6	0.0	-6.3	-0.9	38.0
	E	SAV	-698.5	9.2	13.6	-5.9	-0.2	75.9
6.0	A	SAV	-1173.5	20.5	11.7	-9.5	-3.8	-9.8
	B	SAV	-520.1	8.9	12.6	-4.0	-3.1	73.6
	C	SAV	-940.9	23.3	13.8	-6.8	-4.1	98.5
	D	SAV	-671.8	10.6	16.6	-8.6	-1.4	-15.8
	E	SAV	-796.4	10.5	10.8	-7.7	-0.9	-60.7

Table 19 (continued). December 2018 June 2018 sediment-water exchange, mass units on a daily basis. Dark/light differences are accounted for where appropriate. n.d. indicates non-interpretable fluxes.

Tank	Core	Type	O_2	N_2-N	NH_4^+	NO_x^-	SRP	DON
			mg m^{-2} d^{-1}					
7.0	A	EMV	-660.3	13.5	7.6	-3.6	-1.1	n.d.
	B	EMV	-522.5	4.6	3.9	-1.8	-1.3	n.d.
	C	EMV	-913.2	8.2	6.7	-3.1	-1.3	n.d.
	D	EMV	-218.8	0.6	2.1	-1.1	-3.5	n.d.
	E	EMV	-446.1	6.5	1.3	-0.9	-2.3	n.d.
8.0	A	EMV	-278.5	5.9	11.8	0.0	1.2	0.0
	B	EMV	-520.7	4.9	-10.3	-5.1	-0.8	0.0
	C	EMV	-493.1	1.4	6.0	-2.0	-0.4	-154.2
	D	EMV	-202.8	6.0	5.0	-0.6	-1.0	n.d.
	E	EMV	-288.9	3.2	4.2	-0.3	-0.1	-42.4
9.0	A	EMV	-472.0	10.1	-13.7	0.2	0.0	253.4
	B	EMV	-872.0	17.4	6.4	-1.8	0.0	105.6
	C	EMV	-683.2	29.7	8.8	-1.0	-4.7	42.3
	D	EMV	-840.9	-3.6	9.5	-1.5	-3.6	n.d.
	E	EMV	-1124.7	20.8	11.7	-1.5	0.0	162.8
10.0	A	SAV	-1107.4	2.7	0.0	-1.9	0.0	42.4
	B	SAV	-1156.2	0.0	0.0	-1.2	0.0	10.8
	C	SAV	-780.6	14.1	-29.2	-2.3	-4.9	46.2
	D	SAV	-476.1	12.8	-21.1	-4.8	0.0	21.7
	E	SAV	-1576.0	9.8	0.0	-3.6	0.0	n.d.
11.0	A	EMV	-655.6	4.4	20.9	0.2	-1.6	n.d.
	B	EMV	-769.6	2.4	16.2	0.2	0.0	n.d.
	C	EMV	-603.4	6.3	9.4	0.1	-0.8	n.d.
	D	EMV	-961.8	5.5	47.5	-0.2	-1.3	-158.8
	E	EMV	-817.0	1.1	0.9	0.8	-0.2	n.d.
12.0	A	SAV	-685.6	-10.4	0.0	0.0	0.0	n.d.
	B	SAV	-595.2	12.0	-17.1	0.0	0.0	14.9
	C	SAV	-540.1	6.2	0.0	0.0	0.0	123.4
	D	SAV	-728.1	3.4	0.0	0.0	0.0	63.3
	E	SAV	-371.5	6.7	0.0	0.0	-3.4	100.3

Appendix V: Sediment Pore Water Chemistry

Table 20. Pore Water Chemistry, Mesocosms 1-6

Tank ID	Peeper ID	Depth cm	Treatment	NH_4^+ μmol L^{-1}	NO_x^- μmol L^{-1}	SRP μmol L^{-1}	DON μmol L^{-1}	TN μmol L^{-1}
1	A	2	SAV	691.0	1.3	0.7	0.0	571.3
1	A	8.5	SAV	1049.4	0.5	3.6	277.2	1327.1
1	B	2	SAV	691.2	0.3	9.0	284.6	976.1
1	B	8.5	SAV	1699.7	0.2	14.2	244.6	1944.5
2	A	2	SAV	730.3	0.5	7.6	0.0	596.9
2	A	8.5	SAV	823.2	0.2	19.0	4.1	827.5
2	B	2	SAV	417.6	0.1	6.9	0.0	368.9
2	B	8.5	SAV	672.3	0.5	107.4	195.7	868.5
3	A	2	EMV	134.3	0.2	3.1	57.7	192.1
3	A	8.5	EMV	217.8	0.1	5.7	63.9	281.8
3	B	2	EMV	3.6	0.2	1.4	137.0	140.9
3	B	8.5	EMV	229.2	0.1	4.7	90.9	320.2
4	A	2	EMV	199.8	0.2	9.0	61.3	261.3
4	A	8.5	EMV	984.1	0.2	14.2	0.0	889.0
4	B	2	EMV	10.6	0.2	2.1	222.4	233.1
4	B	8.5	EMV	105.9	0.2	8.3	344.8	450.9
5	A	2	SAV	180.5	0.4	2.6	167.6	348.4
5	A	8.5	SAV	576.4	0.1	5.0	40.9	617.4
5	B	2	SAV	484.7	0.2	5.0	119.7	604.6
5	B	8.5	SAV	419.2	0.1	3.1	0.0	386.8
6	A	2	SAV	376.6	0.0	7.3	0.0	207.5
6	A	8.5	SAV	470.0	0.2	11.9	101.2	571.3
6	B	2	SAV	3.9	0.1	2.8	177.9	181.9
6	B	8.5	SAV	781.1	0.2	38.9	23.1	804.4

Table 20 (continued). Pore Water Chemistry, Mesocosms 7-12

Tank ID	Peeper ID	Depth cm	Treatment	NH_4^+ µmol L^{-1}	NO_x^- µmol L^{-1}	SRP µmol L^{-1}	DON µmol L^{-1}	TN µmol L^{-1}
7	A	2	EMV	5.8	0.3	3.3	252.7	258.8
7	A	8.5	EMV	47.9	0.2	4.7	589.8	637.9
7	B	2	EMV	3.4	0.2	2.1	160.4	164.0
7	B	8.5	EMV	50.6	0.1	4.3	218.2	269.0
8	A	2	EMV	26.8	2.5	2.8	137.3	166.5
8	A	8.5	EMV	175.4	0.6	5.9	164.7	340.7
8	B	2	EMV	578.0	4.0	15.2	112.3	694.3
8	B	8.5	EMV	1514.3	0.5	92.7	299.0	1813.8
9	A	2	EMV	122.8	0.4	13.5	281.6	404.8
9	A	8.5	EMV	98.8	0.2	16.8	118.7	217.8
9	B	2	EMV	125.4	3.3	16.6	142.9	271.6
9	B	8.5	EMV	931.7	0.5	83.2	0.0	873.6
10	A	2	SAV	1269.3	2.4	46.5	132.2	1403.9
10	A	8.5	SAV	1935.3	0.6	63.3	198.2	2134.1
10	B	2	SAV	911.1	0.3	12.1	308.0	1219.5
10	B	8.5	SAV	2127.0	0.2	23.5	0.0	942.8
11	A	2	EMV	98.2	0.2	4.5	234.6	333.0
11	A	8.5	EMV	0.4	4.3	1.9	128.5	133.2
11	B	2	EMV	64.5	0.5	12.1	109.2	174.2
11	B	8.5	EMV	47.1	0.1	13.5	173.1	220.3
12	A	2	SAV	437.2	0.2	9.7	85.2	522.6
12	A	8.5	SAV	1445.2	0.2	36.3	219.8	1665.2
12	B	2	SAV	263.6	0.1	9.7	297.3	561.1
12	B	8.5	SAV	550.2	0.2	10.7	82.4	632.8

Appendix VI: Sediment Solid Phase Chemistry

Table 21. Solid Phase Chemistry June 2018, Mesocosms 1-6.

Tank	Core	Depth	Carbon	Nitrogen	Total P	Pheophytin a	Chl a	C/N
		cm	mg g^{-1}	mg g^{-1}	mg g^{-1}	mg m^{-2}	mg m^{-2}	Molar
1	A	0-1	24.6	2.75	0.21	38.9	33	10.4
1	B	0-1	13.9	1.5	0.13	343.4	154.9	10.7
1	C	0-1	7	0.7	0.12	327.3	350.2	11.6
1	D	0-1	12.8	1.5	0.1	287.3	121.1	9.9
1	E	0-1	8.7	1	0.09	162.3	122	10.1
2	A	0-1	6	0.5	0.06	185.8	91.5	13.9
2	B	0-1	5.8	0.6	0.07	166.4	89.8	11.2
2	C	0-1	2.9	0.2	0.06	60	61.8	16.8
2	D	0-1	2.6	0.2	0.04	88.5	55.2	15.0
2	E	0-1	1.9	0.1	0.03	30.2	29.4	22.0
3	A	0-1	12.8	1.3	0.08	449.6	513	11.4
3	B	0-1	15.8	1.5	0.17	379.6	387.3	12.2
3	C	0-1	18.6	1.9	0.11	337.4	328	11.3
3	D	0-1	14.1	1.2	0.12	299	375.8	13.6
3	E	0-1	34.8	4.08	0.29	391.5	339.5	9.9
4	A	0-1	6.3	0.7	0.05	459.7	395.6	10.4
4	B	0-1	17.8	1.8	0.15	67.6	51.9	11.4
4	C	0-1	5.2	0.5	0.04	118.9	85.7	12.0
4	D	0-1	17.8	2	0.17	398.7	591.3	10.3
4	E	0-1	3.5	0.4	0.04	139.7	225.8	10.1
5	A	0-1	7.5	0.8	0.1	167.1	135.1	10.8
5	B	0-1	2.7	0.3	0.05	131.2	164	10.4
5	C	0-1	10.4	1.2	0.09	571	469.7	10.0
5	D	0-1	1.4	0.1	0.03	52.4	58.5	16.2
5	E	0-1	1.5	0.15	0.03	108	145.9	11.6
6	A	0-1	5.1	0.4	0.06	189.9	177.2	14.8
6	B	0-1	12	1	0.08	281.6	171.4	13.9
6	C	0-1	7.2	0.6	0.07	293.9	295	13.9
6	D	0-1	4.4	0.4	0.05	277.1	286.8	12.7
6	E	0-1	2.7	0.2	0.04	92.9	91.5	15.3

Table 21 (continued). Solid Phase Chemistry June 2018, Mesocosms 7-12.

Tank	Core	Depth	Carbon	Nitrogen	Total P	Pheophytin a	Chl a	C/N
		cm	mg g^{-1}	mg g^{-1}	mg g^{-1}	mg m^{-2}	mg m^{-2}	Molar
7	A	0-1	6.2	0.5	0.06	3.6	1.7	14.3
7	B	0-1	2.4	0.2	0.04	89.5	81.6	13.9
7	C	0-1	5.4	0.5	0.05	69.2	81.6	12.5
7	D	0-1	10.9	0.9	0.1	118.6	166.5	14
7	E	0-1	6.9	0.6	0.08	77.8	94.8	13.3
8	A	0-1	11.7	1.1	0.11	165.6	134.3	12.3
8	B	0-1	11.4	1	0.14	284.4	296.7	13.2
8	C	0-1	6	0.6	0.05	163.3	193.7	11.6
8	D	0-1	43.7	4.4	0.27	198.7	202.7	11.5
8	E	0-1	12.7	1.25	0.17	292.6	529.5	11.8
9	A	0-1	6.3	0.65	0.22	442.4	426.5	11.2
9	B	0-1	13.6	1.3	0.13	396.6	482.1	12.1
9	C	0-1	7.4	0.8	0.09	418.7	319.3	10.7
9	D	0-1	1.8	0.2	0.05	101.2	96.4	10.4
9	E	0-1	8.5	0.9	0.14	991	1586.3	10.9
10	A	0-1	5.8	0.6	0.05	309.1	227.2	11.2
10	B	0-1	4.5	0.5	0.04	265.8	84.9	10.4
10	C	0-1	3.7	0.4	0.05	265	309	10.7
10	D	0-1	6.0	0.6	0.05	623.8	618.1	11.6
10	E	0-1	3.8	0.45	0.07	250.9	317.3	9.8
11	A	0-1	27.2	2.6	0.21	2061.5	1091.9	12.1
11	B	0-1	24.1	2.2	0.24	366.8	214.3	12.7
11	C	0-1	16.0	1.5	0.15	525.5	346.1	12.3
11	D	0-1	11.9	1.1	0.17	583.8	486.2	12.5
11	E	0-1	1.5	0.1	0.03	141.3	120.3	17.4
12	A	0-1	4.2	0.3	0.05	126.4	76.6	16.2
12	B	0-1	5.9	0.6	0.06	122.3	80.8	11.4
12	C	0-1	1.7	0.1	0.04	76.5	61	19.7
12	D	0-1	3.8	0.3	0.06	149.4	131	14.7
12	E	0-1	5.5	0.6	0.06	188.3	140.1	10.6

Table 22. Solid Phase Chemistry December 2018, Mesocosms 1-6.

Tank	Core	Depth	Carbon	Nitrogen	Total P	Pheophytin a	Chl a	C/N
		cm	mg g^{-1}	mg g^{-1}	mg g-1	mg m^{-2}	mg m^{-2}	Molar
1	A	0-1	0.4	0.04	0.40	0.17	169.6	252.0
1	B	0-1	0.2	0.01	0.10	0.04	38.6	39.1
1	C	0-1	0.2	0.03	0.30	0.05	106.3	120.7
1	D	0-1	0.1	0.01	0.10	0.05	95.9	95.5
1	E	0-1	0.1	0.01	0.10	0.05	149.1	156.9
2	A	0-1	0.4	0.04	0.40	0.13	180.7	265.2
2	B	0-1	0.1	0.01	0.08	0.19	252.1	185.7
2	C	0-1	0.1	0.01	0.08	0.03	153.7	228.5
2	D	0-1	0.4	0.04	0.40	0.05	48.7	38.9
2	E	0-1	0.9	0.08	0.80	0.22	81.6	130.4
3	A	0-1	0.8	0.07	0.70	0.11	123.7	136.1
3	B	0-1	0.3	0.03	0.30	0.11	111.9	117.6
3	C	0-1	0.8	0.09	0.90	0.14	101.5	134.4
3	D	0-1	0.7	0.09	0.90	0.07	84.4	121.6
3	E	0-1	0.2	0.01	0.10	0.08	121.8	173.3
4	A	0-1	1.5	0.18	1.80	0.15	69.0	67.2
4	B	0-1	0.4	0.03	0.30	0.22	216.8	318.3
4	C	0-1	0.4	0.03	0.30	0.07	22.4	16.8
4	D	0-1	2.8	0.23	2.30	0.49	18.6	10.8
4	E	0-1	0.3	0.02	0.20	0.21	63.0	61.9
5	A	0-1	0.2	0.01	0.10	0.16	84.3	131.7
5	B	0-1	0.4	0.03	0.30	0.09	264.1	530.4
5	C	0-1	0.2	0.02	0.20	0.07	137.7	148.1
5	D	0-1	0.5	0.05	0.50	0.05	62.4	117.1
5	E	0-1	0.6	0.05	0.50	0.15	60.1	61.9
6	A	0-1	0.2	0.01	0.10	0.06	170.0	247.5
6	B	0-1	0.2	0.02	0.20	0.05	131.0	91.9
6	C	0-1	0.2	0.01	0.10	0.06	135.6	153.4
6	D	0-1	0.2	0.02	0.20	0.04	152.6	193.2
6	E	0-1	0.3	0.03	0.30	0.11	140.9	114.5

Table 22 (continued). Solid Phase Chemistry December 2018, Mesocosms 1-6.

Tank	Core	Depth	Carbon	Nitrogen	Total P	Pheophytin a	Chl a	C/N
		cm	mg g^{-1}	mg g^{-1}	mg g^{-1}	mg m^{-2}	mg m^{-2}	Molar
7	A	0-1	1.3	0.10	0.04	68.7	51.3	15.0
7	B	0-1	8.1	0.70	0.11	115.3	85.8	13.4
7	C	0-1	2.4	0.20	0.15	135.0	219.2	13.9
7	D	0-1	3.5	0.20	0.06	71.6	138.8	20.2
7	E	0-1	2.0	0.10	0.09	71.7	98.1	23.1
8	A	0-1	1.3	0.10	0.09	101.5	130.0	15.0
8	B	0-1	2.6	0.30	0.07	187.3	234.3	10.0
8	C	0-1	1.3	0.08	0.04	131.0	170.6	18.8
8	D	0-1	1.7	0.20	0.05	192.1	274.1	9.8
8	E	0-1	1.3	0.08	0.04	60.4	107.4	18.8
9	A	0-1	2.0	0.10	0.07	75.5	126.0	23.1
9	B	0-1	2.9	0.30	0.09	156.7	212.2	11.2
9	C	0-1	1.7	0.10	0.05	167.2	164.4	19.7
9	D	0-1	1.3	0.08	0.06	476.0	614.4	18.8
9	E	0-1	2.9	0.20	0.08	121.5	128.2	16.8
10	A	0-1	1.7	0.20	0.12	118.5	91.5	9.8
10	B	0-1	1.8	0.20	0.09	211.3	179.5	10.4
10	C	0-1	1.8	0.10	0.12	305.3	375.7	20.8
10	D	0-1	3.8	0.30	0.07	500.0	570.2	14.7
10	E	0-1	11.3	1.20	0.11	172.8	203.8	10.9
11	A	0-1	1.3	0.10	0.04	96.1	72.5	15.0
11	B	0-1	3.7	0.40	0.14	44.3	81.3	10.7
11	C	0-1	4.6	0.30	0.12	292.4	287.3	17.7
11	D	0-1	1.5	0.10	0.07	207.5	137.0	17.4
11	E	0-1	6.9	0.70	0.22	100.5	88.4	11.4
12	A	0-1	6.0	0.50	0.11	153.5	94.6	13.9
12	B	0-1	1.5	0.10	0.19	106.2	58.3	17.4
12	C	0-1	7.9	0.60	0.17	80.6	93.7	15.2
12	D	0-1	8.6	0.60	0.13	91.0	95.9	16.6
12	E	0-1	1.9	0.20	0.05	137.6	129.5	11.0

Table 23. Grainsize, Water Content, Bulk Density, December 2018, Mesocosms 1-6.

Tank	Core	Depth	Sand	Silt	Clay	Water Content	Bulk Density
		cm	%	%	%	%	g cm^{-3}
1	A	0-3	99.2	0.2	0.6	27.5	1.4
1	B	0-3	98.4	0.8	0.8	22.3	1.9
1	C	0-3	98.8	0.3	0.9	26.1	1.3
1	D	0-3	98.5	0.0	1.8	26.0	1.8
1	E	0-3	98.5	0.3	1.2	28.7	1.5
2	A	0-3	97.6	0.2	2.2	26.5	1.6
2	B	0-3	98.4	0.6	0.9	27.5	1.4
2	C	0-3	98.3	0.1	1.6	24.0	1.1
2	D	0-3	98.2	0.3	1.5	22.9	1.5
2	E	0-3	96.8	0.3	2.9	39.3	0.8
3	A	0-3	95.3	0.4	4.3	46.2	0.8
3	B	0-3	95.6	0.7	3.7	32.2	1.2
3	C	0-3	96.2	0.3	3.5	33.8	1.1
3	D	0-3	96.9	0.2	2.8	40.2	0.9
3	E	0-3	96.5	0.8	2.7	35.9	1.1
4	A	0-3	98.1	0.6	1.3	66.7	0.3
4	B	0-3	97.2	0.2	2.6	37.4	1.0
4	C	0-3	98.1	0.4	1.5	22.3	1.3
4	D	0-3	97.6	0.5	1.9	32.8	1.3
4	E	0-3	98.4	1.5	0.1	48.0	0.8
5	A	0-3	97.3	1.1	1.6	27.9	1.4
5	B	0-3	98.2	0.0	1.9	33.9	1.1
5	C	0-3	97.9	0.5	1.7	26.6	1.3
5	D	0-3	98.7	0.3	1.0	26.4	1.1
5	E	0-3	98.5	0.3	1.2	29.0	1.3
6	A	0-3	98.1	0.4	1.4	32.0	1.3
6	B	0-3	98.5	0.4	1.1	28.5	1.3
6	C	0-3	98.6	0.3	1.2	25.9	1.5
6	D	0-3	99.2	0.0	0.8	27.9	1.5
6	E	0-3	98.9	0.2	0.9	23.2	1.4

Table 23 (continued). Grainsize, Water Content, Bulk Density, December 2018, Mesocosms 7-12.

Tank	Core	Depth	Sand	Silt	Clay	Water Content	Bulk Density
		cm	%	%	%	%	g cm^{-3}
7	A	0-3	85.5	1.0	13.5	30.4	1.1
7	B	0-3	77.0	1.2	21.9	33.3	1.0
7	C	0-3	79.3	1.7	19.0	40.5	1.0
7	D	0-3	86.7	0.9	12.4	39.8	1.3
7	E	0-3	92.8	1.0	6.1	21.6	1.9
8	A	0-3	86.0	2.5	11.5	32.6	0.9
8	B	0-3	87.7	1.6	10.7	64.5	0.5
8	C	0-3	95.2	1.2	3.6	35.3	1.1
8	D	0-3	95.9	2.0	2.2	41.9	1.1
8	E	0-3	95.9	1.6	2.6	31.8	1.1
9	A	0-3	96.7	0.9	2.5	27.0	0.9
9	B	0-3	99.1	0.3	0.6	31.7	1.0
9	C	0-3	99.7	0.8	0.0	44.0	1.0
9	D	0-3	98.4	-0.2	1.7	31.0	0.9
9	E	0-3	98.5	0.6	0.9	45.0	1.0
10	A	0-3	99.1	0.8	0.1	39.2	1.2
10	B	0-3	99.2	1.0	0.0	32.3	1.1
10	C	0-3	99.4	0.7	0.0	35.5	1.3
10	D	0-3	99.4	0.3	0.3	34.9	1.1
10	E	0-3	99.3	0.2	0.4	25.8	1.6
11	A	0-3	98.8	0.0	1.6	35.9	1.0
11	B	0-3	97.5	0.7	1.7	35.4	1.2
11	C	0-3	97.3	0.9	1.8	36.3	1.2
11	D	0-3	98.8	0.3	0.9	25.1	1.6
11	E	0-3	98.6	0.7	0.6	35.3	1.1
12	A	0-3	98.9	0.3	0.8	43.8	0.9
12	B	0-3	98.2	1.5	0.3	33.9	1.2
12	C	0-3	98.5	0.0	1.6	31.8	1.4
12	D	0-3	98.8	0.5	0.8	29.4	1.1
12	E	0-3	99.2	0.0	0.9	35.4	1.3

Table 24. Areal C, N and P Concentrations, Mesocosms 1-6

Tank	Replicate	C	N	P	C	N	P
		June			December		
		g m^{-2}					
1	A	336.6	37.6	2.91	47.9	5.5	2.32
1	B	268.8	29.0	2.44	42.5	1.9	0.83
1	C	92.8	9.3	1.61	29.2	4.0	0.70
1	D	228.8	26.8	1.73	23.2	1.8	0.88
1	E	128.1	14.7	1.38	19.1	1.5	0.71
2	A	98.1	8.2	1.04	62.1	6.5	2.17
2	B	83.1	8.6	1.03	18.6	1.1	2.71
2	C	31.7	2.2	0.64	14.2	0.9	0.35
2	D	38.4	3.0	0.58	59.1	5.9	0.81
2	E	15.6	0.8	0.28	70.4	6.6	1.77
3	A	143.5	14.6	0.94	14.6	1.1	0.44
3	B	152.5	14.5	1.61	78.2	6.8	1.07
3	C	186.8	19.1	1.06	24.1	2.0	1.49
3	D	177.3	15.1	1.50	44.0	2.5	0.78
3	E	671.1	78.5	5.54	38.5	1.9	1.83
4	A	53.2	5.9	0.41	71.0	5.9	0.91
4	B	213.5	21.6	1.85	39.6	3.6	1.33
4	C	58.0	5.6	0.43	86.9	10.0	1.61
4	D	157.3	17.7	1.52	64.5	8.0	0.58
4	E	39.2	4.5	0.45	19.1	1.1	0.94
5	A	23.6	2.5	0.33	48.2	5.7	0.48
5	B	28.2	3.1	0.51	44.9	3.1	2.26
5	C	140.3	16.2	1.17	47.2	4.0	0.94
5	D	18.0	1.3	0.34	359.4	29.5	6.24
5	E	12.0	1.2	0.22	22.4	1.6	1.65
6	A	47.1	3.7	0.55	18.5	0.9	0.65
6	B	116.6	9.7	0.81	28.2	2.9	0.85
6	C	69.0	5.8	0.66	16.3	1.0	0.44
6	D	38.2	3.5	0.44	11.3	0.7	0.56
6	E	27.7	2.1	0.46	30.3	2.1	0.79

Table 24 (continued). Areal C, N and P Concentrations, Mesocosms 7-12

Tank	Replicate	C	N	P	C	N	P
		June			December		
		g m^{-2}					
7	A	58.8	4.7	0.58	12.3	0.9	0.84
7	B	11.7	1.0	0.17	12.7	1.5	0.33
7	C	57.2	5.3	0.53	13.8	0.8	0.48
7	D	117.6	9.7	1.06	18.3	2.2	0.52
7	E	76.5	6.6	0.89	14.4	0.9	0.49
8	A	168.4	15.8	1.59	21.6	1.4	2.23
8	B	120.0	10.5	1.48	43.2	3.2	0.91
8	C	77.0	7.7	0.63	24.4	2.6	0.91
8	D	498.5	50.2	3.07	52.5	5.7	0.58
8	E	164.7	16.2	2.19	71.3	6.5	1.92
9	A	77.2	8.0	2.71	20.8	2.5	1.46
9	B	149.0	14.2	1.47	19.7	2.2	0.94
9	C	99.1	10.7	1.25	24.1	1.3	1.59
9	D	19.7	2.2	0.53	41.5	3.3	0.76
9	E	132.0	14.0	2.25	175.5	18.6	1.78
10	A	55.8	5.8	0.47	12.5	1.0	0.42
10	B	53.4	5.9	0.50	43.9	4.7	1.65
10	C	45.3	4.9	0.58	56.4	3.7	1.42
10	D	98.1	9.8	0.85	24.5	1.6	1.17
10	E	42.1	5.0	0.80	76.5	7.8	2.39
11	A	347.4	33.2	2.73	20.4	1.3	0.82
11	B	307.8	28.1	3.08	28.1	2.6	0.70
11	C	233.5	21.9	2.23	21.9	1.5	0.83
11	D	173.6	16.1	2.43	32.1	2.9	0.60
11	E	21.6	1.4	0.46	47.5	4.3	1.65
12	A	38.5	2.7	0.44	55.0	4.6	0.97
12	B	72.5	7.4	0.72	18.4	1.2	2.27
12	C	23.9	1.4	0.57	111.2	8.4	2.37
12	D	43.2	3.4	0.71	97.8	6.8	1.44
12	E	70.6	7.7	0.76	24.4	2.6	0.65

Appendix VII: Use of the N_2:Ar approach to measure wetland denitrification

The measurement of denitrification in wetland soils and flooded sediments has generally followed one of three approaches (Cornwell et al. 1999):

1. Acetylene block (Sorensen 1978). This method hinders transformation of N_2O to N_2 and allows easy analysis of denitrification by accumulation of N_2O (Knowles 1990; Shiau et al. 2016; Thompson et al. 2000; Van Raalte and Patriquin 1979). Most studies using this approach yield "potential" denitrification.
2. Isotope pairing using ^{15}N techniques (Nielsen 1992). This approach uses $^{15}NO_3^-$ additions to measure denitrification, with an ability to distinguish between denitrification driven by water column and nitrification sources of nitrate. This approach has been widely used in Europe and elsewhere (Koop-Jakobsen 2008; Racchetti et al. 2011).
3. N_2:Ar approach (Kana et al. 1994). The changes in this gas ratio are precise to ≤ 0.02% and can measure denitrification in intact cores (Cornwell et al. 2008; Cornwell et al. 2016; Owens and Cornwell 2016). Wetland applications have included systems impacted by sewage and farm runoff with the earliest applications to tidal freshwater sediments (Merrill and Cornwell 2000). Wetland studies using this approach are listed in Table 27 and data is shown in Figures 53 and 54.

Advantages/disadvantages of each approach

1. Acetylene block. This approach is simple and less costly, at least for the measurement end of the process. The main disadvantage of the acetylene block approach is that these are generally potential measurements, usually useful for site to site comparison, but not generally relevant to actual denitrification rates. Acetylene also blocks nitrification, often a source of nitrate for denitrification and concerns for the effectiveness of the block have been made.
2. Isotope pairing. This technique works well in many environments, though there has been concern whether the label reaches the zone of denitrification (Middelburg et al. 1996). It is relatively costly, usually uses small cores for incubation, and often does not include measurements of other parameters such as oxygen and DIN. A key advantage is its value in determining denitrification pathways and its sensitivity at low rates.
3. N_2:Ar approach. The main advantage of this approach is the simplicity of the experiments and the lack of disturbance of the sediment. It is the only approach amenable to light/dark experiments so that the effect of autotrophic processes can

be identified in a single incubation. It is not sensitive at low rates when denitrification is a minor N cycling pathway and can be affected, as the other techniques, by bubbles of methane or oxygen. It has been widely applied in freshwater, estuarine and wetland environments.

Examples of the N_2/Ar approach in wetlands are shown in Table 1. In addition, data from two of our studies are shown in Figures 1-3.

Table 25. Wetland studies using the N_2:Ar approach.

Authors	Site	Comments
(Merrill 1998; Merrill 1999; Merrill and Cornwell 2000)	Chesapeake Bay tidal marshes	First studies using N2:Ar in wetlands
(Poe et al. 2003)	North Carolina created freshwater wetland	Very high nitrate system.
(Scott et al. 2008)	Texas created wetland	
(Hopfensperger et al. 2009)	Potomac River freshwater tidal marsh	Paper includes both acetylene and N_2/Ar data
(Inglett et al. 2013)	Method	This methodological approach is very similar to ours
(Jacobs and Harrison 2014)	Floating wetlands	
(Owens and Cornwell 2010)	Murderkill Marsh	This marsh receives all of the wastewater from Kent County, DE

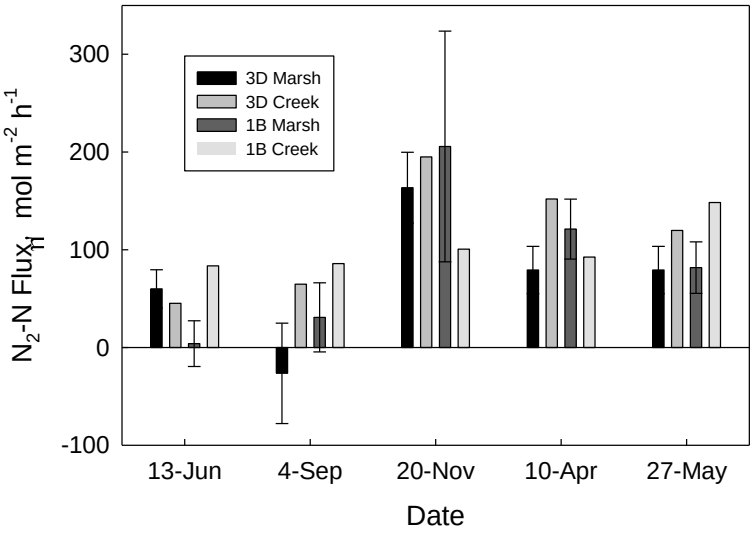

Figure 53. Denitrification at Poplar Island, a restoration site constructed of dredged materials.

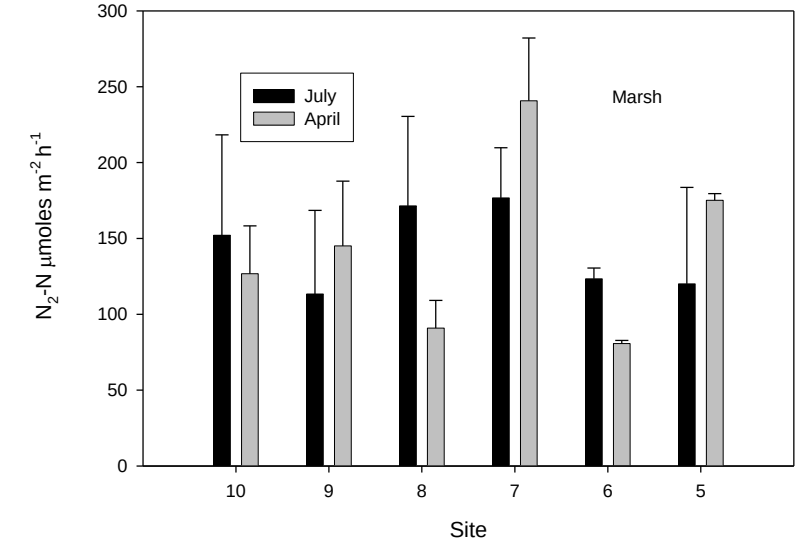

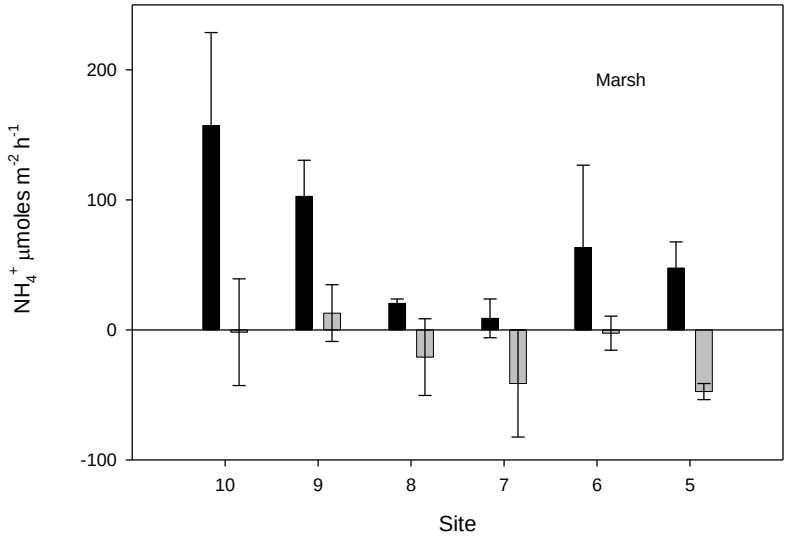

Figure 54. Di-nitrogen and ammonium fluxes from Murderkill Marsh (Delaware) across a salinity gradient. Station 10 is the freshwater endmember and station 5 near the Delaware Bay.